

# **Basic Theoretical Concepts**

I. Dobson

T. Van Cutsem

C. Vournas

C.L. DeMarco

M. Venkatasubramanian

T. Overbye

C.A. Canizares

## **CHAPTER 2 from Voltage Stability Assessment: Concepts, Practices and Tools August 2002**

IEEE Power Engineering Society

Power System Stability Subcommittee Special Publication

IEEE product number SP101PSS

ISBN 0780378695

# Contents

<b>2 BASIC THEORETICAL CONCEPTS</b>	<b>2-1</b>
2.1 DESCRIPTION OF PHYSICAL PHENOMENON	2-1
2.1.1 Time Scales	2-1
2.1.2 Reactive Power, System Changes and Voltage Collapse	2-2
2.1.3 Stability and Voltage Collapse	2-4
2.1.4 Cascading Outages and Voltage Collapse	2-5
2.1.5 Maintaining Viable Voltage Levels	2-5
2.2 BRIEF REMARKS ON THEORY	2-6
2.3 POWER SYSTEM MODELS FOR BIFURCATIONS	2-8
2.4 SADDLE NODE BIFURCATION & VOLTAGE COLLAPSE	2-10
2.4.1 Saddle-node Bifurcation of the Solutions of a Quadratic Equation	2-11
2.4.2 Simple Power System Example (Statics)	2-11
2.4.3 Simple Power System Example (Dynamics)	2-12
2.4.4 Eigenvalues at a Saddle-node Bifurcation	2-14
2.4.5 Attributes of Saddle-node Bifurcation	2-18
2.4.6 Parameter Space	2-18
2.4.7 Many States and Parameters	2-18
2.4.8 Modeling Requirements for Saddle-node Bifurcations	2-21
2.4.9 Evidence Linking Saddle-node Bifurcations with Voltage Collapse	2-22
2.4.10 Common Points of Confusion	2-23
2.5 LARGE DISTURBANCES AND LIMITS	2-24
2.5.1 Disturbances	2-24
2.5.2 Limits	2-25
2.6 FAST AND SLOW TIME-SCALES	2-29
2.6.1 Time-scale Decomposition	2-29
2.6.2 Saddle Node Bifurcation of Fast Dynamics	2-31
2.6.3 A Typical Collapse with Large Disturbances and Two Time-scales	2-33
2.7 CORRECTIVE ACTIONS	2-35
2.7.1 Avoiding Voltage Collapse	2-35
2.7.2 Emergency Action During a Slow Dynamic Collapse	2-38
2.8 ENERGY FUNCTIONS	2-39
2.8.1 Load and Generator Models for Energy Function Analysis	2-42
2.8.2 Graphical Illustration of Energy Margin in a Radial Line Example	2-46

2.9 CLASSIFICATION OF INSTABILITY MECHANISMS	2-52
2.9.1 Transient Period	2-52
2.9.2 Long-term Period	2-52
2.10 SIMPLE EXAMPLES OF INSTABILITY MECHANISMS	2-54
2.10.1 Small Disturbance Examples	2-54
2.10.1.1 Example 1	2-54
2.10.1.2 Example 2	2-56
2.10.1.3 Example 3	2-56
2.10.2 Large Disturbance Examples	2-58
2.10.2.1 Example 4	2-58
2.10.2.2 Example 5	2-58
2.10.3 Corrective Actions in Large Disturbance Examples	2-59
2.10.3.1 Example 6	2-60
2.10.3.2 Example 7	2-60
2.11 A NUMERICAL EXAMPLE	2-62
2.11.1 Stability Analysis	2-64
2.11.2 Time Domain Analysis	2-67
2.11.3 Conclusions	2-70
2.12 GLOSSARY OF TERMS	2-71
2.13 REFERENCES	2-74
APPENDIX 2.A HOPF BIFURCATIONS AND OSCILLATIONS	2-79
2.A.1 Introduction	2-79
2.A.2 Typical Supercritical Hopf Bifurcation	2-79
2.A.3 Typical Supercritical Hopf Bifurcation	2-80
2.A.4 Hopf Bifurcation in Many Dimensions	2-80
2.A.5 Comparison of Hopf with Linear Theory	2-80
2.A.6 Attributes of Hopf Bifurcation	2-88
2.A.7 Modeling Requirements for Hopf Bifurcation	2-88
2.A.8 Applications of Hopf Bifurcation to Power Systems	2-88
APPENDIX 2.B SINGULARITY INDUCED BIFURCATIONS	2-90
2.B.1 Introduction	2-90
2.B.2 Differential-algebraic Models	2-90
2.B.3 Modeling Issues Near a Singularity Induced Bifurcation	2-91
2.B.4 Singularity Induced Bifurcation	2-92

APPENDIX 2.C	GLOBAL BIFURCATIONS AND COMPLEX PHENOMENA	2-94
2.C.1	Introduction	2-94
2.C.2	Four Types of Sustained Phenomena	2-94
2.C.3	Steady State Conditions at Stable Equilibria	2-94
2.C.4	Sustained Oscillations at Stable Periodic Orbits	2-94
2.C.5	Sustained Quasiperiodic Oscillations at Invariant Tori	2-97
2.C.6	Sustained Chaotic Oscillations at Strange Attractors	2-97
2.C.7	Mechanisms of Chaos in Nonlinear Systems	2-98
2.C.8	Transient Chaos	2-98

# Chapter 2

## BASIC THEORETICAL CONCEPTS

Chapter 2 begins by reviewing the physical phenomenon of voltage collapse in Section 2.1 and then describes basic theoretical concepts for voltage collapse in a tutorial fashion. The theoretical concepts include saddle-node bifurcations, controller limits, large disturbance and time scale analysis, and energy functions and are briefly introduced in Section 2.2. Section 2.3 presents a brief discussion on the various power system models used for voltage collapse; more details regarding system modeling can be found throughout the chapter. Based on the explanations of voltage collapse mechanisms presented in detail in Sections 2.4, 2.5 and 2.6, corrective actions are discussed in Section 2.7. Section 2.8 concentrates on discussing, with the help of a simple example, the use of energy functions in voltage collapse analysis. The mechanisms are classified in Section 2.9 and illustrative examples are given in Section 2.10. Section 2.11 presents a complete numerical example to illustrate several of the issues discussed throughout the chapter. Finally, terms which may be unfamiliar are explained in the glossary in Section 2.12.

Other types of bifurcations and more exotic phenomena are discussed in the appendices.

### 2.1 DESCRIPTION OF PHYSICAL PHENOMENON

This section reviews some of the basic features of voltage collapse. The presentation is brief and selective because much good material on the physical aspects of voltage collapse exists in previous IEEE publications [40, 41] and books [18, 34, 51].

#### 2.1.1 Time scales

Voltage collapses take place on the following time scales ranging from seconds to hours:

- (1) Electromechanical transients (e.g. generators, regulators, induction machines) and power electronics (e.g. SVC, HVDC) in the time range of seconds.

- (2) Discrete switching devices, such as load tap-changers and excitation limiters acting at intervals of tens of seconds.
- (3) Load recovery processes spanning several minutes.

In voltage collapse, time scale 1 is called the transient time scale. Time scales 2 and 3 constitute the “long-term” time scale for voltage stability analysis (this long-term time scale is sometimes referred to as “midterm”). Electromagnetic transients on transmission lines and synchronous machines (e.g. DC components of short circuit currents) occur too quickly to be important in voltage collapse. Hence, it is assumed throughout this chapter that all electromagnetic transients die out so fast that a sinusoidal steady state remains and we can analyze voltages and currents as time varying phasors (see further discussion in Appendix 2.B). It follows that for a balanced three phase system, real power is equal to the sum of the powers momentarily transferred by the three phases, and reactive power at each phase is the amplitude of a zero mean power oscillation at twice the system frequency. Increase in load over a “long” time scale can be significant in voltage collapse. Figure 2.1-1 outlines a power system model relevant to voltage phenomena which is decomposed into transient and long-term time frames.

Voltage collapses can be classified as occurring in transient time scales alone or in the long-term time scale. Voltage collapses in the long-term time scale can include effects from the transient time scale; for example, a slow voltage collapse taking several minutes may end in a fast voltage collapse in the transient time scale.

### **2.1.2 Reactive Power, System Changes and Voltage Collapse**

Voltage collapse typically occurs on power systems which are heavily loaded, faulted and/or have reactive power shortages. Voltage collapse is a system instability in that it involves many power system components and their variables at once. Indeed, voltage collapse often involves an entire power system, although it usually has a relatively larger involvement in one particular area of the power system.

Although many other variables are typically involved, some physical insight into the nature of voltage collapse may be gained by examining the production, transmission and consumption of reactive power. Voltage collapse is typically associated with the reactive power demands of loads not being met because of limitations on the production and transmission of reactive power. Limitations on the production of reactive power include generator and SVC reactive power limits and the reduced reactive power produced by capacitors at low voltages. The primary limitations on the transmission of power are the high reactive power loss on heavily loaded lines, as well as possible line outages that reduce transmission capacity. Reactive power demands of loads increase with load increases, motor stalling, or changes in load composition such as an increased proportion of compressor load.

There are several power system changes known to contribute to voltage collapse.

- Increase in loading

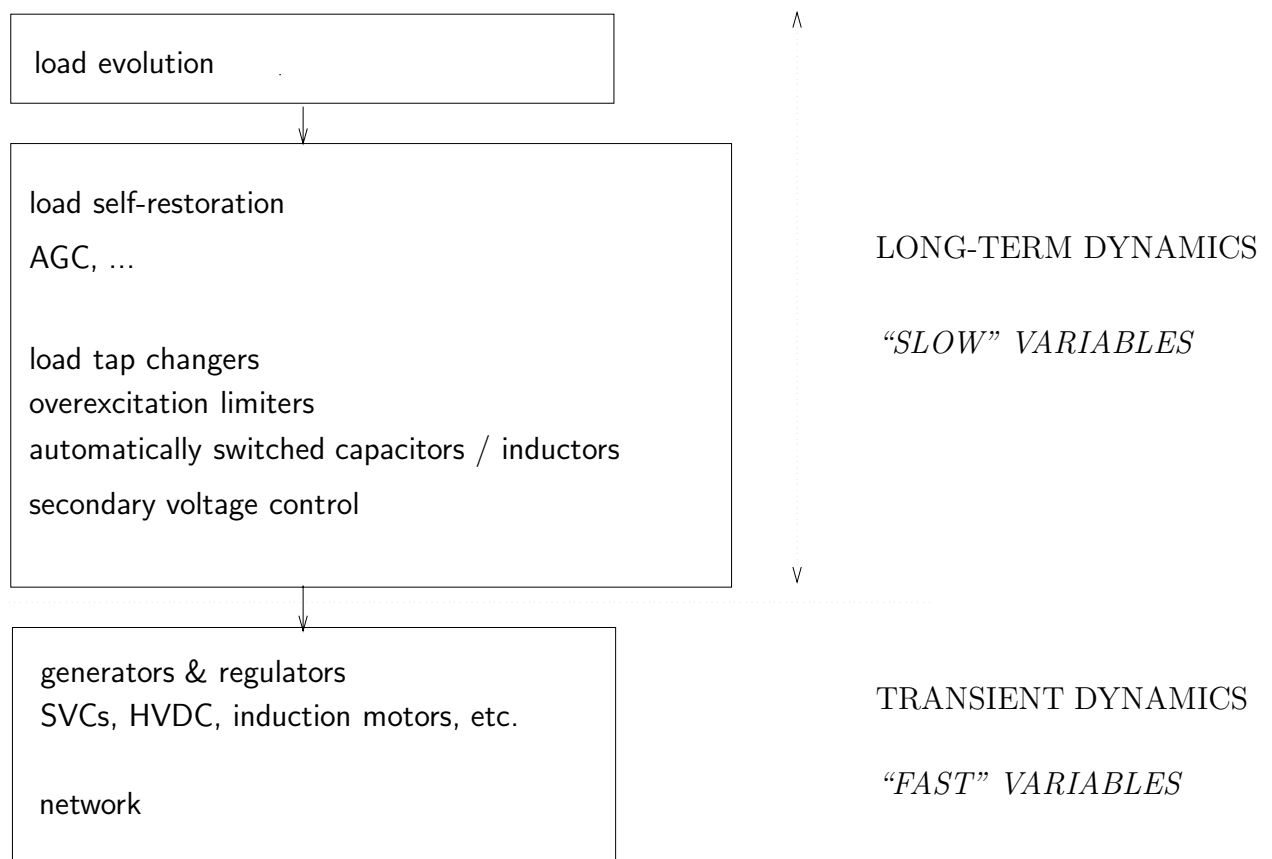


Figure 2.1-1. Voltage collapse time scales.

- Generators, synchronous condensers, or SVC reaching reactive power limits
- Action of tap-changing transformers
- Load recovery dynamics
- Line tripping or generator outages

Most of these changes have a significant effect on reactive power production, consumption and transmission. Switching of shunt capacitors, blocking of tap-changing transformers, redispatch of generation, rescheduling of generator and pilot bus voltages, secondary voltage regulation, load shedding, and temporary reactive power overload of generators are some of the control actions used as countermeasures against voltage collapse.

### 2.1.3 Stability and Voltage Collapse

To discuss voltage collapse a notion of stability is needed. There are dozens of different definitions of stability, and several of these are presented in Section 2.12 for reference. One of the definitions is small disturbance stability of an operating point:

An operating point of a power system is *small disturbance stable* if, following any small disturbance, the power system state returns to the identical or close to the pre-disturbance operating point.

A power system operating point must be stable in this sense.

Suppose a power system is at a stable operating point. It is routine for one of the changes discussed above to occur and the power system to undergo a transient and restabilize at a new stable operating point. If the change is gradual, such as in the case of a slow load increase, the restabilization causes the power system to track the stable operating point as this point gradually changes. This is the usual and desired power system operation.

Exceptionally, the power system can lose stability when a change occurs. One common way in which stability is lost in voltage collapse is that the change causes the stable operating point to “disappear” due to a bifurcation, as discussed in more detail below. The lack of a stable operating point results in a system transient characterized by a dynamic fall of voltages, which can be identified as a voltage collapse problem. The transient collapse can be complex, with an initially slow decline in voltages, punctuated by further changes in the system followed by a faster decline in voltages. Thus the transient collapse can include dynamics at either or both of the transient and long-term time scales defined above. Corrective control actions to restore the operating equilibrium are feasible in some cases. Mechanisms of voltage collapse are explained in much more detail in the following sections.



### 2.1.4 Cascading Outages and Voltage Collapse

Voltage collapse can also be caused by a cascade of power system changes, as for example a series of line trippings with generator reactive power limits being reached in succession. Cascading outages are complex and somewhat difficult to reproduce and analyze, as a given series of outages depend on a particular sequence of interdependent events, which eventually lead the system to collapse. These outages are a significant factor in voltage collapse and, due to their complexity, are typically analyzed using simulation tools that are able to adequately reproduce the sequence of events for each individual cascading outage.

### 2.1.5 Maintaining Viable Voltage Levels

One important problem related to voltage collapse is that of maintaining viable voltage levels. Voltage magnitudes are called viable if they lie in a specified range about their nominal value [38]. Transmission system voltage levels are typically regulated to within 5% of nominal values. It is necessary to maintain viable voltage levels as system conditions and the loads change.

Voltage levels are largely determined by the balance of supply and consumption of reactive power. Since inductive line losses make it ineffective to supply large quantities of reactive power over long lines, much of the reactive power required by loads must be supplied locally. Moreover generators are limited in the reactive power they can supply and this can have a strong influence on voltage levels as well as voltage collapse.

Devices for voltage level control include

- Static and switchable capacitor/reactor banks
- Static Var control
- Under-load tap changing (ULTC) transformers
- generators

A low voltage problem occurs when some system voltages are below the lower limit of viability but the power system is operating stably. Since a stable operating point persists and there is no dynamic collapse, the low voltage problem can be regarded as distinct from voltage collapse. Low voltages and their relation to voltage collapse are now discussed.

Increasing voltage levels by supplying more reactive power generally improves the margin to voltage collapse. In particular, shunt capacitors become more effective at supplying reactive power at higher voltages. However, low voltage levels are a poor indicator of the margin to voltage collapse. Increasing voltage levels by tap changing transformer action can decrease the margin to voltage collapse by in effect increasing the reactive power demand.

There are some relations between the problems of maintaining voltage levels and voltage collapse, but they are best regarded as distinct problems since their analysis is

different and there is only partial overlap in control actions which solve both problems. The rest of this chapter does not address the low voltage problem.

## 2.2 BRIEF REMARKS ON THEORY

This section discusses the role of theory in voltage collapse analysis and summarizes the main themes of Chapter 2.

**Why a Theoretical Perspective?** Voltage collapse is an inherently nonlinear phenomenon and it is natural to use nonlinear analysis techniques such as bifurcation theory to study voltage collapse and to devise ways of avoiding it. The aim of the theoretical perspective presented in this chapter is to explain some of the ideas used by theorists so as to encourage their practical use in understanding and avoiding voltage collapse.

Theory should help to explain and classify phenomena, and supply ideas and calculations so that events can be imagined and worked out. The theory presented here exploits and adapts ideas from mathematics, science and other parts of engineering, particularly nonlinear dynamical systems theory. Some standard terms are used in order to promote the desirable links between power system engineering and other subjects.

Although power system engineers routinely solve nonlinear problems, nonlinear theory to support these efforts is often unfamiliar. The authors believe that bifurcation theory and other nonlinear theories need not be difficult to grasp and use. The following sections try to explain the main ideas clearly without the mathematical apparatus needed to state and prove the results precisely. Thus the following presentation prefers to use the “pictures” that theorists think with rather than equations.

Excellent and accessible introductory texts on nonlinear dynamics and bifurcations are [48, 49, 52]. For illustrative examples of nonlinear dynamics and bifurcations see [4]. More specific background material can be found in some of the various references cited throughout this chapter. One way to track the more recent development of theory for voltage collapse is to consult the conference proceedings [27, 28, 29].

**Bifurcations:** Bifurcation theory assumes that system parameters vary slowly and predicts how the system typically becomes unstable. The main idea is to study the system at the threshold of instability. Regardless of the size or complexity of the system model, there are only a few ways in which it can typically become unstable and bifurcation theory describes these ways and associated calculations. Many of these ideas and calculations can be used or adapted for engineering purposes.

*What every power systems engineer should know about bifurcations:*

- (1) Bifurcations assume slowly varying parameters and describe qualitative changes such as loss of stability.
- (2) In a saddle-node bifurcation, a stable operating equilibrium disappears as parameters change, and the consequence is that system states dynamically col-

lapse. This basic fact can be used to explain the dynamic fall of voltage magnitudes in voltage collapse.

- (3) In a Hopf bifurcation, a stable equilibrium becomes oscillatory unstable and the consequence is either stable oscillations or a growing oscillatory transient.

**Large Disturbances and Fast and Slow Time scale Analysis:** Bifurcation theory assumes slowly varying parameters and does not account for the large disturbances found in many voltage collapses. However, some useful concepts of bifurcation theory can be used, although with some care, to study large disturbance scenarios. Voltage collapses often have an initial period of slow voltage decline. One key idea is to divide the dynamics into fast and slow. Then the slow decline can be studied by approximating the stable, fast dynamics as instantaneous. Later on in the voltage collapse, these fast dynamics can lose their stability in a bifurcation and a fast decline of voltage ensues. This fast-slow time scale theory suggests corrective actions which, if done quickly, can restore power system stability during the initial slow collapse.

**Modeling:** As might be expected, there is no single system model that can be used to study all possible voltage collapse problems. Power flow models have been typically used for voltage collapse studies, as these allow for a quick and approximate analysis of the changes in operating conditions that lead to the onset of the conditions which eventually drive the system to collapse. However, there is a clear need for better models than simple classical power flow models in voltage collapse analysis, as these types of models do not represent accurately some of the main devices and controls that lead to collapse problems, particularly loads (e.g. dynamic response) and generator voltage regulators (e.g. over/under-excitation limits). With this basic idea in mind, various system models are considered and briefly discussed throughout the various sections of this chapter.

**Energy Functions:** Energy function analysis offers a different “geometric” view of voltage collapse. In this approach, a power system operating stably is like a ball which lies at the bottom of a valley. Stability can be viewed as the ball rolling back to the bottom of the valley when there is a disturbance. As parameters of the power system change, the landscape of mountains and mountain passes surrounding the valley changes. A voltage collapse corresponds to a mountain pass being lowered so much that with a small perturbation the ball can roll from the bottom of the valley over the mountain pass and down the other side of the pass. The height of the lowest mountain pass can be measured by means of its associated potential energy, and then used as an index to monitor the proximity to voltage collapse. This potential energy is typically approximated by means of an energy function directly associated with the system model used for stability analysis, and is used as a relative measure of the stability region of an operating point (bottom of the valley), as discussed in more detail below.

**Interactions of Tap Changers, Loads and Generator Limits:** Certain voltage collapse problems can be studied by examining the interaction of load tap changer dynamics, system loading and generator reactive power limits, (e.g. [60, 61]). If the system frequency is assumed to be unchanging so that swing equations do not

become involved in the dynamics, then the effect of these interactions on voltage collapse can be successfully analyzed in terms of stability regions. A stability region is the region surrounding a stable operating point for which the state will return to that operating point. A sufficiently large stability region surrounding an operating point is desirable and the system becomes unstable if the stability region disappears. As the loading increases, reactive power limits apply and load tap changers act, the stability region can shrink or even disappear leading to voltage collapse. This view of the problem gives insight into how load tap changer dynamics, system loading and generator reactive power limits act to cause voltage collapse and shows how tap changer blocking can forestall voltage collapse.

**Instabilities due to Limits:** As loading increases, reactive power demand generally increases and reactive power limits of generators or other voltage regulating devices can be reached. These reactive power limits can have a large effect on voltage stability. The equations modeling the power system change when a reactive power limit is encountered. The effect of encountering the reactive power limit is that the margin of stability is suddenly reduced. In some cases, the power system operating point can become unstable or disappear when the limit is reached and this causes a voltage collapse.

**Other Nonlinear Phenomena:** Power systems are large dynamical systems with significant nonlinearities. Thus it is quite possible that power systems can display “exotic” dynamical behaviour such as chaos, as many other nonlinear systems do. Indeed, some idealized mathematical models of power systems do, in certain operating regions, produce chaos and other unusual behaviour.

Despite everyone’s best efforts to operate the power system stably, unexpected or unexplained events sometimes happen. How would one recognize chaos or other unusual behavior in such events? One approach is based on the fact that nonlinear theory provides a gallery of typical behaviors that nonlinear systems can have. Some of these, particularly saddle-node and Hopf bifurcations, help to explain certain phenomena in power systems such as monotonic collapses and oscillations, respectively. Other more uncommon behaviors such as chaos also have qualitative features which can be recognized, and learning these features opens new possibilities in interpreting unusual results.

## 2.3 POWER SYSTEM MODELS FOR BIFURCATIONS

Bifurcation analysis requires that the power system model be specified as equations which contain two types of variables: states and parameters. The states vary dynamically during system transients. Examples of states are machine angles, bus voltage magnitudes and angles and currents in generator windings. (The convenient choice of power system states varies considerably depending on the power system models being used. Thus different power system models are often written down using different choices of power system states.) Parameters are quantities that are regarded as varying slowly to gradually change the system equations. Examples of parameters are the (smoothed) real power demands at system buses. It is often convenient to regard

control settings as parameters so that the effect of the slow variation of the control settings can be studied. The choice of which variables are states and which variables are parameters is an important part of the power system modeling and should be stated explicitly in the power system model.

We now discuss in more detail the assumption of slow parameter variation, which is often called the quasistatic assumption. The parameters are assumed to vary quasistatically for bifurcation analyses, i.e., the parameters are considered as variable inputs to the system neglecting their dynamics. Thus, although the parameters vary, the system dynamics are computed assuming that parameters are fixed at a given value. The quasistatic approximation holds when the parameter variation is slow enough compared with the dynamics of the rest of the system.

Both the system states and the system parameters are vectors. The state vector is geometrically imagined as a point in “state space” and the parameter vector is geometrically imagined as a point in “parameter space”. If there are  $n$  states and  $m$  parameters, the state space is  $n$  dimensional and the parameter space is  $m$  dimensional. Pictures of the state and parameter space in 1, 2 or 3 dimensions are very valuable in visualizing the ideas of bifurcation analysis for power systems, but it should be emphasized that realistic power system examples involve many states and parameters. One objective of bifurcation analysis is to give insight into system stability as well as calculation methods to help deal with realistic power system problems which involve many states and parameters at once.

As is usual in power systems analysis, the equations used to represent the power system are critically dependent on the bifurcation phenomenon under study. Useful bifurcation analyses have been done with power systems modeled by differential equations, differential-algebraic equations and static (algebraic) equations. One can think of the power system being modeled, at least in principle, as differential equations. If some of the dynamics always act extremely quickly to restore algebraic relations between the states, then it can be a good approximation to use the algebraic relations together with the remaining differential equations as a differential-algebraic model. These models and their special features are discussed in Appendix 2.B. Some useful bifurcation calculations do not require knowledge of the complete differential equations and static equations are sufficient. These models are discussed in Section 2.4.

The equations and power system models discussed so far contain only smooth functions and are fixed in form. Also the equations do not vary with time, except for the quasistatic approximation of parameter variations. These restrictions are usually necessary for conventional bifurcation analyses. However power systems stability and dynamics is often influenced by discrete events such as outages or device or control limits being reached and these phenomena may change the form of the equations or introduce time dependence. For example, detailed models of generator reactive power limits cause the limit and the system equations to change based on the time that a limit has been exceeded. In general, these effects are not at present easily accounted for in conventional bifurcation analysis. However, it is still valuable to study with bifurcations the loss of power system stability given that a particular configuration of system limits have been reached. Moreover, methods based on bifurcation analysis

can be incorporated into software that does take account of the system limits.

Another important limitation of bifurcation analysis that sizable step changes or rapid changes in parameters are not accounted for. These parameter changes cause the state to be perturbed far from its steady state condition. These large disturbances and also the effects of limits are discussed in Section 2.5.

There are two approaches to representing loads in the following sections. In one approach, the quantities that characterize load (such as  $P$  and  $Q$ , demanded real and reactive current, or load impedance) are viewed as external “inputs.” That is, their predicted behaviors are typically specified as functions of time, or some other, single underlying variable (e.g. total MVA, with each individual load bus powers being a fixed, specified percentage of the total). In this approach, the dynamic modeling of the power system does not include the loads. As an alternate approach, when sufficient information is available, one may construct a dynamic model to predict load recovery with time. Voltage collapse analyses using this approach capture the relevant slow time scale behavior as an evolution of state variables within the model, rather than as externally prescribed inputs. This approach typically uses external inputs only to specify discontinuous changes in the system, such as line tripping or generator outage.

Either approach to load modeling yields quasistatic parameters for bifurcation analysis under suitable conditions. If the load powers are regarded as inputs and they are slowly varying, they can be regarded as quasistatic parameters. If the load dynamics are represented and the load dynamics are slow enough that they are decoupled from other system dynamics, then the load variations can be regarded as quasistatic parameters. Treatment of slow time scale load changes as externally specified parameters is used in the bifurcation analysis of Section 2.4, and in the energy function methods of Section 2.8. Modified bifurcation analyses that capture slow time scale load recovery within a two time scale dynamic model are described in Section 2.6.

Power system loads are sometimes thought of as varying stochastically and this aspect of modeling is described in Section 2.8.

## 2.4 SADDLE-NODE BIFURCATIONS & VOLTAGE COLLAPSE

A saddle-node bifurcation is the disappearance of a system equilibrium as parameters change slowly. The saddle-node bifurcation of most interest to power system engineers occurs when a *stable* equilibrium at which the power system operates disappears. The consequence of this loss of the operating equilibrium is that the system state changes dynamically. In particular, the dynamics can be such that the system voltages fall in a voltage collapse. Since a saddle-node bifurcation can cause a voltage collapse, it is useful to study saddle-node bifurcations of power system models in order to understand and avoid these collapses.

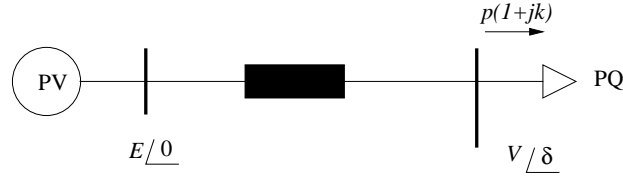


Figure 2.4-1. Single machine PV bus supplying a PQ load bus with constant power factor.

### 2.4.1 Saddle-node Bifurcation of the Solutions of a Quadratic Equation

Saddle-node bifurcation is an inherently nonlinear phenomenon and it cannot occur in a linear model. However the phenomenon of saddle node bifurcation is familiar from as simple a nonlinear model as a quadratic equation. Suppose the quadratic equation has two real roots (equilibrium solutions). As the coefficients (parameters) of a quadratic equation change slowly, the two real roots move and it is possible and routine for the real roots to coalesce and disappear. The bifurcation occurs at the critical case of a double root which separates the case of two real roots from the case of no real roots.

For example, consider the quadratic equation  $-x^2 - p = 0$ . The variable  $x$  represents the system state and  $p$  represents a system parameter. When  $p$  is negative, there are two equilibrium solutions  $x_0 = \sqrt{-p}$  and  $x_1 = -\sqrt{-p}$ . If  $p$  increases to zero, then both equilibria are at the double root  $x = 0$ . If  $p$  increases further and becomes positive, there are no equilibrium solutions. The bifurcation occurs at  $p = 0$  at the critical case separating the cases of two real solutions from no real solutions.

### 2.4.2 Simple Power System Example (Statics)

Now consider a single machine PV bus supplying a PQ load of constant power factor ( $k = \tan \phi = \text{constant}$ ) through a transmission line, as depicted in Figure 2.4-1. We choose the real power  $p$  as a slowly varying parameter which describes the system loading. The system state vector  $x = (V, \delta)$  specifies the load voltage phasor. The variation of load voltage magnitude  $V$  with loading  $p$  is shown in Figure 2.4-2. For low loading there are two equilibrium solutions; one with high voltage and the other with low voltage. The high voltage solution has low line current and the low voltage solution has high line current. As the loading slowly increases, these solutions approach each other and finally coalesce at the critical loading  $p^*$ . If the loading increases past  $p^*$ , there are no equilibrium solutions. The equilibrium solutions disappear in a saddle-node bifurcation at  $p^*$ .

Figure 2.4-2, which plots one of the state variables against the loading parameter, is called a bifurcation diagram and the bifurcation occurs at the nose of the curve. The power system can only operate at equilibria which are stable so that the system dynamics act to restore the state to the equilibrium when it is perturbed. In practice, the high voltage equilibrium is stable and the low voltage equilibrium is unstable. (Here for simplicity we neglect Hopf bifurcations and singularity induced bifurcations

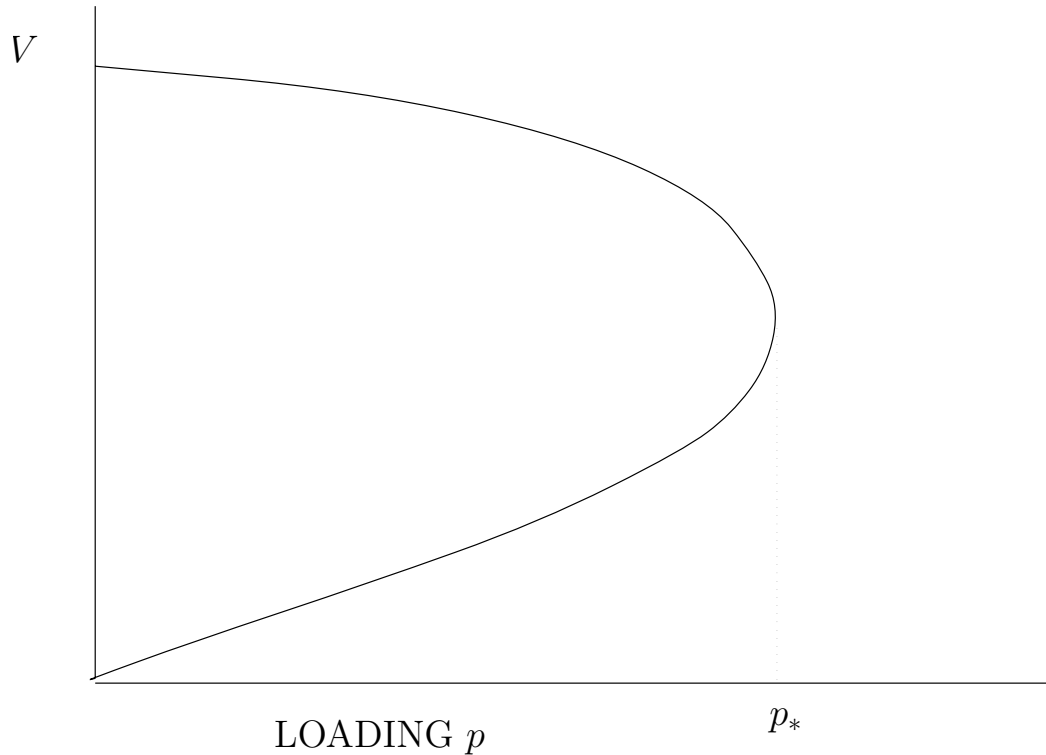


Figure 2.4-2. Bifurcation diagram showing one state versus parameter  $p$ .

which can alter the stability of the high and low voltage equilibria. A description of these bifurcations and their effects in the stability of the equilibrium points are discussed in the appendices.) The stability of the high voltage equilibrium ensures that as the loading is slowly increased from zero, the system state will track the high voltage equilibrium until the bifurcation occurs.

Since the system has two states  $V$  and  $\delta$ , a more complete picture in Figure 2.4-3 shows the variation of both  $\delta$  and  $V$  of the equilibrium solution as loading increases. The lower angle solution for  $\delta$  corresponds to the stable high voltage solution. The noses of the two curves signal the same event of the stable and unstable equilibria coalescing and therefore the noses occur at the same loading  $p^*$ .

### 2.4.3 Simple Power System Example (Dynamics)

It is also useful to visualize the state space for various loading conditions as shown in Figures 2.4-4, 2.4-5 and 2.4-6 because this allows the effect of the system dynamics to be seen. The coordinates for the state space are the states  $V$  and  $\delta$ .

Figure 2.4-4 shows both equilibria at a moderate loading. The arrows indicate the system dynamics or transients. For example, if the state is slightly perturbed in any direction from the high voltage, stable equilibrium, the arrows show that the



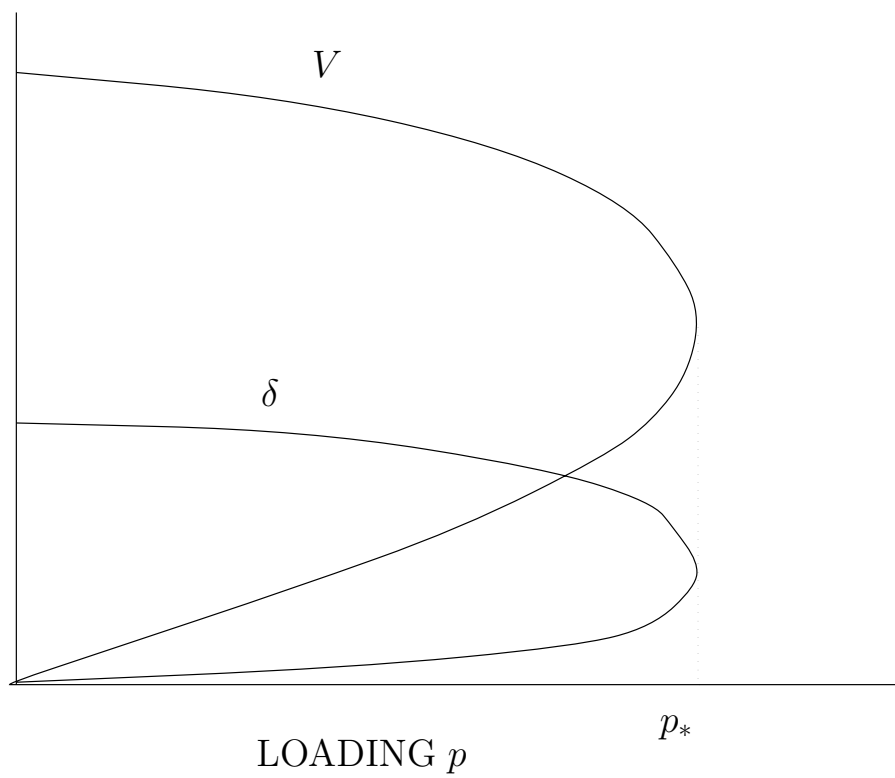


Figure 2.4-3. Bifurcation diagram showing two states versus parameter  $p$ .

state will move back to the stable equilibrium. On the other hand, almost all slight perturbations from the low voltage unstable equilibrium result in the state moving dynamically away from the unstable equilibrium.

Figure 2.4-5 shows the equilibria coalesced into one equilibrium at the critical loading  $p^*$  at bifurcation. The arrows show that this equilibrium is unstable (that is, some of the arrows point away from the equilibrium so that the usual small, random perturbations in the state will inevitably lead to instability). Moreover, the unstable dynamics tend to move the state along the thick curve. Movement along the thick curve in Figure 2.4-5 implies that the voltage magnitude  $V$  declines monotonically and the angle  $\delta$  increases. This dynamic movement is an explanation and mechanism for the dynamic fall in voltages in voltage collapse [23].

Before bifurcation, the system state tracks a stable equilibrium as the loading varies slowly. Therefore static equations can be used to follow the operating point (assuming that the solution of the static equations found is indeed the stable equilibrium). At bifurcation, the equilibrium becomes unstable and the resulting transient voltage collapse requires a dynamic model. Thus, to understand voltage collapse, system dynamics must be considered.

In some fault situations the power system can have a loading greater than the bifurcation loading. In this case there is no operating equilibrium and the system dynamics are as shown in Figure 2.4-6. The voltage would dynamically collapse following the arrows in Figure 2.4-6.

The assumption of slow parameter variation means that the parameters vary slowly with respect to the system dynamics. For example, before bifurcation when the system state is tracking the stable equilibrium, the system dynamics act more quickly to restore the operating equilibrium than the parameter variations do to change the operating equilibrium.

#### 2.4.4 Eigenvalues at a Saddle-node Bifurcation

Consider the system Jacobian evaluated at a stable equilibrium. Note that the system Jacobian of a dynamic power system model typically differs from the power flow Jacobian. However, as discussed in Section 2.4.8, static power system models and the Jacobians of these static models do suffice for some useful saddle-node bifurcation computations.

If the system Jacobian is asymptotically stable (the usual case), all eigenvalues have negative real parts. What happens as loading increases slowly to the critical loading is that one of the system Jacobian eigenvalues approaches zero from the left in the complex plane. The bifurcation occurs when the eigenvalue is zero. The main use of the system Jacobian is that it determines the stability of the system linearized about an equilibrium. For this to make sense, the equilibrium must exist. If the loading is increased past the critical loading there is no equilibrium nearby, and this use of Jacobians makes no sense.

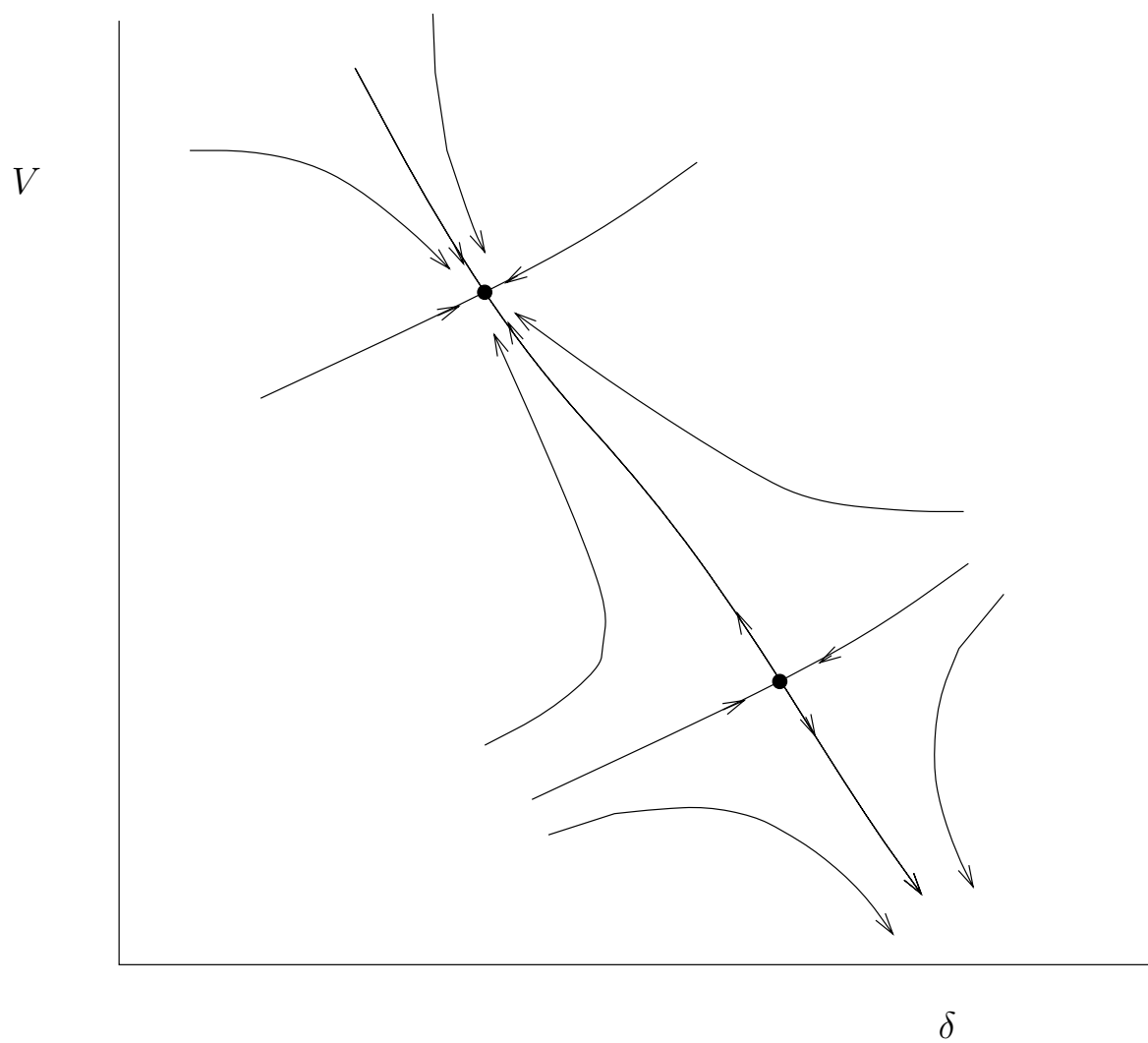


Figure 2.4-4. State space at moderate loading.

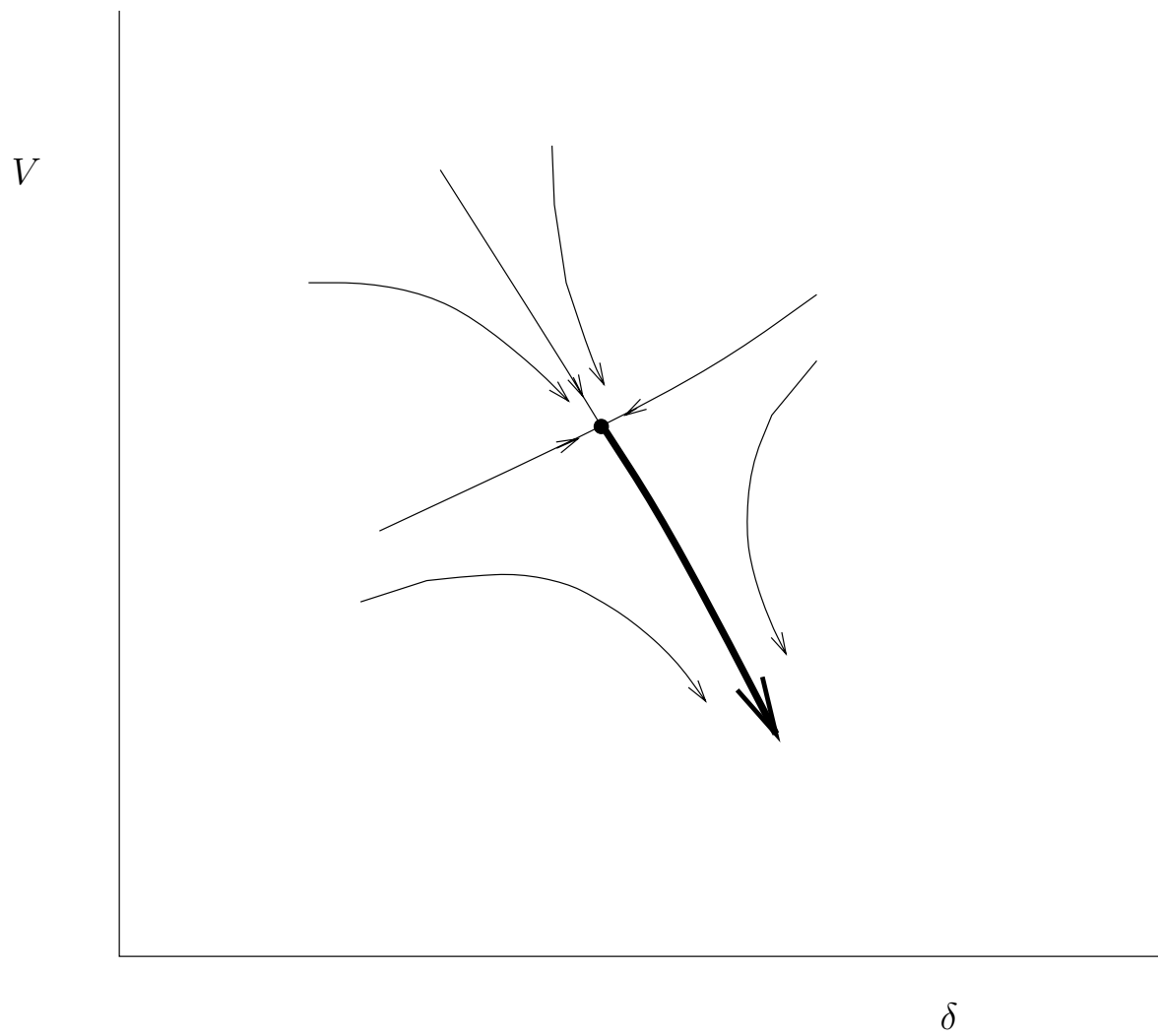


Figure 2.4-5. State space at saddle-node bifurcation.

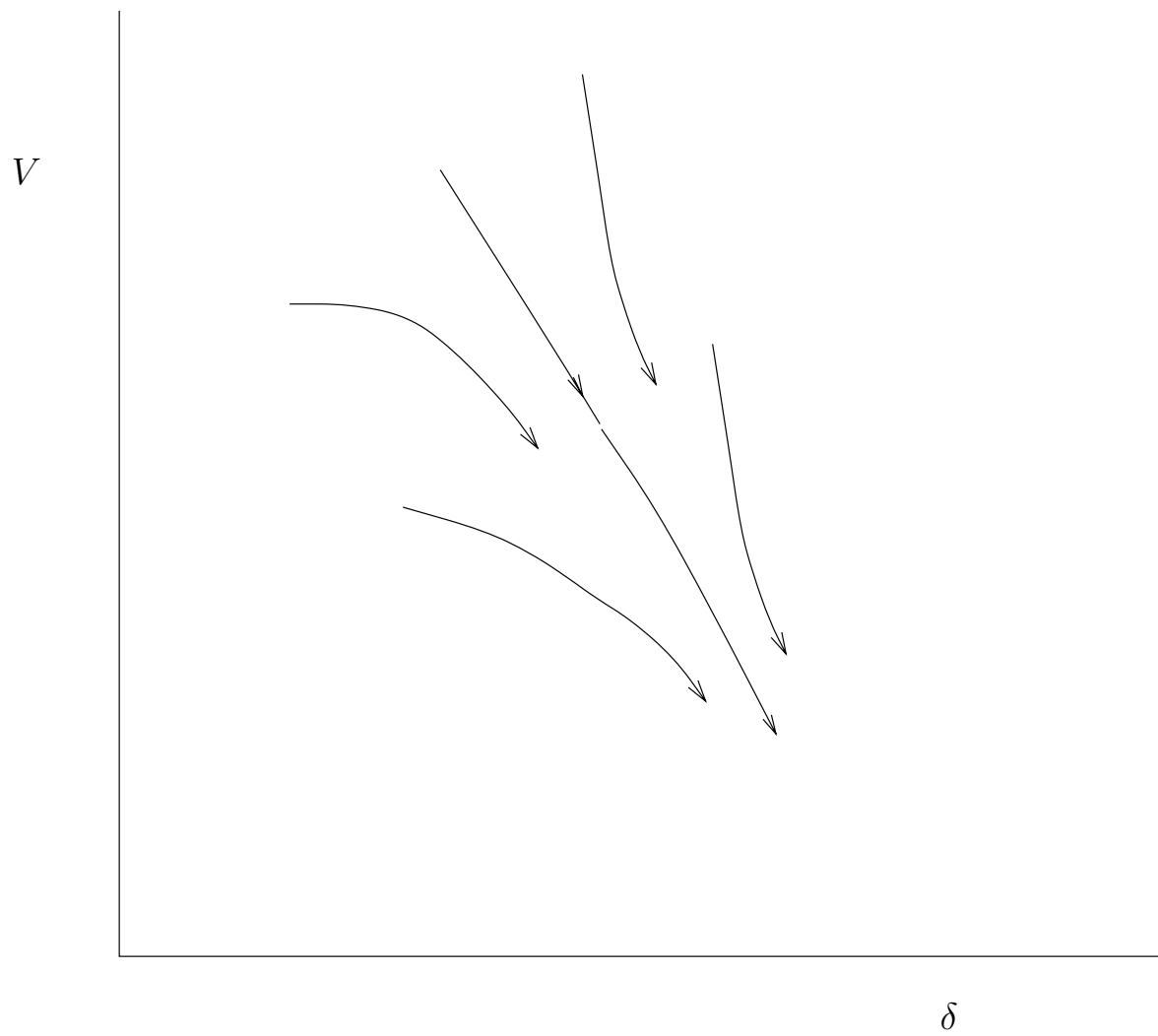


Figure 2.4-6. State space after saddle-node bifurcation.

### 2.4.5 Attributes of a Saddle-node Bifurcation

There are several useful indications of a saddle-node bifurcation. All the following conditions occur at a saddle-node bifurcation and can be used to characterize or detect saddle-node bifurcations:

- (1) Two equilibria coalesce. One of these equilibria must be unstable.
- (2) The sensitivity with respect to the loading parameter of a typical state variable is infinite. This follows from the infinite slope of the bifurcation diagram at the nose as shown in Figure 2.4-3.
- (3) The system Jacobian has a zero eigenvalue.
- (4) The system Jacobian has a zero singular value.
- (5) The dynamics of the collapse at the bifurcation are such that states change monotonically and the rate of collapse is at first slow and then fast. The typical time history predicted by the theory is shown in Figure 2.4-7.

### 2.4.6 Parameter Space

It is useful to visualize the parameter space when there are a few parameters as a guide to imagining the case of many parameters. Figure 2.4-8 shows the parameter space when the real powers consumed by two loads are chosen as parameters. The power system is operable in the unshaded region because there is a stable equilibrium corresponding to real powers in the unshaded region. The shaded region contains real power loads for which there is no equilibrium and the power system is not operable. Separating the two regions is the curve of critical loadings at which there is a saddle-node bifurcation. The curve is the set of parameters at which there is a bifurcation and is called the *bifurcation set*. Starting from  $p^0$  and stressing the system along direction  $d$ , the system finally reaches the bifurcation set at  $p^*$  where it loses equilibrium.

If the power system is operating at a loading in the unshaded region, then avoiding bifurcation and voltage collapse can be viewed as the geometric problem of ensuring that the system loading does not come close to the bifurcation set.

### 2.4.7 Many States and Parameters

The simple example discussed so far shows the essence of a typical saddle-node bifurcation in a large power system. However, there are many states and parameters involved in the bifurcation of the large power system.

Suppose that there are 500 independently varying loading parameters. Then the parameter space has 500 dimensions and the bifurcation set is a hypersurface of 499 dimensions which bounds the operable region of parameter space. It is impossible to visualize such a high dimensional set, but geometrical calculations of the proximity

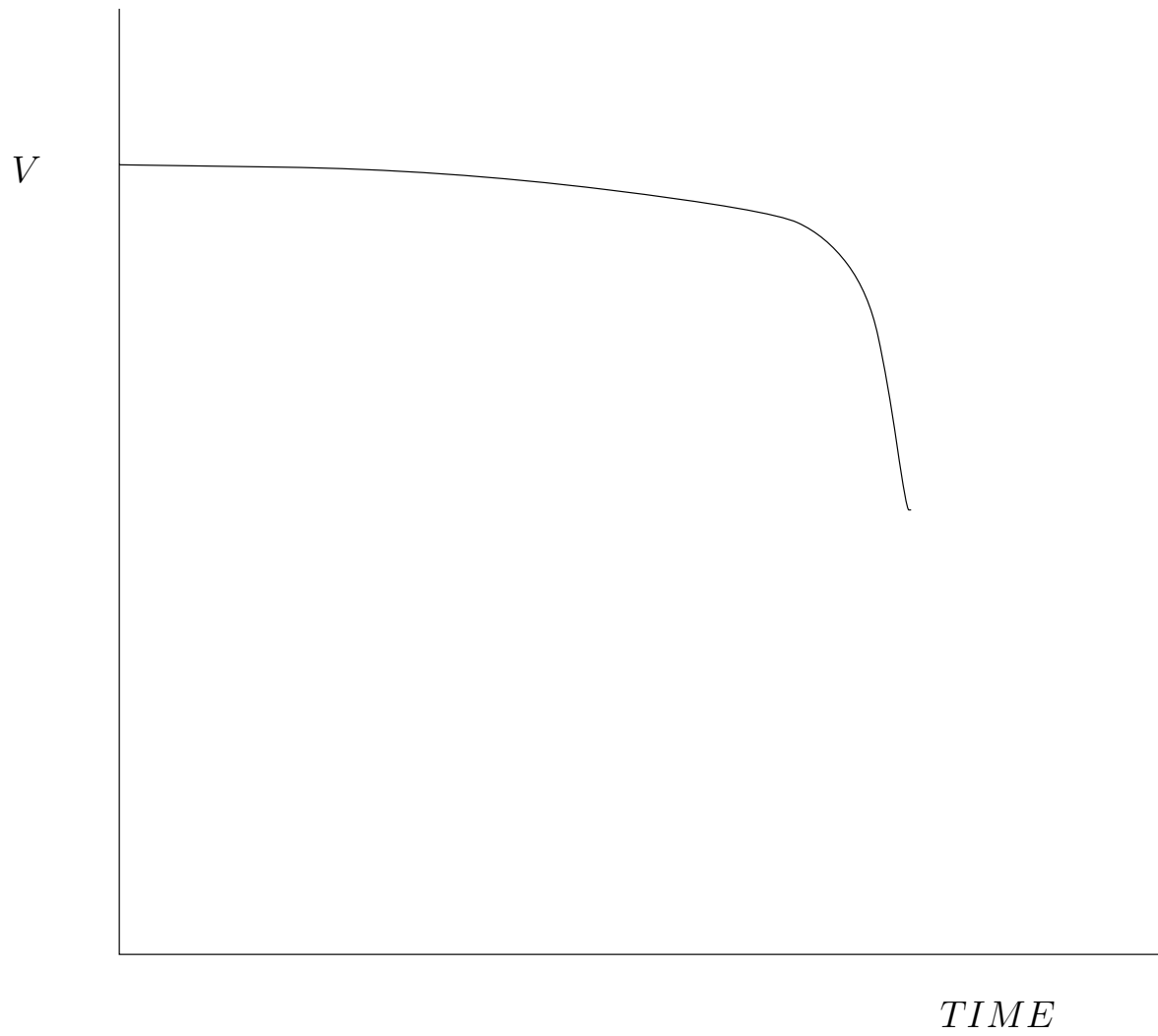


Figure 2.4-7. Time history of voltage collapse at saddle-node bifurcation.

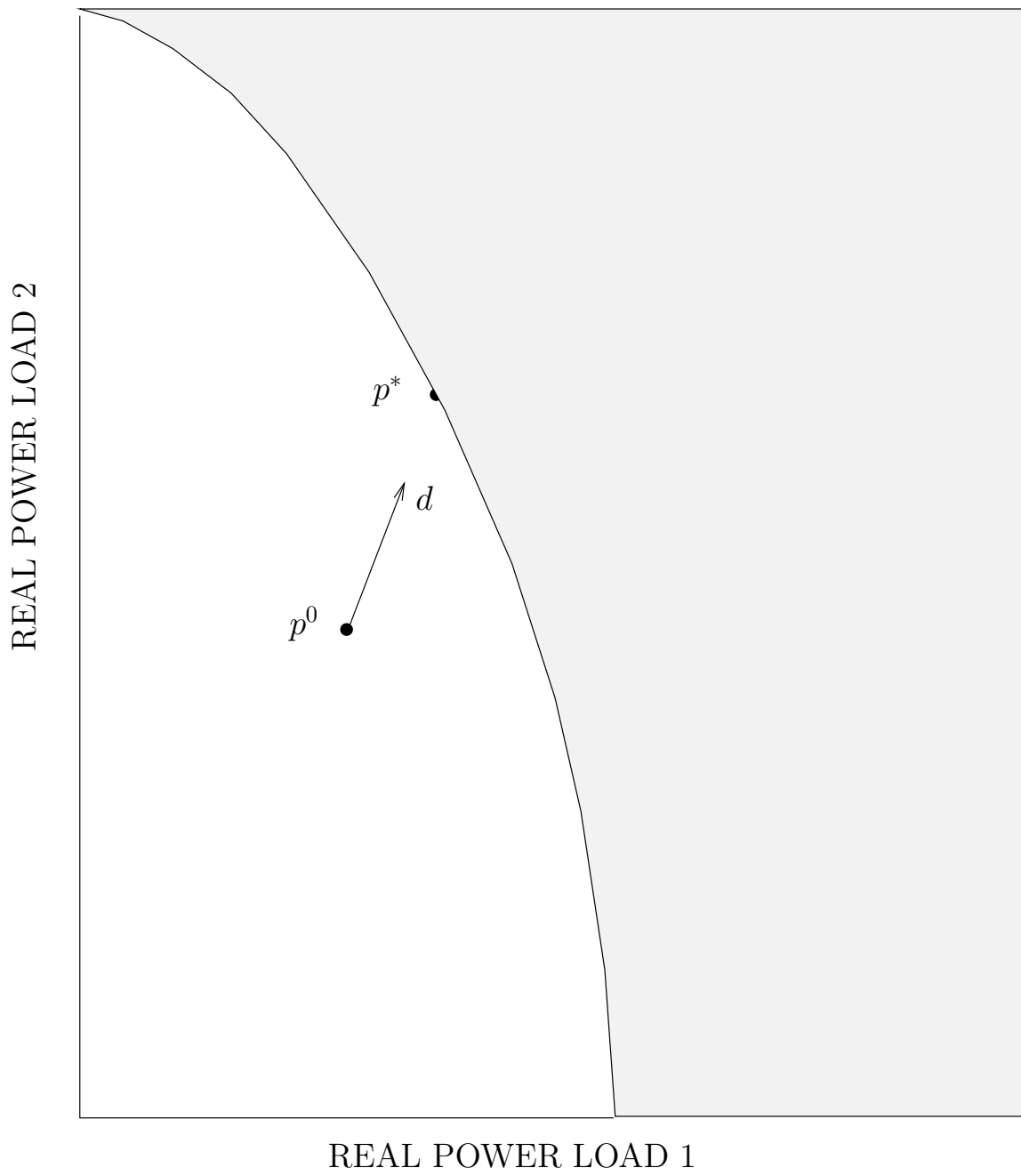


Figure 2.4-8. Load power parameter space.



of the current loading to the bifurcation set can still be done and used to help avoid bifurcation and voltage collapse.

In the state space the relative participation of state variables in the voltage collapse can be computed. (It is given by the components of the right eigenvector corresponding to the zero eigenvalue of the system Jacobian evaluated at the bifurcation. Note that this right eigenvector coincides with the right singular vector corresponding to the zero singular value of the corresponding system Jacobian.) This is useful in identifying the area of the power system in which the collapse is concentrated. It is also possible to evaluate the most effective controls or parameters to avoid the bifurcation [31] (these computations use the corresponding left eigenvector of the system Jacobian). Thus, computations related to the bifurcation can supply useful engineering information.

#### 2.4.8 Modeling Requirements for Saddle-node Bifurcations

The understanding of saddle-node bifurcation requires a dynamic model in order to explain why the voltages fall dynamically. However, some computations concerning saddle-node bifurcations require only a static model.

If a dynamic model is required, the power system is modeled by a set of differential equations with a slowly changing parameter. Differential-algebraic equations are a valid replacement for the differential equations if the algebraic equations are assumed to be enforced by underlying dynamics which are both fast and stable.

If a static model is required, the equilibrium of the power system is modeled by a set of algebraic equations with a slowly varying parameter. It is valid, but not essential, to obtain the algebraic equations by setting the right hand sides of differential or differential-algebraic equations to zero. Computations which only require static models are advantageous because the results do not require load dynamics and other dynamics to be known. When using static models to obtain practical results, there is a caveat that there must be a way of identifying the stable operating equilibrium of the power system. In principle, this requires a dynamic model, but the stable operating point is often known by observing the real power system, or by experience, or by knowing the stable operating equilibrium at lower loading and tracking this equilibrium by gradually increasing the loading.

The following computations associated with saddle-node bifurcations require dynamic models:

- (1) Predicting the outcome of the dynamic collapse.
- (2) Any problem involving significant step changes in states or parameters (see Section 2.5).
- (3) Computations involving eigenvalues or singular values away from the bifurcation.

The following computations associated with saddle-node bifurcations only require static models [7, 26]:

- (1) Finding the bifurcation.
- (2) Computations involving the distance to bifurcation in parameter space.
- (3) Predicting the initial direction of the dynamic collapse and the states initially participating in the dynamic collapse.
- (4) Predicting which buses have the lowest voltages before the collapse.

Two cautions about modeling dynamic collapses should be made. First, the results are only as good as the model assumed for the power system. For example, the simple dynamical model assumed in Section 2.4.3 would require elaboration of the load and generator models to be realistic. Fortunately, the qualitative features of a saddle-node bifurcation do not depend on the particular model so that in some sense all saddle node bifurcations that occur, even in different models, are similar. However, the quantitative features of a saddle-node bifurcation, such as the values of state and parameters at which it occurs and the extent to which states participate in the collapse, are usually of vital interest to engineers and these can depend heavily on the form and constants assumed for the power system model. The second caution concerns the range of validity of power system models. For example, if voltage magnitudes fall sufficiently, then system protections may operate to change the system and this must be regarded as changing the system model. Load models may only be validated near nominal voltage levels and are often questionable at lower voltages. Also a very fast drop in voltages invalidates the quasistationary phasor assumptions of some power system models as explained in Appendix 2.B.

### **2.4.9 Evidence Linking Saddle-node Bifurcations with Voltage Collapse**

Consider a power system with a slowly increasing load which increases indefinitely. Eventually, the generation and transmission will be unable to support the load in steady state and the operating equilibrium will be lost. Under these assumptions, saddle-node bifurcation theory applies and explains how the operating equilibrium disappears and predicts that in the ensuing transient there will be an initially slow but accelerating monotonic decline in the system states.

However, some voltage collapses involve more quickly changing loads, large disturbances and discrete events. In these cases, the assumptions required for analysis with saddle-node bifurcations may not be strictly satisfied. It still may be possible to analyze part of the sequence of events using saddle-node bifurcations, as, for example, when a large disturbance weakens the system and then an increase in load causes the operating equilibrium to disappear. On the other hand, a large disturbance can cause the operating equilibrium to disappear suddenly without passing gradually through a saddle-node bifurcation. That is, if the large disturbance had artificially been made to happen slowly, the system would have passed through a saddle-node bifurcation. The effect of the large disturbance is that the dynamics changes suddenly from that of Figure 2.4-4 to that of Figure 2.4-6. This phenomenon is described in much more

detail in Section 2.5. In this case one might guess that since the system was quite close to a saddle-node bifurcation, that the dynamics after the operating equilibrium was lost should be quite similar to those at the saddle-node bifurcation. That is, there should be an initially slow but accelerating monotonic decline in the system states.

Traces of voltage collapse incidents typically contain an initially slow but accelerating monotonic decline in the system states. Indeed, the form of the collapse shown in Figure 2.4-7 is often prominent in traces of voltage collapse. Other events are quite often superimposed on this decline. Of course, the decline does end in practice, due to a variety of system protections acting (e.g., undervoltage relays). Saddle-node bifurcation is best thought of as a useful idealization that helps to explain the form of the collapse when the operating equilibrium is lost. One good way to test or confirm the explanatory power of the saddle-node bifurcation theory in a practical context is to look through traces of voltage collapse events such as in [40] to check for portions of the trace which resemble the initially slow but accelerating monotonic decline predicted or suggested by bifurcation theory.

#### 2.4.10 Common Points of Confusion

This subsection addresses some common pitfalls which are known hazards for the unwary.

**Parameter space versus state space:** It is important when applying bifurcations to always keep in mind which variables have been chosen to be states and which variables have been chosen to be parameters. (Recall that these choices are made as part of specifying the power system model.) Difficulties with properly identifying states and parameters in a system model is the leading cause of confusion when bifurcation theory is applied.

**Nose curves are not always bifurcation diagrams:** If one draws a nose curve with a state variable on the vertical axis and a parameter on the horizontal axis, then this nose curve is a bifurcation diagram. It follows that the nose will correspond to a saddle-node bifurcation and typically a voltage collapse of the assumed power system model. For example, a nose curve of a bus voltage against a load bus power is a bifurcation diagram *if* the load bus power is a parameter of the power system model. However, it happens quite often that the power system model is chosen to have a parameter which is not the load power. In this case, as the parameter is varied, the load power and the bus voltage still change and the nose curve of a bus voltage against the load bus power is still nose shaped, but it is not a bifurcation diagram. In particular, a saddle bifurcation can possibly occur, but it can occur anywhere on the curve and is not related to the nose. However, the nose is of course a maximum power point. (There is nothing wrong with such a curve as long as no one mistakes it for a bifurcation diagram.) Redrawing the curve so that bus voltage is plotted against the true parameter will produce a bifurcation diagram, and if the bifurcation diagram has a nose, it will correspond to a saddle-node bifurcation. Examples 1 and 2 in Section 2.10.1 show that changing the parameter from load power to another parameter move the bifurcation away from the maximum power point.

**Infinite sensitivity at the nose does not explain voltage collapse:** It is true that all system states become infinitely sensitive to general parameter variations at a saddle-node bifurcation. However, it does not follow from this infinite sensitivity that a parameter variation will cause a large change in the state. To understand this, look at the nose curve of a bifurcation diagram such as Figure 2.4-2. The infinite sensitivity corresponds to a vertical tangent at the nose. However, it is clear that the *steady state voltage* as described by the nose curve does not change much near the nose of the curve, despite its large *rate of change* near the nose. When the parameter increases through the bifurcation, the operating point disappears and dynamics drive the collapse as described in Section 2.4.3. The collapse cannot be understood by examining the steady state nose curve alone and is not caused by the infinite sensitivity at the nose; the correct explanation of the collapse relies on dynamics.

## 2.5 LARGE DISTURBANCES AND LIMITS

Many voltage collapse incidents have resulted from large disturbances such as the loss of transmission or generation equipment (often, but not always combined with high loading). Contingency evaluation is the heart of system security assessment at all levels of decision. Moreover, generators and SVCs reaching reactive power limits and tap changing transformers reaching tap limits are important in voltage collapse. It is thus essential to understand voltage instability mechanisms triggered by large disturbances and limits [15, 60, 61, 63].

### 2.5.1 Disturbances

A large disturbance such as the loss of transmission or generation equipment can be modeled by a discrete change in the system equations or parameters. For example, the loss of a transmission line can be modeled either by removing the line from the system equations or by making the line series admittance and shunt capacitances zero.

Suppose that the power system is initially operating at a stable equilibrium and a large disturbance occurs. After the disturbance, there may be a new equilibrium corresponding to the previous stable equilibrium. Because the disturbance causes the equations to change, the new equilibrium will generally be in a different position than the previous stable equilibrium. It is also possible that there is no new equilibrium corresponding to the previous stable equilibrium.

Just after the disturbance, the system state is at the position of the previous stable equilibrium, which is generally no longer an equilibrium, and a transient will occur. The initial condition of the transient is the pre-disturbance stable equilibrium. There are several possible outcomes for this transient:

1. The state restabilizes at the new equilibrium. This possibility is the routine response of the power system to a disturbance in which stability is maintained. However, the disturbance causes the *margin* of stability to change discretely.

In particular, line or generation outages can cause the margin of stability to be abruptly reduced.

2. There is no new equilibrium and the transient continues as a voltage collapse. In some sense, this possibility is the large disturbance equivalent of the loss of stability when parameters change slowly and stability is lost when the equilibrium disappears in a saddle-node bifurcation (see Section 2.4). When the parameters vary slowly, the system starts with operation at a stable equilibrium, the equilibrium becomes less stable and then finally disappears in a saddle-node bifurcation. Further slow changes in the parameter would further modify the system dynamics. These changes to the state space in the slowly varying parameter case are illustrated in Figures 2.4-4-2.4-6 in Section 2.4. In the large disturbance case, the system moves abruptly from operation at a stable equilibrium (Figure 2.4-4) to the dynamics after the saddle bifurcation has occurred (Figure 2.4-6). The effect of the large disturbance can also be visualized in the loading parameter space: In Figure 2.5-1, the loading parameters keep their pre-disturbance values  $p^0$  but the bifurcation set moves so that  $p^0$  falls outside the bifurcation set, which means that the system has lost its equilibrium.
3. The transient diverges from the new equilibrium. This can occur for two reasons:
  - (a) The disturbance causes the new equilibrium to be unstable.
  - (b) The new equilibrium is stable but the initial system state just after the disturbance is sufficiently far from the new equilibrium that the transient does not return to the new equilibrium. This can be expressed as “the initial state is not attracted to the new equilibrium” or “the initial state is not in the basin of attraction of the new equilibrium”. This instability mechanism is further discussed in Section 2.7.

## 2.5.2 Limits

Reactive power limits on generators and the tap limits on tap changing transformers have a significant effect on voltage collapse. In general, the system equations change nonsmoothly when these limits are encountered. In some cases the effect of the limit is that one of the system state variables become constant or interchanges with a constant. For example, if tap changing transformers are modeled by first order lag differential equations in the tap ratio, then encountering the maximum tap limit has the effect of changing the tap ratio from a state variable to a constant. It is usual for the operating equilibrium to remain fixed, but the stability margin will change discretely and it is possible for the new equilibrium to be unstable and to cause a voltage collapse.

Various approaches to modeling and analyzing the effects of limits on voltage collapse have been proposed [60, 61, 24, 55, 13, 17, 18, 59]. Some of the modeling and analysis issues are under discussion in the research community. Here we present an elementary explanation of the effect of generator power limits and then briefly survey

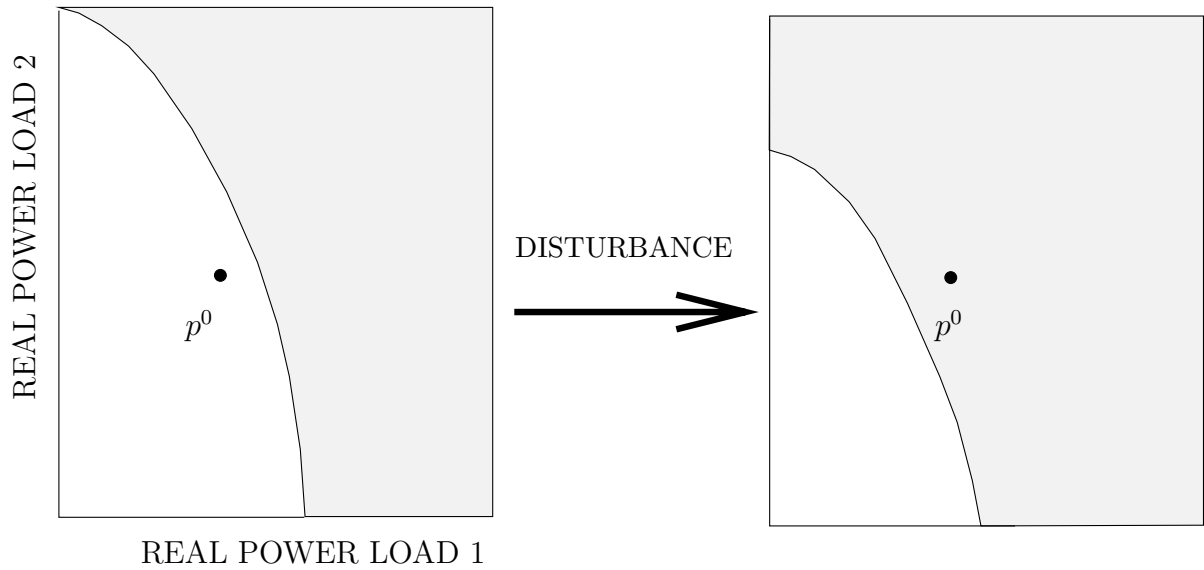


Figure 2.5-1. A disturbance moves the bifurcation set.

some of these approaches. (Generator reactive power limits are more fully discussed in Section 2.3.)

We examine PV curves when a generator reactive power limit is encountered. As shown in Figure 2.5-2, there is a PV curve derived from the power system equations when generator reactive power limit is off and another PV curve derived from the power system equations when the generator reactive power limit is on. The vertical axis of Figure 2.5-2 shows a load voltage, not the voltage at the generator. The parameter on the horizontal axis is the system loading so that each PV curve is also a bifurcation diagram. For simplicity we assume that the top portion of each PV curve is stable and the bottom portion of each PV curve is unstable.

Suppose that the power system is initially at position A on the PV curve with the limit off. As the loading increases, the load voltage falls and the generator reactive power output increases. The generator reaches its reactive power limit at point B and the application of this limit changes the power system equations and the PV curve to the limited case. The equilibrium remains fixed and in particular the load voltage remains fixed at point B. Since the equilibrium remains on the top portion of the PV curve with the limit on, the equilibrium remains stable. However, as expected, the margin of stability is reduced by the reactive power limit since the nose of the PV curve with the limit on is closer to point B. If the load increases further, the equilibrium will move along the PV curve with the limit on until the voltage collapses at the nose due to a saddle node bifurcation.

It is also possible for the equilibrium to become immediately unstable when the reactive power limit is applied as shown in Figure 2.5-3. Figure 2.5-3 is similar to Figure 2.5-2, except that when the limit is applied, the equilibrium ends up on the

bottom portion of the PV curve with the limit on and so is unstable. Since the equilibrium is unstable, voltage collapse ensues. Point B in Figure 2.5-3 when the limit is encountered is the practical stability limit of loading in this power system. A numerical example of this instability phenomenon is given in section 2.11. This instability phenomenon has been found to be the applicable limit of stability in a number of practical cases. Terminologies for the instability include “immediate instability”, “limit-induced bifurcation” and “breaking point”. The phenomenon often occurs at high loading quite close to the saddle node bifurcation.

Now we briefly discuss some of the modeling and analysis approaches that handle generator reactive power limits. Note that continuation and midterm and time domain analysis software routinely takes account of generator limits in order to correctly estimate the system loadability or trajectory with respect to voltage collapse. The approaches sketched below aim to develop analytic frameworks to handle generator limits.

If a generator with no reactive power limit is simply represented as a PV bus, then a crude way to represent the effect of the reactive power limit is to change the PV bus into a PQ bus. In this change, the reactive power balance equation is the same, but the constant  $V$  becomes a state variable and the state variable  $Q$  becomes a constant. The system equilibrium does not move.

To calculate the loadability as constrained by the limit instability phenomenon, [17, 18] model the generator excitation system using inequality constraints and formulate maximizing loadability as an optimization problem. Techniques from optimization theory handle the inequality constraints so as to find either the saddle node bifurcation (point B in Figure 2.5-2) or the loadability limit caused by the generator limit (point B in Figure 2.5-3). [59] examines the properties of the loadability surface due to the generator limit.

Detailed models of the generator excitation and voltage control system represent the dynamics of the excitation and voltage control systems and the limiters in these control systems (e.g. [55]). In the case of windup limits, the output of the limiter changes to a constant when the limit is encountered and this changes the right hand side of the power system equations in a nonsmooth way. In the case of non-windup limits, the state variable is constrained by an inequality constraint. The effect of the inequality constraint is to bound the state space and the corresponding equality constraint is a boundary or edge of the state space. When the limit is encountered, the inequality becomes an equality and the limited state variable becomes a constant. In the limited system, the state space dimension is reduced by one and the system trajectories are confined to the boundary of the state space. The limit causes a nonsmooth change in the system and the stability of equilibria changes discretely when the limit is encountered. [55] analyzes the non-windup limit case in which the equilibrium becomes unstable as a “limit-induced bifurcation” in which a stable equilibrium of the unlimited system merges in a nonsmooth way with an unstable equilibrium of the limited system at the boundary of the state space.

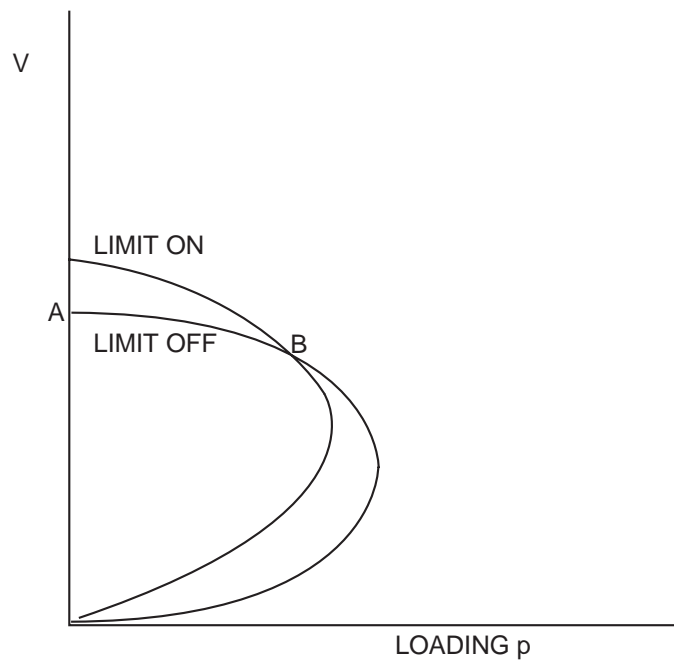


Figure 2.5-2. Equilibrium B remaining stable when a reactive power limit is encountered.

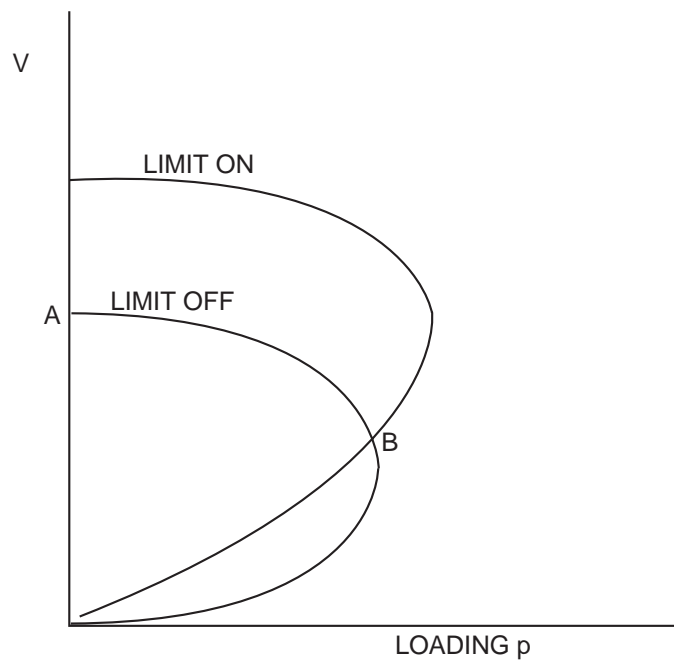


Figure 2.5-3. Equilibrium B becoming immediately unstable when a reactive power limit is encountered.



## 2.6 FAST AND SLOW TIME SCALES

### 2.6.1 Time scale Decomposition

The fast-slow time scale decomposition is carried out using the analysis known as singular perturbations [33, 43]. The standard model of a two time scale system is:

$$\begin{aligned}\dot{x} &= f(x, y) \\ \epsilon \dot{y} &= g(x, y)\end{aligned}$$

where  $x$  is the “slow” state vector,  $y$  is the “fast” state vector and  $\epsilon$  is a small number. The first approximation to a time scale decomposition is the assumption  $\epsilon \rightarrow 0$ , in which case the second equation becomes algebraic corresponding to equilibrium conditions for the fast variables. Therefore, the slow component  $y_s$  of the fast state variables  $y$  can be evaluated as a function of the slow variables  $x_s$ . Thus the approximate *slow* subsystem is defined by the following differential-algebraic equations:

$$\begin{aligned}\dot{x}_s &= f(x_s, y_s) \\ 0 &= g(x_s, y_s)\end{aligned}$$

This is the quasi steady-state representation of a two time scale system. Further approximation is possible using an expansion in powers of  $\epsilon$ , but this is beyond the scope of this brief presentation.

We illustrate the quasi steady state approximation in Figure 2.6-1 in the case of a two state system with one fast variable  $y$  and one slow variable  $x$ . The equilibrium condition  $g = 0$  defines a curve in the  $xy$  plane, which we call the fast dynamics equilibrium manifold (in this two-dimensional system, the curve is called a manifold so that the terminology applies to multivariable systems as well). When  $\epsilon$  is very small, this is a good approximation of the “slow manifold” of the two time scale system.

The equilibria of the full system are the points on the manifold defined by  $g = 0$ , for which also  $f = 0$ . In Figure 2.6-1 two such equilibria are shown, one stable and one unstable. Each point  $x_s, y_s$  of the fast dynamics equilibrium manifold is the equilibrium point of a fast subsystem defined as:

$$\epsilon \dot{y}_f = g(x_s, y_s + y_f) \tag{2.1}$$

where  $y_f = y - y_s$  is the fast component of  $y$ . The time scale decomposition is valid only when the fast subsystem defined above is stable at its equilibrium point  $y_f = 0$ .

With this assumption, the behavior of the two time scale system can be approximated as follows: For an initial condition outside the fast dynamics equilibrium manifold a fast transient is excited at first. One common possibility is that the fast transient acts to put the system state onto the fast dynamics equilibrium manifold before the slow variables have time to change considerably. For example, an initial condition such as point A on Figure 2.6-1 leads to a fast downwards transient to the

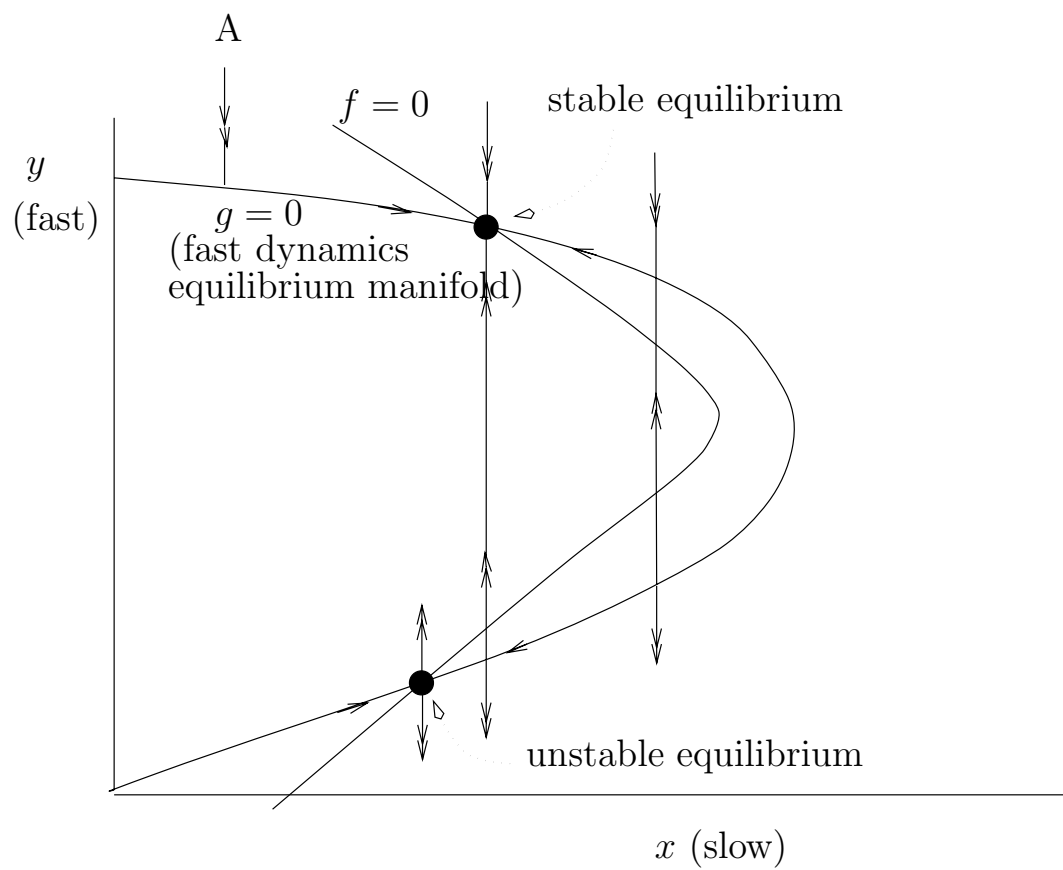


Figure 2.6-1. System with fast and slow time scales.

upper portion of the fast dynamics equilibrium manifold. Following this fast transient, the system will remain on the fast dynamics equilibrium manifold and it will slowly move towards the stable equilibrium.

When large disturbances are considered, the existence of a stable fast dynamics equilibrium after a disturbance is not the only requirement for a valid time scale decomposition; the pre-disturbance state of the system must also belong to the region of attraction of the post disturbance stable equilibrium of the fast dynamics. For the system of Figure 2.6-1 the region of attraction of the stable part of the fast dynamics equilibrium manifold is easily determined; all initial conditions above the unstable part of the fast dynamics equilibrium manifold are attracted to the stable part. On the other hand, an initial condition lying below the unstable part of the fast dynamics equilibrium manifold initiates a collapse, even though a stable equilibrium still exists.

### 2.6.2 Saddle-node Bifurcation of Fast Dynamics

As the slow dynamics drive the system along the fast dynamics equilibrium manifold, the fast subsystem defined above changes and the fast dynamics may lose stability. If the slow dynamics are thought of as slowly varying parameters, then the instability of the fast dynamics may be understood as a bifurcation of the fast dynamics [17]. In the fast equations (2.1),  $x_s$  may be thought of as the bifurcation parameter (note that  $y_s$  depends on  $x_s$ ). (We often expect the slow dynamics to arise from the disappearance of the operating equilibrium due to a disturbance, as discussed in Section 2.5. In this case it should be noted that stability is already lost before the bifurcation of the fast dynamics in which the fast dynamics lose stability.)

Consider, for instance, a system for which the fast dynamics equilibrium manifold is the nose curve of Figure 2.6-2. Point B is a saddle-node bifurcation of the fast dynamics. The fast subsystem is stable on the upper part of the fast dynamics equilibrium manifold and unstable on the lower part of the fast dynamics equilibrium manifold. If  $\epsilon$  is assumed sufficiently small, the fast dynamics are approximated by vertical lines moving towards stable points of the fast dynamics equilibrium manifold and away from unstable points of the fast dynamics equilibrium manifold. In this particular system, the slow dynamics are such that the slow state  $x$  always increases.

Consider now the response of the system starting from an initial point A lying above the nose curve. At first the fast dynamics will drive the system to the stable upper part of the fast dynamics equilibrium manifold. This will be a fast transient. Then the system will move slowly along the fast dynamics equilibrium manifold driven by the slow dynamics. This process can continue until point B is reached. At B, the two fast dynamics equilibria coalesce in a saddle-node bifurcation. The dynamic consequence of the bifurcation is collapse of the fast dynamics as the state follows the vertical arrows near B.

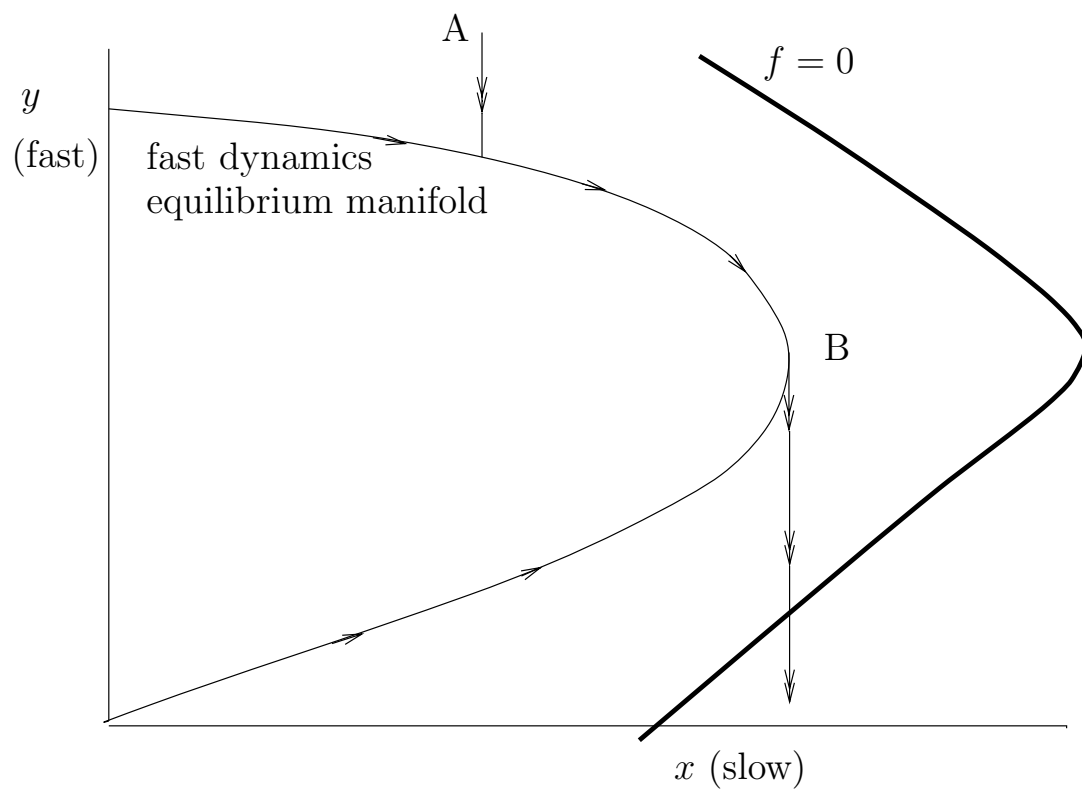


Figure 2.6-2. Bifurcations of fast dynamics equilibria.

### 2.6.3 A Typical Collapse with Large Disturbances and Two Time scales

Let us illustrate a typical collapse triggered by large disturbances and involving fast and slow dynamics. The system is initially at a stable equilibrium and the following sequence of events takes place:

- (1) A disturbance happens and the system re-stabilizes.
- (2) A second disturbance happens and the operating equilibrium is lost. (This is the large disturbance equivalent of a saddle-node bifurcation as discussed in Section 2.4.)
- (3) Due to this loss of equilibrium, a slow collapse begins and lasts for some time.
- (4) In this case, the slow collapse leads to a saddle-node bifurcation of the fast dynamics, which causes a faster collapse and hence a total system disruption.

(This chapter defines the collapse to begin with the instability (2) and to include the slow and fast dynamics of (3) and (4). Some authors prefer to identify the collapse with the fast dynamics of (4) only.)

The sequence of events can be illustrated with pictures of the functions  $f$  and  $g$  in Figure 2.6-3. The two large disturbances are represented by discrete changes in the system equations so that  $g$  becomes  $g_0, g_1, g_2$ . For simplicity we suppose that  $f$  is not affected by the disturbances so that the curve  $f = 0$  remains the same throughout. The equilibrium points of the various system equations are the intersection points of the fast dynamics equilibrium manifolds  $g_0 = 0, g_1 = 0, g_2 = 0$  with  $f = 0$ .

The initial stable equilibrium  $S_0$  is the upper intersection of  $g_0 = 0$  with  $f = 0$ . The first disturbance changes  $g_0$  to  $g_1$  and the resulting transient indicated in Figure 2.6-3 first quickly moves the state to the fast dynamics equilibrium manifold  $g_1 = 0$ , and then slowly restores the state to the new stable equilibrium  $S_1$ . Enough time is assumed to pass so that the re-stabilization at  $S_1$  is achieved. Note that the first large disturbance has reduced the margin to voltage collapse since the system is now closer to a saddle-node bifurcation.

The second large disturbance changes  $g_1$  to  $g_2$ . A fast transient quickly moves the state to the fast dynamics equilibrium manifold  $g_2 = 0$ . Since  $g_2 = 0$  has no equilibrium points, slow dynamics will move the state along  $g_2 = 0$ . In Figure 2.6-3, the state moves along  $g_2 = 0$  to the right. The system state will eventually reach a saddle-node bifurcation of the fast dynamics, and it will depart from the fast dynamics equilibrium manifold  $g_2 = 0$  with a fast transient which is a fast collapse.

The second large disturbance changing  $g_1$  to  $g_2$  is a quick change from a system with two equilibria to a system with no equilibria. If the large disturbance were instead thought of as a gradual change, the system would pass through a saddle node bifurcation at which the equilibria coalesced and disappeared as described in Section 2.4.

Now we give a more concrete example of the more general collapse above by choosing to think of the fast dynamics as the network transients and the slow dynamics

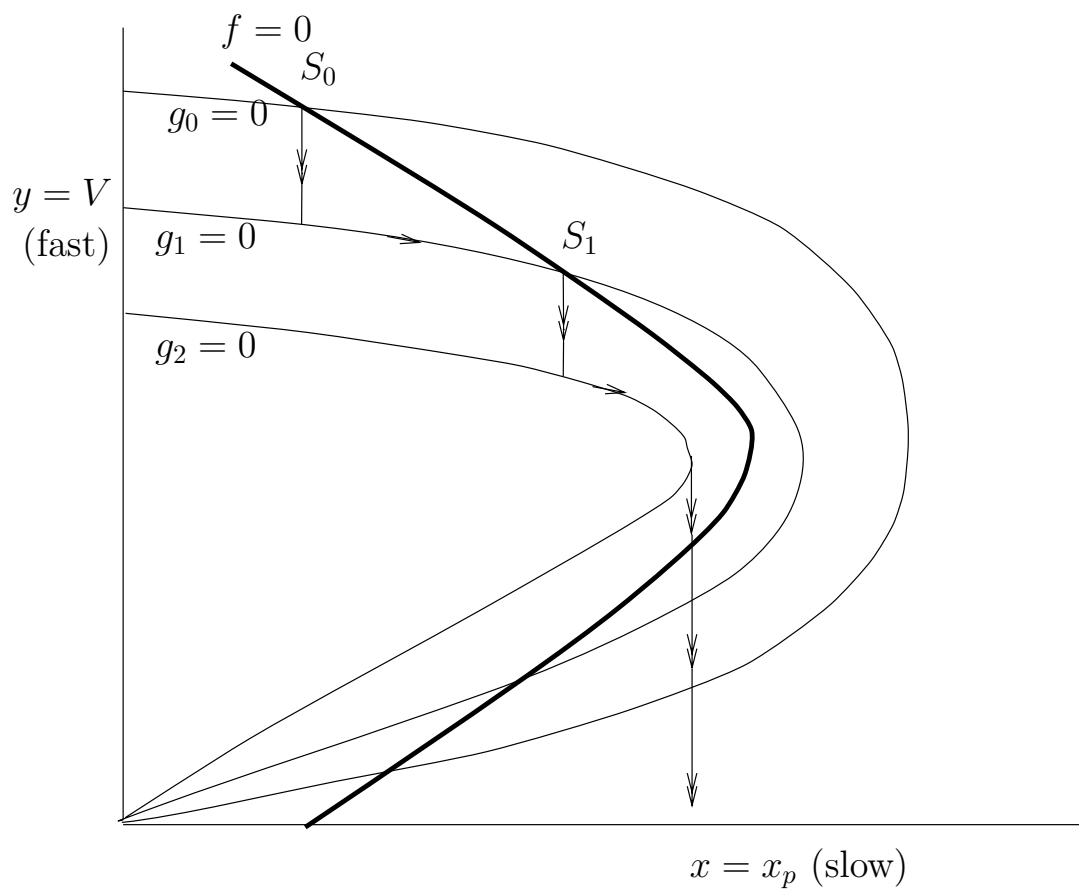


Figure 2.6-3. Time collapse with large disturbances and 2 time scales.

as the load recovery to constant power. (For simplicity, the load is assumed to be constant power in steady state.) In terms of the variables of the load model discussed in Section 2.3,  $y$  is identified as the load voltage  $V$  and  $x$  is identified as the internal load state  $x_p$ . Then the curves  $g_0 = 0$ ,  $g_1 = 0$ ,  $g_2 = 0$  represent the network capability and the large disturbances could be caused by network outages. The curve  $f = 0$  represents the constant load power in steady state.

In Figure 2.6-3, the system is presented with the slow variable  $x_p$  on the horizontal axis. Since  $x_p$  is the slowly varying variable, the saddle-node bifurcation of the fast dynamics occurs at the nose of the fast dynamics equilibrium manifold  $g_2 = 0$ . It is often useful to present the system with instantaneous real power  $P$  on the horizontal axis. This skews the diagram so that it appears as in Figure 2.6-4. In Figure 2.6-4, the fast dynamics move at angle so that typically both voltage and power drop quickly when a disturbance occurs. Also the constant power characteristic  $f = 0$  appears as a vertical line. Figures 2.6-3 and 2.6-4 present two views of the same collapse and it is useful to understand both views when reading the literature.

## 2.7 CORRECTIVE ACTIONS

Understanding and visualizing voltage collapse mechanisms suggests approaches for preventative actions to avoid voltage collapse or emergency or corrective actions to restore stability if voltage collapse begins.

### 2.7.1 Avoiding Voltage Collapse

Suppose the power system is operating at a stable equilibrium but is dangerously close to voltage collapse. What control actions will best avoid voltage collapse?

It is useful to visualize the situation in the loading parameter space. Recall from Section 2.4 that the current loading is a point in the loading parameter space and the critical loadings at which voltage collapse occurs is the bifurcation set, a hypersurface in the loading parameter space; see Figure 2.7-1.

First suppose that the power system is at the saddle-node bifurcation so the current loading is at point B on the bifurcation set in Figure 2.7-1. Changing the loading by shedding some combination of loads corresponds to moving in a particular direction in the loading parameter space. It is geometrically clear that the best direction to move away from the bifurcation set is along the vector  $N$  normal to the bifurcation set at B. Thus the normal vector  $N$  defines an optimum combination of loads to shed. If load is to be shed at only one bus, this bus can be chosen to correspond to the largest component of  $N$ . Once the bifurcation has been determined, it is straightforward to compute  $N$ . (In particular,  $N$  depends on the left eigenvector corresponding to the zero eigenvalue of the Jacobian evaluated at the bifurcation.) The normal vector  $N$  also has an important interpretation as Lagrange multipliers in an optimization formulation [14].

Suppose that the power system loading is at point A, and the margin to voltage collapse is measured along a loading increase direction as shown in Figure 2.7-1 so

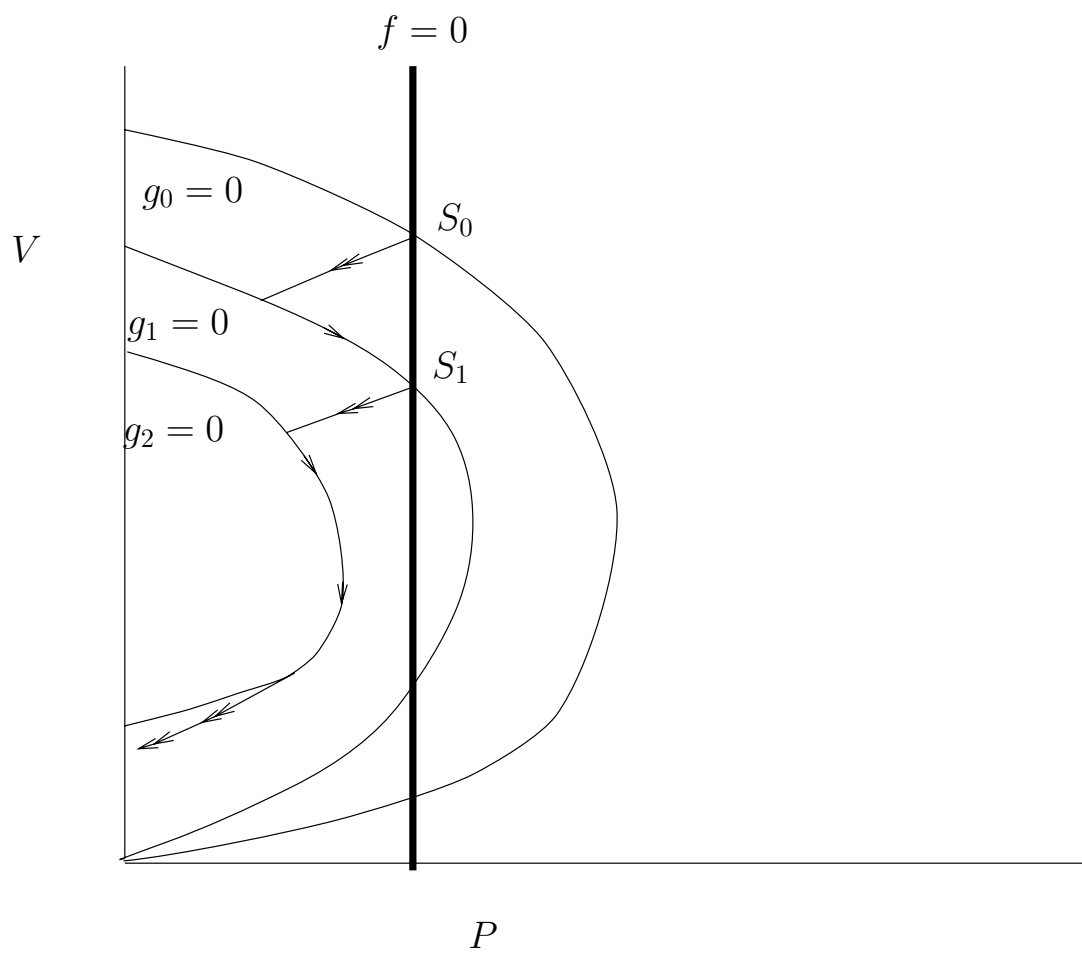


Figure 2.6-4. Another view of typical collapse.



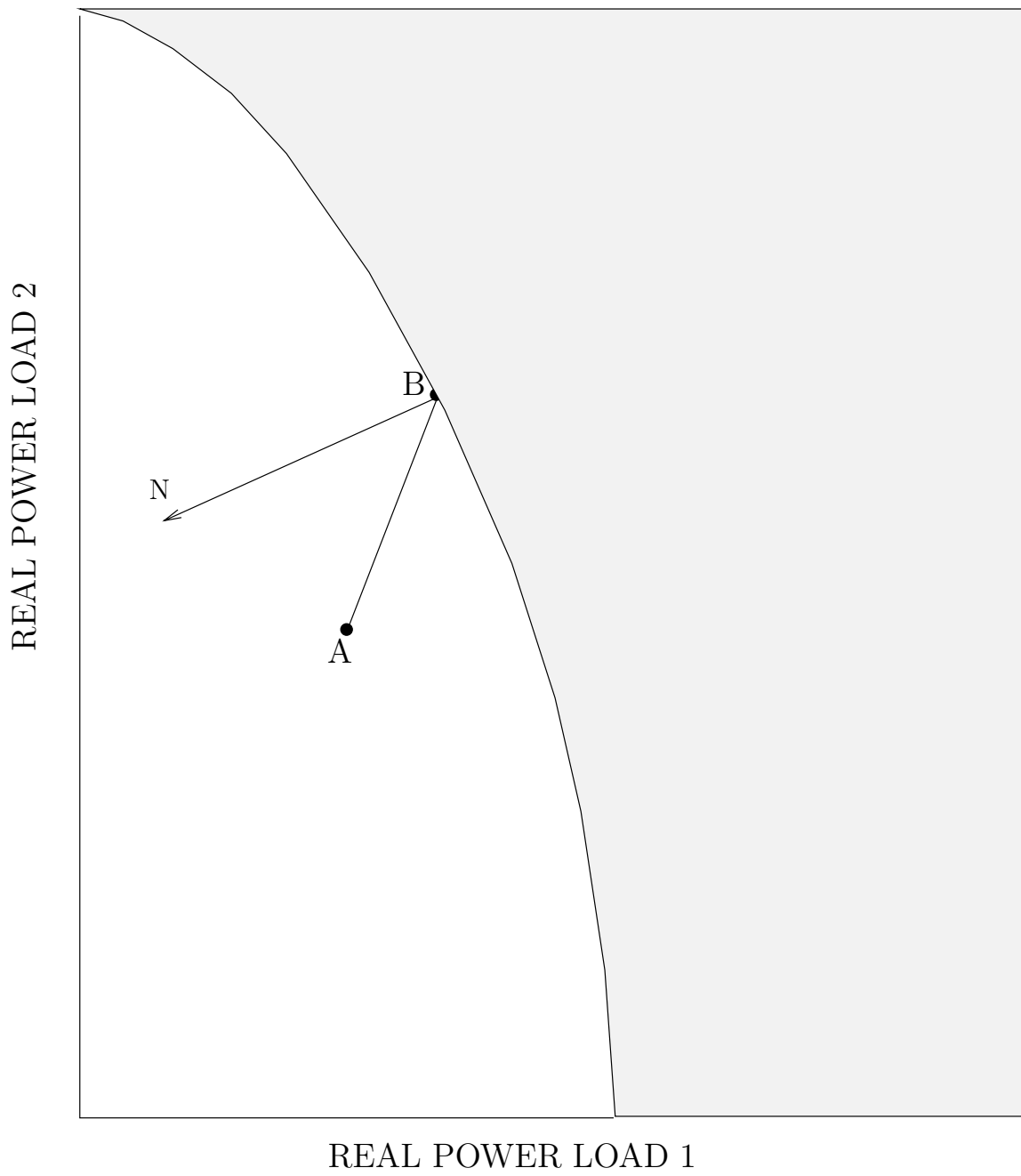


Figure 2.7-1. Corrective action in load power space.

that the margin is the length of AB. It turns out that the optimum direction to move A to maximize the margin is also given by the vector N normal to the bifurcation set at B [25] (Appendix 2.A).

These ideas lead to consider the effectiveness of changing *any* power system parameter to increase the margin to voltage collapse. This is done by adding the power system parameters to the loading parameter space and performing similar normal vector calculations [31].

Another analytical technique for determining the most effective preventative controls is to try to maintain the Jacobian at an operating point sufficiently far from singularity [37, 53]. This can be done by computing the smallest singular value of the Jacobian and its sensitivity to controls. If the smallest singular value becomes too small, then controls are selected based on the sensitivities to restore the smallest singular value to an acceptable minimum value. At the saddle-node bifurcation, the singular value approach and the normal vector approach become identical.

### 2.7.2 Emergency Actions During a Slow Dynamic Collapse

Suppose that a large disturbance has caused loss of the operating equilibrium and that slow dynamics are acting as described in Section 2.6; that is, the state moves dynamically along the fast dynamics equilibrium manifold but the saddle-node bifurcation of the fast dynamics and the fast collapse have not yet been reached. In the case of load recovery to constant steady state power, the slow dynamics cause the load voltage to decline slowly and instantaneous load power to increase slowly as the load attempts to recover to constant steady state power. The idea of the emergency control is to reduce the steady state load power to the value of the instantaneous load power to attempt to restore a stable operating equilibrium [16]. The reduction in steady state load power creates an equilibrium at the current state. This new equilibrium is stable because before the saddle-node bifurcation of the fast dynamics, the fast dynamics are stable and the reduction in the steady state power stabilizes the slow dynamics. However, if the emergency action is taken after the saddle-node bifurcation of the fast dynamics, then stability would probably be lost. In practical terms this means that the control action should take place fast enough.

It is also useful to show the interaction of load recovery and corrective actions in load power parameter space. In Figure 2.7-2, two different load power quantities are plotted on the same picture. The first quantity is the steady state load powers regarded as parameters of the power system; this is the usual load power parameter space. The second quantity is the transient load power consumed by the loads at an instant of time (these load powers are time varying phasors, not instantaneous powers). These two load powers are equal in steady state and are distinct during load recovery. The predisturbance and postdisturbance bifurcation sets are plotted in Figure 2.7-2 in the usual way with steady state load powers assumed to be the system parameters. The parameter value  $p^0$  represents the predisturbance load power. Immediately following the disturbance, the transient power actually consumed by system loads changes abruptly from  $p^0$  to  $p^+$  due to the voltage dependence of various load components. Following this, the load restoration mechanisms come into action

trying to restore the transient load power to the steady state demand  $p^0$ . These slow dynamics are such that the transient load power initially increases towards  $p^0$  as shown by the trajectory starting at  $p^+$  in Figure 2.7-2. As the slow dynamics continue to decrease load voltages, the transient load powers pass through a maximum as the trajectory passes through the postdisturbance bifurcation set  $\Sigma'$ . We call this maximum instantaneous power point a “critical point”. Note that  $\Sigma'$  is only the bifurcation set of the system when the steady state powers are considered to be the system parameters. Thus, the critical point is a saddle-node bifurcation when the steady state powers are considered to be the system parameters. However, when considering the slow dynamics of load recovery, an internal load state is considered to be a parameter and the critical point is not a saddle-node bifurcation of the fast dynamics.

A corrective action decreasing the load demand to its present consumption before reaching the saddle-node bifurcation of the fast dynamics creates a new, stable equilibrium. It is thought that the critical point occurs before the saddle-node bifurcation of the fast dynamics. Therefore, to stabilize the system, it is sufficient to decrease the load demand to its present consumption before reaching the critical point.

Parameter space pictures with several parameters such as Figure 2.7-2 do have the advantage of illustrating which parameters or combinations of parameters are effective in restoring an equilibrium. The normal vector to the bifurcation set can be used to determine the most efficient way to bring  $p^0$  on the other side of the bifurcation set in a similar way to that described in Section 2.7.1. For instance, one can detect the critical point by checking along the trajectory of the collapsing system one of the saddle-node bifurcation conditions listed in Section 4.6 (the sensitivities going to infinity are very convenient; here the saddle-node bifurcation conditions are tested on the system assuming constant steady state load powers). By computing the normal vector at the critical point, one can build the tangent hyperplane, i.e., a linear approximation to the surface  $\Sigma'$ , from which the required changes in  $p^0$  can be estimated. A disadvantage of the parameter space view is that information about the stability of the restored equilibrium is lost.

Blocking of ULTC transformers can also be used to avoid voltage collapse [60, 61] (also see Section 2.10).

## 2.8 ENERGY FUNCTIONS

The energy function to be described here [20] will start from a dynamic model for the power system. It is therefore appropriate to begin with a description of the assumed scenario for voltage collapse, and how dynamics come into play. In particular, why is a dynamic model necessary, and how do predictions made in a dynamic model relate to those from a static analysis?

Let us begin with the obvious observation that the physical power system is a dynamic system; its full range of possible behavior cannot be predicted with a strictly static description. However, in normal operation, the state of the power system is expected to be at or near an operating point. Here we will use the terminology of

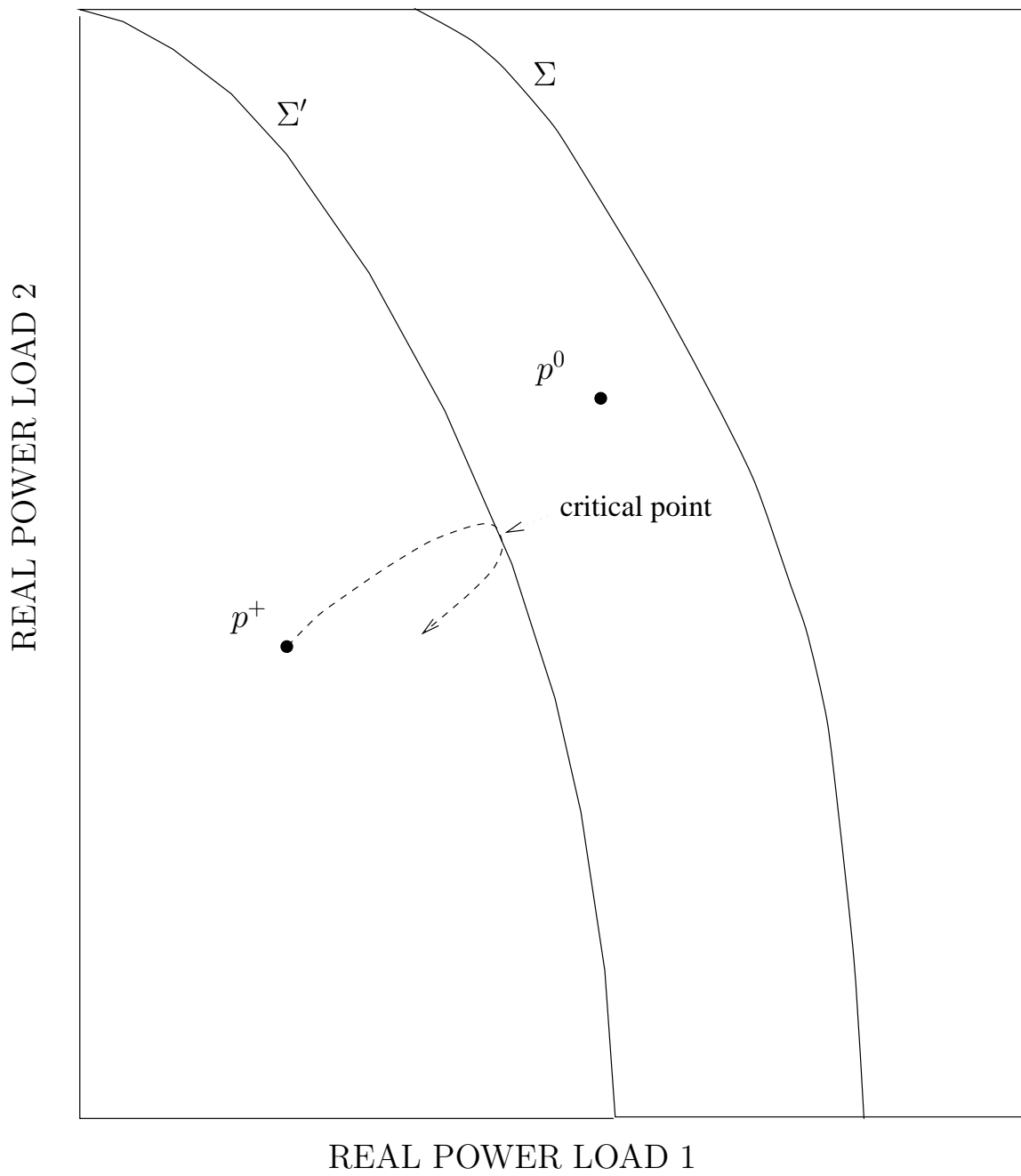


Figure 2.7-2. Load recovery and corrective actions.

“operating point” in a physical sense, separate from any assumptions on the nature of the mathematical model employed to predict system behavior.

As noted in Section 2.3, this approach typically uses a dynamic model for the power system in which load parameters appear as continuous, time varying inputs. If these terms are slowly time varying, one might consider freezing their time evolution at a fixed value. With the external inputs fixed at a constant value, a time invariant model results. The equilibrium of this time invariant model predicts the constant physical operating point that would correspond to the frozen load value. This equilibrium is determined by the solution of a set of algebraic equations such as the power flow equations. In most models, the state vector for a dynamic description will contain components that describe bus voltage magnitude and phase. The values of these magnitude and phase state variables at the “frozen” equilibrium will be determined by the solution to what are essentially power flow equations (perhaps slightly augmented to include some internal generator behavior).

As the load inputs vary with time, one could parameterize by time the sequence of equilibria obtained, and call this a “time varying equilibrium point.” Despite the intuitive appeal of this terminology, note that the result does not, in general, satisfy the rigorous mathematical definition of an equilibrium in the original model with time varying inputs. However, the true, nonequilibrium state of the time varying system may be expected to remain close to this “time varying equilibrium point” provided a number of conditions are met.

First, observe that the normal behavior of the load with respect to time is given by a slowly varying (time scale of minutes to hours) average part, and a small (a few percent of load magnitude), rapidly varying part that is usually modeled as a zero mean random process [6, 30]. As the average load value evolves in time, the position of the frozen equilibrium will move in the state space. Intuitively, one expects that the true state will track this quasistatic motion of the frozen equilibrium provided the equilibrium remains “sufficiently stable.” Clearly, a key question in the analysis to follow will be how to measure degree of stability in a nonlinear model driven by slowly varying inputs.

This quasistatic evolution of the frozen equilibrium is clearly related to the observed behavior in many reported instances of voltage collapse. For the analysis here, the assumed scenario will be taken as follows. First, the power system often experiences some large “discrete event” disturbance(s) that put it into an operating condition that is insecure (often with reduced reactive “reserves”). The interesting point is that these initial disturbances do not immediately lead to the breakdown of the system; some significant time period (minutes to hours) follows during which the system evolves and approaches the bifurcation point. The most common pattern following the large disturbance seems to be a gradual increase in load or in some cases, a decline in reactive sources available as generator protective mechanisms reach their maximum reactive output. The increase in load can be due to an increase in base load (see Section 2.4) or due to tap changer action or general load recovery after the initial disturbance (see Section 2.6). As the frozen equilibrium tracks these parameter variations, the voltage magnitudes decline. One also expects that the frozen equilibrium is getting progressively less and less stable. If this process continues unchecked,

system parameters ultimately reach a saddle-node bifurcation where stability of the equilibrium is completely lost, and the system state diverges along a trajectory that ultimately displays voltage magnitudes very rapidly declining towards zero.

If one accepts the scenario above as a reasonable description of the process of voltage collapse, static analyses are sufficient only to predict the evolution of the slowly moving frozen equilibrium, and to identify the saddle-node bifurcation where the equilibrium disappears entirely. To quantify the degree of stability of the operating point requires some knowledge of the dynamic model, even if one does not actually solve for trajectories of the dynamic model. The most obvious approach would be to linearize the frozen system about its equilibrium, and examine its eigenvalues. As any eigenvalue moves from the left half of the complex plane towards the imaginary axis, the linearized frozen equilibrium is getting less stable. While researchers rarely state their results in these terms, this idea is closely related to voltage collapse proximity measures that examine the smallest singular value or smallest magnitude eigenvalue of the power flow Jacobian. The relationship becomes clear if one reviews the results of [12], which shows that in a certain class of dynamic models singularity of the power flow Jacobian implies that the linearized dynamic model has an eigenvalue on the imaginary axis.

The drawback of linearized analyses is that they can accurately predict behavior only in a neighborhood of the equilibrium of the frozen system. To see the potential drawbacks from a power systems application standpoint, imagine an operating condition where a generator is close to its reactive power limit. So long as the generator has not yet reached its Mvar limit, the linearization at the frozen equilibrium will not depend on the value of this limit. Yet intuitively, one expects that if the Mvar limit on the generator was increased, the system would be less vulnerable to voltage collapse. Moreover, if one accepts the premise that loads have a small magnitude random component, the state will not remain precisely at the frozen equilibrium, but rather will “wander” in a neighborhood of this point. Traditional voltage collapse analyses in single line examples have shown that the sensitivity of the state to load variations increases as the system approaches collapse, so the deviation of the state from the frozen equilibrium may be expected to get larger as the system parameters approach values that lead to collapse. Therefore, one may expect an analysis based on a linearization at the frozen equilibrium will get progressively less accurate as the system gets closer to collapse. It is this observation that motivates the nonlinear proximity measure to be derived here.

### **2.8.1 Load and Generator Models for Energy Function Analysis**

The model developed here includes voltage dependence of reactive power loads, static tap changing transformer characteristics (without effects of time delays), and reactive limits on generators. This model will also include simple swing dynamics. Dynamic changes in frequency are not judged important to the voltage collapse scenario, but the relationship between voltage magnitudes and phase angles predicted by active

power balance at generator buses (the equilibrium of the swing equations) may be significant. Including the full differential equations that predict swing dynamics actually proves more convenient in this analysis, and does not change the computational burden associated with evaluation of energy margins. Indeed, to show that the energy function derived is formally a Lyapunov function, it will prove convenient to formulate all constraints in the model as differential equations. We begin by examining how this is done for reactive power balance equations.

This analysis will adopt the sign convention of positive for injections, with loads being represented as negative injections. Further, we will assume that the average value of reactive load can be modeled as a continuous function of voltage magnitude at the load bus; denote this function  $Q_i(V_i)$ . The expression for reactive power absorbed by the network can be found in any standard text treating power flow analysis, and can be written as a function of the vector  $\delta$  of phase angles (relative to a reference bus), and the vector  $V$  of bus voltage magnitudes; denote this expression at bus  $i$  as  $g_i(\delta, V)$ . The resulting reactive power balance equation becomes:

$$0 = Q_i(V_i) - g_i(\delta, V) \quad (2.2)$$

Consider the behavior predicted by (2.2). Suppose the reactive demand at the load were to undergo a step increase. Equation (2.2) would predict an instantaneous, discontinuous change in the bus voltage(s) to compensate for this change. The approach proposed here is to relax the algebraic constraint to a differential equation that predicts nearly the same equilibrium behavior, but allows the response of voltage to be continuous with some very fast time constant. It proves convenient to first normalize (2.2), dividing the equality by  $V_i^{-1}$  to obtain:

$$0 = V_i^{-1}(Q_i(V_i) - g_i(\delta, V)) \quad (2.3)$$

Given that voltage magnitudes are restricted to be strictly positive by assumption, the solutions to (2.2) and (2.3) are identical. The relaxation process to obtain a differential equation introduces a small time constant  $\epsilon$  to yield:

$$\dot{V}_i = 1/\epsilon V_i^{-1} (Q_i(V_i) - g_i(\delta, V)) \quad (2.4)$$

Clearly, the equilibria of (2.4) are identical to the solutions of (2.3). To obtain consistent behavior between a model based on (2.3) and that of a model based on (2.4), standard results in singular perturbations (described in [19]) require that the linearization of (2.4) be stable in a neighborhood about the solution of interest for (2.3) (i.e., the solution of the full powerflow). Satisfaction of this condition depends in part on the exact form of the voltage dependence of the load. This analysis to confirm stability for a particular load model is left to the reader; here we will simply state without proof that experience with a wide range of load models shows the linearization of (2.4) about reasonable (per unit voltage magnitude above 0.7) operating points is

typically stable. However, behavior of (2.4) differs from (2.3) if one examines stability in the vicinity of “low voltage” power flow solutions (voltage magnitude less than 0.4). The algebraic constraint combined with standard small disturbance stability models would predict these equilibria to be stable; the differential model (2.4) predicts such points to be unstable. Unfortunately, because such low voltage solutions are not operable for other reasons (breaker openings), one can not confirm which prediction matches observed physical behavior. The last point concerning this model relates to the choice of  $\epsilon$ . Clearly, this time constant should be small (probably less than 0.01 sec) to match observed voltage behavior in power systems; fortunately, the energy function and voltage collapse proximity measure to be derived do not depend on the choice of  $\epsilon$ .

The model for tap changers depends very heavily on the tap switching logic associated with a particular transformer. If the tap setting changes rapidly in response to under or over voltages, the effect of the tap changer from the primary side may be viewed simply as modifying the static relationship defining voltage dependence of the load. For the reactive portion of the load, this can be accommodated by the structure of (2.4). More challenging is the case where the tap changing logic has a time delay, where the tap does not change until the voltage has been out of range for tens of seconds to several minutes. Some work has been done to develop continuous dynamic models for such switching action [1, 47], and Lyapunov functions for those dynamics alone have been developed. The question of whether or not these dynamic models for “slow acting” tap changers can be incorporated into the analysis proposed here has not yet been addressed.

An honest appraisal of the methodology proposed here would rate the modeling of active loads as its weakest point. At present, in order to rigorously define a Lyapunov function for the dynamic model, active loads can not be functions of bus voltage. If one is willing to relax the requirement that the function be strictly nonincreasing along trajectories, weak dependence of active power loads on voltage can be accommodated. It is because of this failure to strictly satisfy the requirements of a Lyapunov function that the terminology “energy function” is used in the title. The active load does include a term linearly dependent on bus frequency, as is often the case in loads having induction motors as a component.

Many authors have commented on the importance of reactive limits on generators in the voltage collapse phenomenon. The structure of equation suggested in (2.4) may be easily adapted to model this effect. Assume that the generator excitation system at bus  $i$  is normally in a voltage control mode, with voltage setpoint  $V_i^0$ . A simple representation of the excitation system behavior would increase the generators Mvar output when bus voltage drops below  $V_i^0$ , and decrease its output when bus voltage rises above  $V_i^0$ . However, the reactive output has both upper and lower limits, so if the reactive power absorbed by the network exceeds the maximum output of the generator, the bus voltage will go out of its “control band” about  $V_i^0$ . This effect can be modeled by choosing  $Q_i(V_i)$  for the generator as shown in Figure 2.8-1.

For this interpretation of (2.4),  $\epsilon$  should be chosen as the time constant associated with the response of the generators reactive output with respect to terminal voltage regulation errors. Again, because  $\epsilon$  does not enter the voltage collapse proximity index



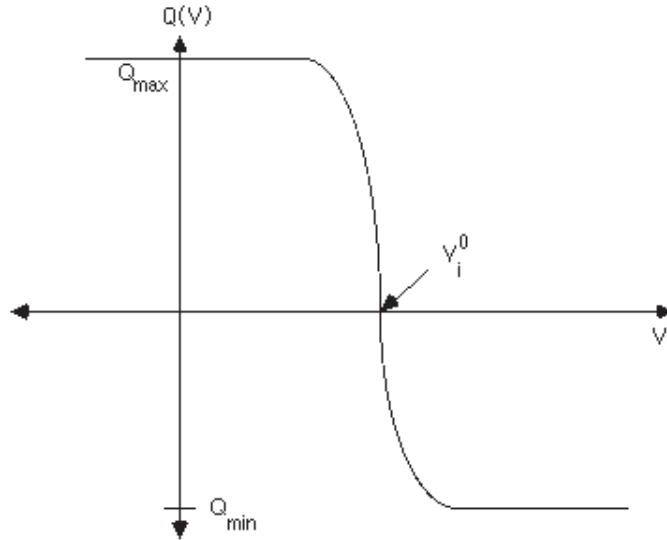


Figure 2.8-1. Generator reactive output versus terminal voltage.

explicitly, the exact choice of this parameter is not critical. For the curve shown in Figure 2.8-1, the equilibrium behavior of (2.4) approaches that of a powerflow model switching the generator bus from PV to PQ when generator limits are encountered.

To understand the use of the energy function to study voltage collapse, it is useful to review its use in transient stability. In that context, the simplest Lyapunov-based stability criterion uses the concept of the closest unstable equilibrium. Roughly, the criteria may be stated as follows. Starting from the post fault equilibrium of interest, expand constant energy contours of the Lyapunov function until they intersect another equilibrium point. Evaluate the Lyapunov function at this “closest unstable equilibrium point.” If the initial energy following the fault is less than this amount, the system will asymptotically return to the desired operating point. This method is generally judged far too conservative, for the following reason. The closest unstable equilibrium point represents the lowest saddle point by which trajectories may escape the potential energy well surrounding the stable equilibrium point. A large transient disturbance (fault, line trip, etc.) that happens to push the system trajectory through this lowest saddle point is a rare, worst case scenario.

However, consider again the conditions associated with voltage collapse. Load is gradually increasing in a way that causes the high voltage equilibrium (normal powerflow solution) to approach the closest unstable equilibrium. The increase in load shrinks the potential well and lowers the saddle point that represents the easiest path of escape. On top of this slow variation of the average load value, we also assume the presence of a small magnitude, broad spectrum random variation in loads. The energy function then provides a measure of this ease with which these small, random load variations push the system state through this closest unstable equilibrium. Given the pervasiveness of these random load variations at any major load distribution substation, it is possible for the system state to be randomly “pushed” in any direction in the state space, unlike the transient stability case, where a specific fault dictates

motion along very particular fault-on trajectory. For this reason, we would argue that the closest unstable equilibrium point is an appropriate critical point for voltage stability studies, even though its use has long been judged ineffective in transient stability studies.

As a further contrast to transient stability use of energy functions, the reader familiar with direct methods in transient stability will recall that calculating the closest unstable equilibrium point in models that include only active power flow equations has proven computationally prohibitive in large scale systems. However, use of the full powerflow equations with reactive power constraints makes the task much easier in our analysis. In a sense, the addition of the reactive power equations limits and changes the nature of the unstable equilibria of interest.

One way to appreciate how the energy function compares with a loading margin is to increase the real power  $P$  at a single load bus and plot the angle  $\delta$  of the load voltage against the real power so as to obtain a  $P\delta$  nose curve. ( $P$  needs to be decreased from the maximum loading at the nose to trace the upper portion of the nose curve.) In this case the (real power) loading margin is the difference in  $P$  at the nose and  $P$  at the nominal operating point. It turns out that the energy function is simply the area enclosed by the nose curve above the nominal loading [44]. This nicely illustrates the relation between the loading margin and the energy function and shows how the energy function includes information about the closeness to instability in the state space as well as the closeness to instability in the loading parameter space. This interpretation of the energy function is analogous to the area interpretations used in transient stability (the equations used in voltage collapse and transient stability differ somewhat as pointed out in the previous paragraph). A similar area interpretation is possible for load reactive power: If, instead, the load real power is held constant and the load reactive power  $Q$  is changed to plot a nose curve of the logarithm of  $V$  against  $Q$ , then it is also true that the energy function is the area under the  $Q$ - $\log V$  curve above the nominal loading.

Another interpretation for the energy function associates it with the expected time for the state to leave the region of attraction under stochastic perturbations [20].

The energy function developed in this section can be used to define a security measure of proximity to voltage collapse as explained in chapter 4.

### 2.8.2 Graphical Illustration of Energy Margin in a Radial Line Example

The canonical example for discussion of voltage stability, pervasive in textbooks for more than forty years, is the case of a single generator serving a radially connected load bus. From a powerflow standpoint, analysis of such a system is particularly simple because one is left with only two degrees of freedom: the relative voltage phase angle between the machine and the load bus, and the voltage magnitude at the load. If one neglects potential energy associated with speed deviations of the generator, as is appropriate in voltage stability applications of energy functions, one is left with a

potential energy term dependent upon these two degrees of freedom in the power flow. As a result, the energy contours of the system may be easily displayed as a potential well in three dimensions (the two degrees of freedom determining the position in a plane, with energy value determining a height of the contour above this plane). These contours will change as the parameters describing the slowly moving average value of load change. Our goal in this section is simply to illustrate our premise that the critical value of load parameters is associated with an “opening up” of the potential well about the operating point. Moreover, we wish to show that an alternate power flow solution, which is unstable in our dynamic model, and typically displays low voltage magnitude, defines the “easiest” path of escape from the potential well as the load values approach their critical values.

Consider a simple one machine, radial line example, as shown in Figure 2.8-2. A small point that further distinguishes this application with transient stability, note that we shall assume that in the time frame of interest, the exciter succeeds in holding the terminal voltage of the machine constant, unless reactive limits are encountered. Contrast this with a classical machine model in transient stability, for which a fictitious internal voltage behind transient reactance is held constant. For the figures below, the terminal bus voltage is held constant at 1.0 per unit, and no reactive limits are enforced on the generator. The radial transmission system is a lossless short line model. The nominal, slowly varying load behavior is constant PQ, with the Q value successively increased. It is the increase in this value of reactive demand that will drive our simple system to loss of stability.

For this example, the potential energy can be defined as [21]

$$E_P = 10.0(V \cos \delta - V_o \cos \delta_o) + 5.0(V^2 - V_o^2) - 2.0(\delta - \delta_o) + Q \ln \left( \frac{V}{V_o} \right)$$

where  $V_o$  and  $\delta_o$  stand for the stable equilibrium point, which corresponds to the basic power flow solution of the system. Figures 2.8-3, 2.8-4, 2.8-5, and 2.8-6 show the energy potential well, i.e. the plots of  $E_P$  with respect to  $V$  and  $\delta$ , as the reactive load  $Q$  increases; observe that the bottom of the well corresponds to the equilibrium point  $(V_o, \delta_o)$ . Several observations are in order. As predicted, the depth of the potential well, in a particular direction, decreases with increasing reactive load. In particular, the potential well “opens up” along a direction that is primarily one of decreasing voltage magnitude (with a small component in the direction of increasing phase angle difference across the line). The (initially) stable equilibrium point near 1.0 per unit bus voltage, 20 to 30 degrees phase angle, is a local minimum point in the energy well. The saddle point, which is the lowest point on the “lip” of the potential well, is defined by an alternate, low voltage power flow solution. This solution is an unstable equilibrium in our dynamic model. As the reactive loading is increased, the “opening up” of the potential well is also characterized by the saddle point approaching, and ultimately coalescing with, the stable equilibrium. The point where these two equilibria coalesce is a saddle-node bifurcation of our model. However, the energy contours clearly provide extra insight into the degree of stability possessed by the system as the bifurcation approaches.

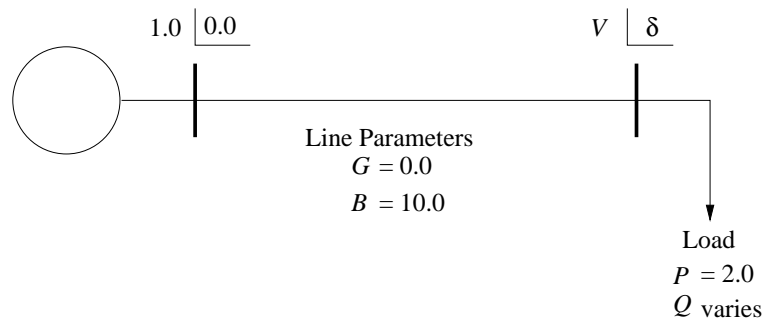


Figure 2.8-2. One line diagram of radial example.

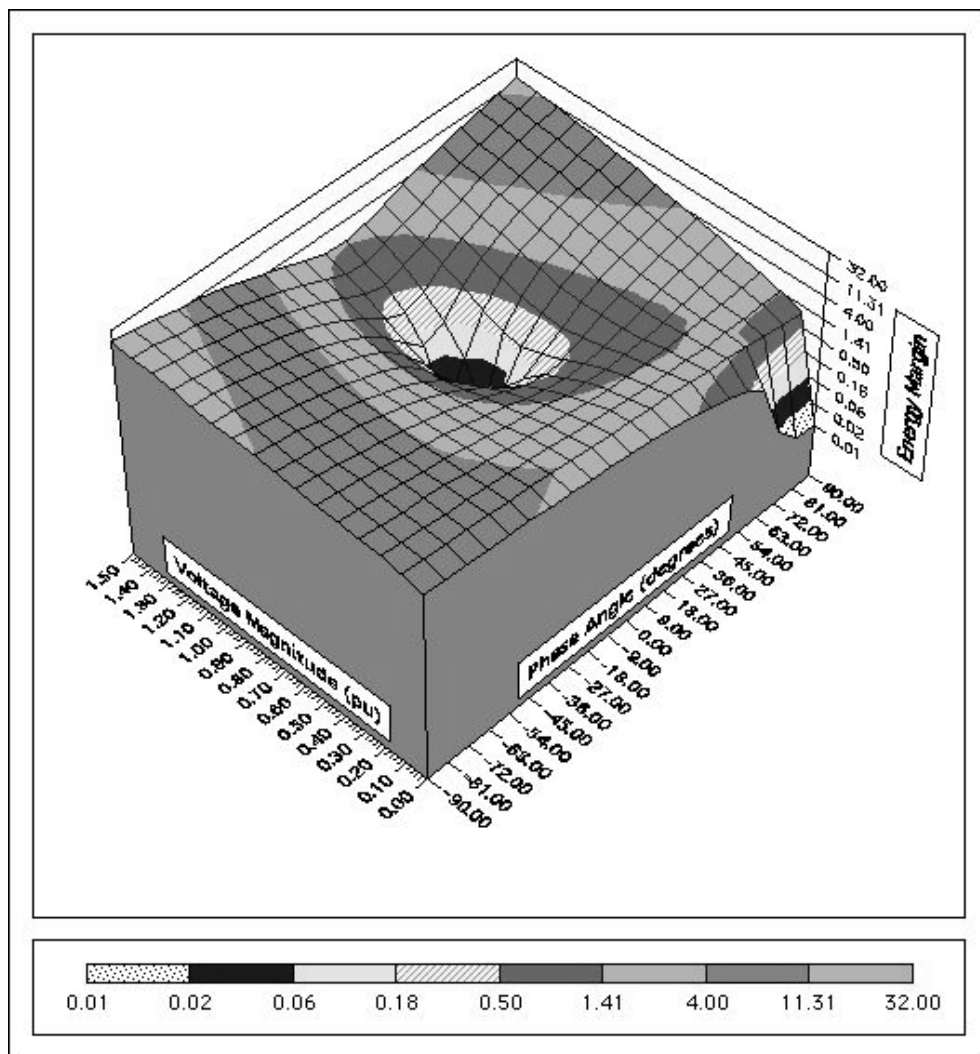


Figure 2.8-3. Energy potential well;  $Q=0.5$ .

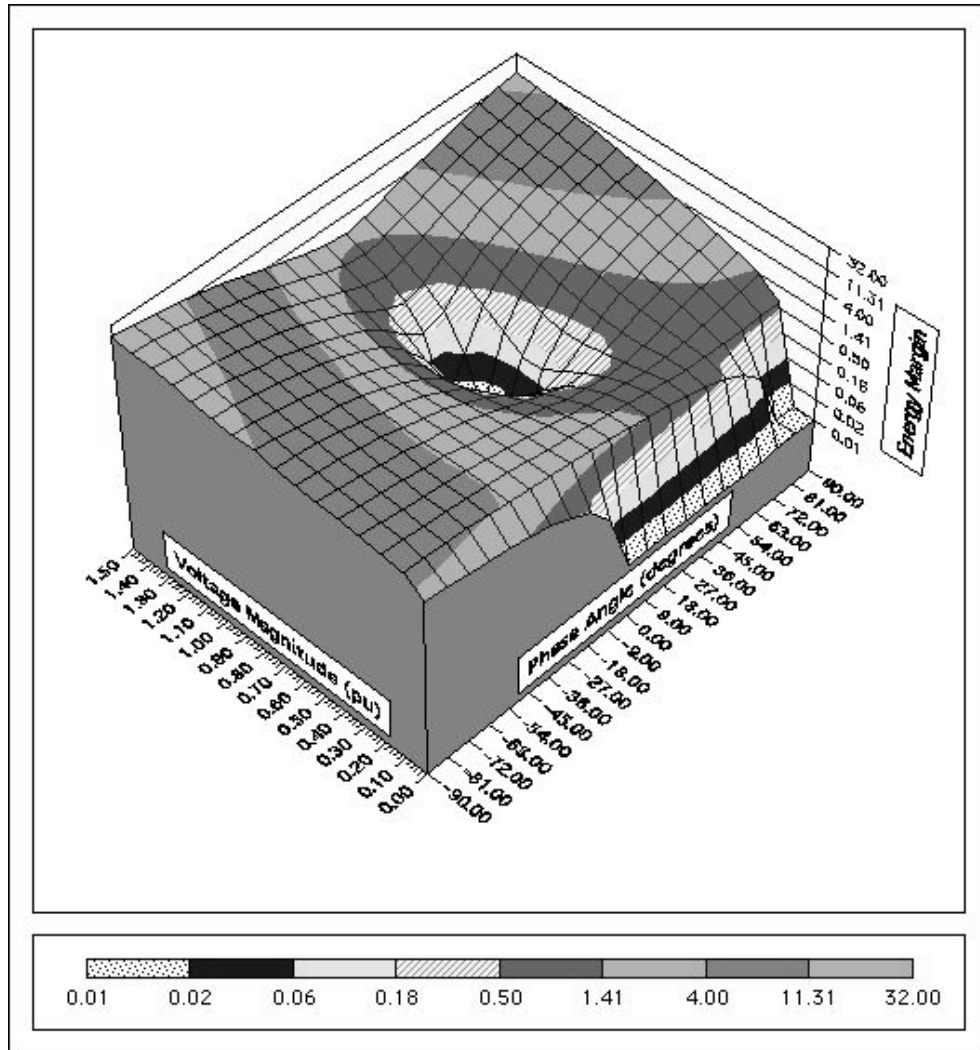


Figure 2.8-4. Energy potential well;  $Q=1.0$ .

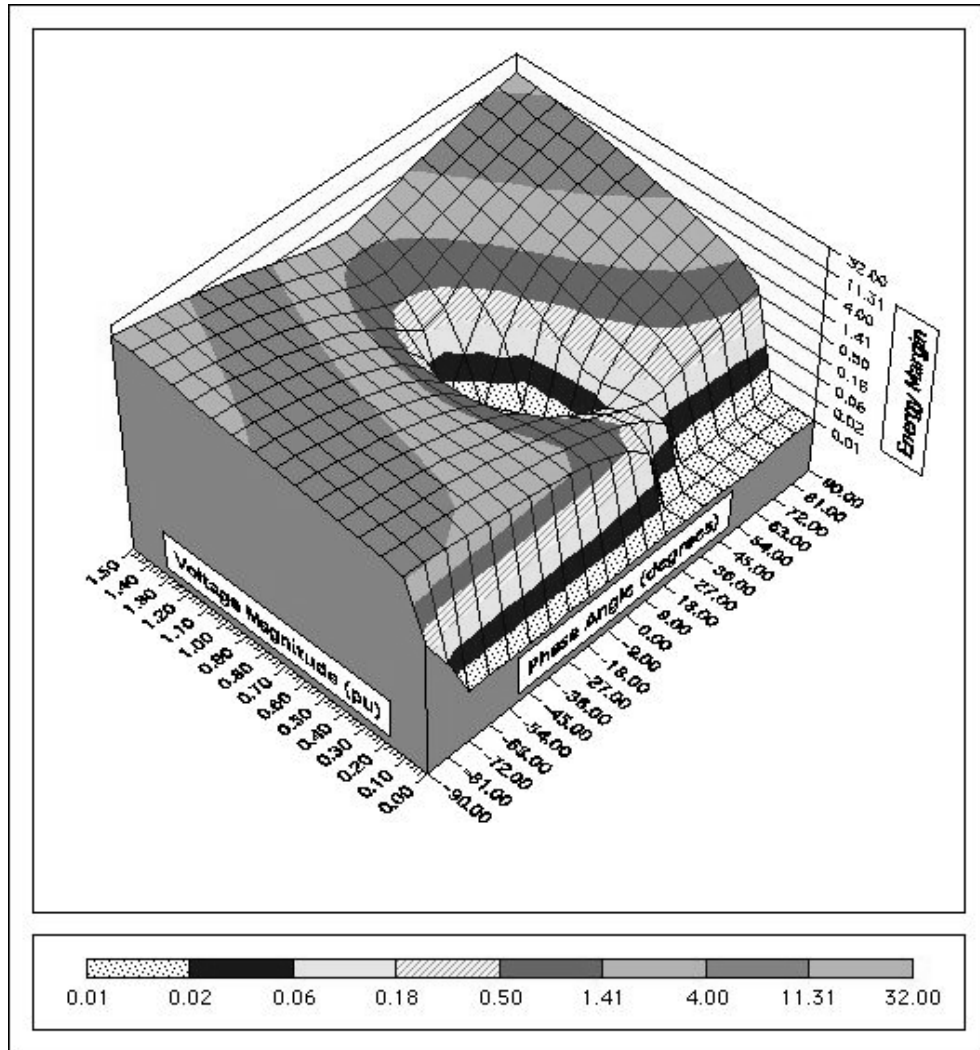


Figure 2.8-5. Energy potential well;  $Q=1.5$ .

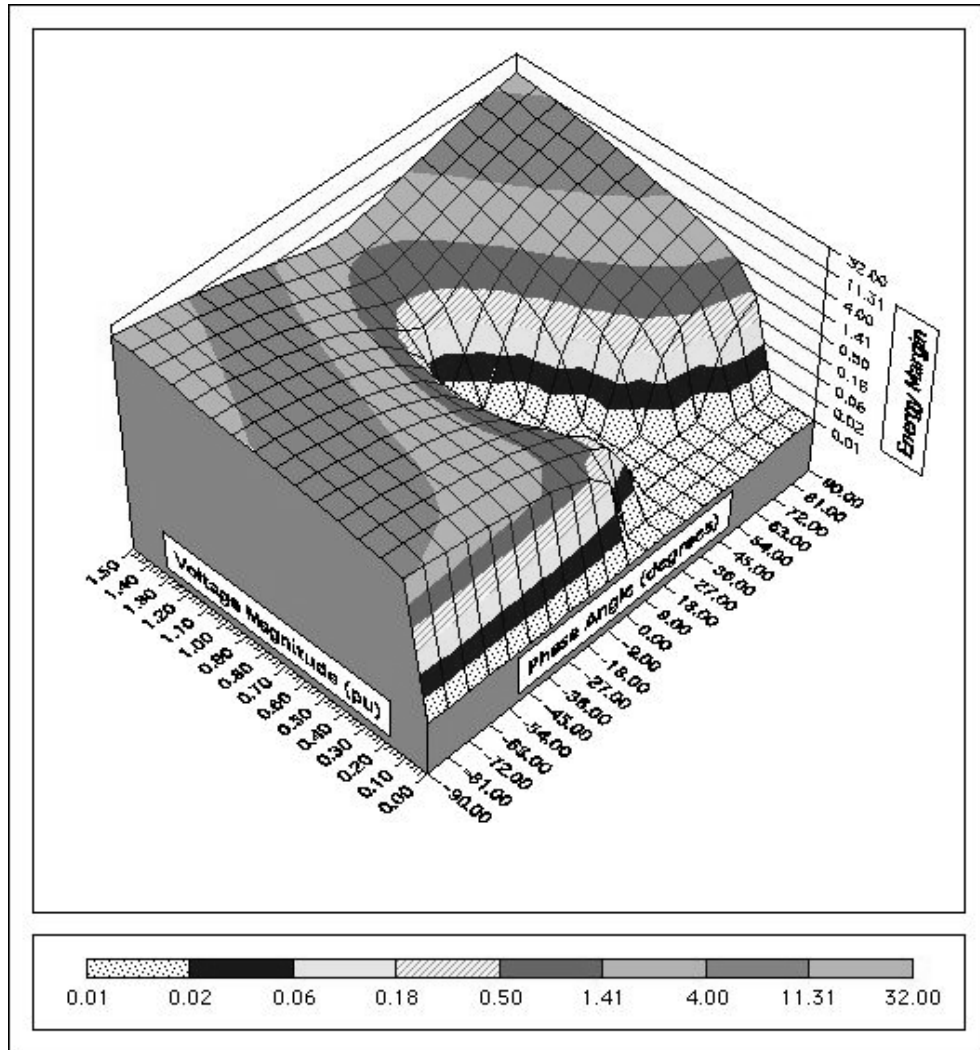


Figure 2.8-6. Energy potential well;  $Q=1.75$ .

## 2.9 CLASSIFICATION OF INSTABILITY MECHANISMS

The objective of this section is to relate the above concepts of large disturbance and time scale decomposition to power system phenomena and models. We provide a classification of loss of stability mechanisms relevant to voltage phenomena.

Figure 2.1-1 at the beginning of the chapter outlines a power system model relevant to voltage phenomena and decomposed into transient and long-term time frames. The corresponding variables are respectively the fast and slow variables of Section 2.6. A good separation between the two time scales is assumed, allowing the quasi steady state approximation to be used and the overall system instability to be decomposed in several well defined categories. Let us assume a large disturbance and consider the possible unstable system responses that might result.

### 2.9.1 Transient Period

In the transient period immediately following the disturbance the slow variables do not respond yet and may be considered constant. The three major instability mechanisms are

T1: loss of equilibrium of the fast dynamics.

T2: lack of attraction towards the stable post-disturbance equilibrium of the fast dynamics.

T3: post-disturbance equilibrium oscillatory unstable.

The transient period is the usual time frame of angular stability studies. For instance, the loss of synchronism following too slow a fault clearing is a typical T2 mechanism. This is also the time frame of *transient voltage stability*, which results from loads trying to restore their power in the transient time frame. Typical examples are induction motor loads and HVDC components.

An example of T1 voltage instability is the stalling of an induction motor fed through a long transmission line, after some circuit tripping makes the transmission impedance too large. Motor stalling causes the voltage to collapse. The motor mechanical and electrical torque curves do not intersect any longer, leaving the system without a post-disturbance equilibrium.

An example of T2 voltage instability is the stalling of induction motors after a short-circuit. In heavily loaded motor and/or slowly cleared fault conditions, the motor cannot reaccelerate after the fault. The mechanical and electrical torque curves intersect but at fault clearing, the motor slip is larger than the unstable equilibrium value.

### 2.9.2 Long-term Period

If the system survives the transient period after the disturbance, the slow variables start evolving. As discussed in Section 2.6, these slow variables can be considered as



slowly changing parameters for the fast dynamics. Let us assume first that the fast dynamics are stable. Following the initial disturbance, the long-term dynamics may become unstable in basically two ways:

LT1: a loss of equilibrium.

LT2: a lack of attraction towards a stable equilibrium.

The above scenarios lead to what is known as *long-term voltage instability*. A majority of voltage incidents experienced throughout the world were of this type.

LT1 is the most typical voltage mechanism, with the loads trying either to recover their predisturbance powers through ULTC actions or to reach their long-term characteristics through self-restoration.

A typical example of LT2 instability would be an LT1 scenario followed by a corrective action (e.g. shunt compensation switching or load shedding) which restores a stable equilibrium but too late, so that the system is not attracted by the post-control equilibrium. A third mechanism LT3 of slowly growing oscillations is also conceivable.

We finally consider the case where the changes in slow variables causes the fast dynamics to become unstable. If those changes are smooth enough, this can be seen as a bifurcation of the fast dynamics. According to whether this is a saddle-node or a Hopf bifurcation, the system undergoes

T-LT1: a loss of equilibrium point of the transient dynamics caused by the long-term dynamics.

T-LT2: in practice, as the transient dynamics approach situation T-LT1, the domain of attraction of the stable transient equilibrium point shrinks. Hence, if changes in slow dynamics are not slow enough, a lack of attraction may occur before reaching T-LT1 instability.

T-LT3: an oscillatory instability of the transient dynamics caused by the long-term dynamics.

Typical examples of T-LT1 instability in power systems are loss of synchronism (especially for field current limited machines) and motor stalling following the system degradation caused by long-term instability LT1 or LT2. The latter is the cause, the former the result.

ULTC blocking for instance may be used to slow down, or stop the degradation caused by long-term instability and prevent the system from reaching T-LT1 instability. There is little chance to avoid the catastrophic collapse during the T-LT1 instability.

It should be noted however that LT1 (or LT2) may well occur without triggering T-LT1 or T-LT2 instabilities. One reason may be ULTCs reaching their limits (e.g. in systems having a single level of ULTCs between transmission and distribution) or self-restoration saturating. These limits “stabilize” the system.

There are less realistic or real-life cases reported in the voltage stability literature about T-LT3. This could occur in systems having voltage and electromechanical oscillation problems compounded.

Detailed power system examples illustrating all the mechanisms discussed here are given in the next section.

## 2.10 SIMPLE EXAMPLES OF INSTABILITY MECHANISMS

This section provides simple examples to illustrate instability mechanisms described in previous sections [15, 17]. They have been made as simple as possible to emphasize a single mechanism at a time. The explanations rely on the traditional PV curves.

We focus on long-term voltage instability, driven by ULTC transformers and load self-restoration. Following the time scale decomposition ideas of Sections 2.6 and 2.12, we first concentrate on long-term instability mechanisms, assuming that the transient dynamics is stable. Then we discuss cases where this assumption stops being valid.

### 2.10.1 Small Disturbance Examples

#### 2.10.1.1 Example 1

We consider the simple system of Figure 2.10-1. A load is fed by a generator through a transmission line and an ULTC transformer. For the sake of simplicity, we assume an ideal transformer (or merge its leakage reactance with the line) and a purely active (unity power factor) load. The ULTC transformer is aimed at keeping the low voltage  $V_2$  at the  $V_2^0$  set point value.

The *transient* load characteristic is voltage dependent, according to the exponential model:

$$P = P^0 \left( \frac{V_2}{V_2^0} \right)^{\alpha_T}$$

where we take  $\alpha_T > 1$  and the ULTC set point  $V_2^0$  as the voltage reference. The transformer being ideal,  $P$  is also the power entering the transformer (see Figure 2.10-1). The latter imposes:

$$V_2 = rV$$

Hence the load power can be expressed as a function of  $V$ :

$$P = P^0 \left( \frac{rV}{V_2^0} \right)^{\alpha_T} \quad (2.5)$$

To each value of  $r$  corresponds one transient load characteristic as seen from the network. The transient load characteristics are shown with dotted lines in Figure 2.10-2. In this system the fast dynamics are the transient load dynamics: if there is a disturbance, the load voltage and power change quickly along the transient load characteristic.

In this system the slow or long-term dynamics comes from the ULTC. The equilibrium is such that  $V_2 = V_2^0$  (ignoring the ULTC dead-band for simplicity), which

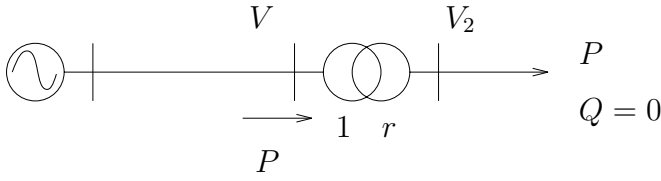


Figure 2.10-1. Simple power system example.

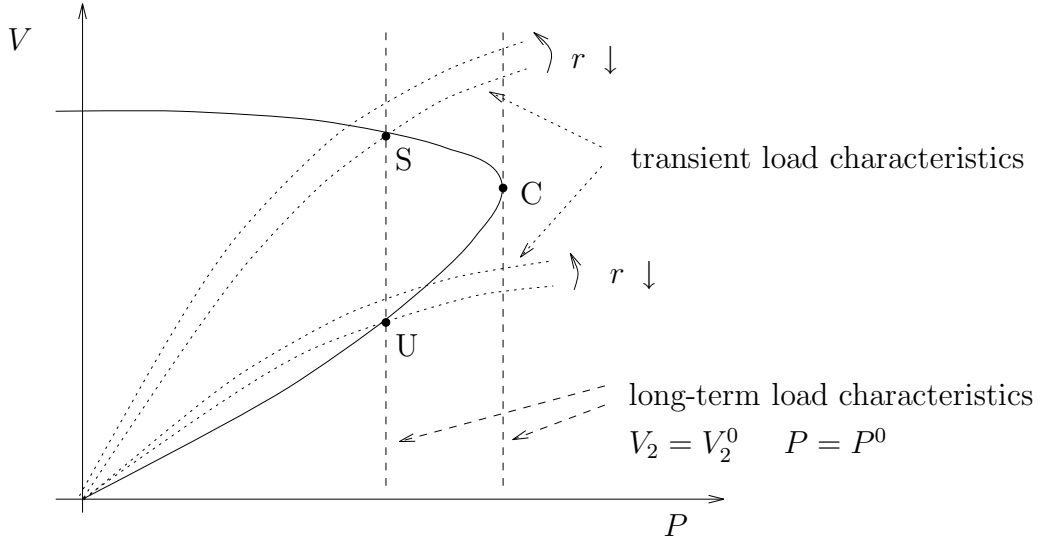


Figure 2.10-2. Example 1.

means that  $P = P^0$ . In other words, for a given demand  $P^0$ , the long-term load characteristic appears as a constant power, vertical dashed line in Figure 2.10-2.

Assuming the fast dynamics are stable, the characteristic of the network and generator is the well known PV curve shown with a solid line in Figure 2.10-2. Note that there is no long term generator dynamics in this example (we do not consider excitation limitation). The PV curve is also the fast dynamics equilibrium manifold explained in Section 2.6. If there is a disturbance and the fast dynamics are stable, they act to quickly restore the voltage and power to the PV curve along the transient load characteristic. The slow ULTC dynamics then act to move the voltage and power along the PV curve. Point C at the nose of the PV curve corresponds to the maximum power that can be delivered to the load.

For a given demand  $P^0$ , we thus have two equilibria, denoted by S and U in Figure 2.10-2. The stability of these points can be checked intuitively by slightly disturbing the ULTC ratio  $r$ . Figure 2.10-2 shows for instance the effect of a small decrease in  $r$  (the same conclusions would be drawn by considering an increase in  $r$ ):

- At point S, the decrease in  $r$  yields a lower load power and hence a lower

secondary voltage. Therefore the ULTC will react by increasing  $r$  and the operating point will come back to S. S is thus stable.

- At point U, the decrease in  $r$  yields a higher load power and hence a higher secondary voltage. Therefore, the ULTC will react by further decreasing  $r$ , making the operating point further depart from U. U is thus unstable.

As the demand  $P^0$  increases, the two equilibria converge to each other. At point C they coalesce and disappear. Point C is a *saddle-node bifurcation* when the demand  $P^0$  is considered to be the parameter.

### 2.10.1.2 Example 2

In the previous example, the long-term load characteristic was constant power due to ULTC action. Therefore the saddle-node bifurcation and maximum load points coincided. This is no longer true if the load restores to a characteristic other than constant power.

To illustrate this, we consider the same system as in Figure 2.10-1 but we replace the transformer and passive load with a self-restoring load. The latter restores to

$$P = P^0 \left( \frac{V}{V^0} \right)^{\alpha_L}$$

where we take  $0 < \alpha_L < 1$ . (Example 1 corresponds to  $\alpha_L = 0$ .)

The corresponding PV curves are shown in Figure 2.10-3. The dashed curves are two long-term characteristics. If the demand  $P^0$  increases, the long-term stable equilibrium moves from A to M to C. At point M the load power is maximal. In between M and C the equilibrium is still stable but the load power decreases as  $P^0$  increases. When reaching the saddle-node bifurcation C, the system becomes unstable.

The distinct natures of points C and M comes from the long-term dependence of load power on voltage. The long-term constant power assumption used in many fast voltage stability analyses is justified for the many systems where load restores due to ULTCs, provided the latter do not hit their limits, nor are blocked and the dead band effect is neglected. For other load behaviors, the loadability limit - although of practical interest - does not correspond to a stability limit.

### 2.10.1.3 Example 3

We come back to Example 1 where we assume now that the *transient* load characteristics has some constant power part (if one would incorporate the reactive counterpart, this might represent some motor component of the load; induction motors restore to almost constant active power in the transient time frame). The long-term load characteristics is unchanged: constant power due to ULTC action. The corresponding curves are shown in Figure 2.10-4.

Consider the equilibria S, U and S' in Figure 2.10-4. The intuitive stability check of Example 1 now shows that:

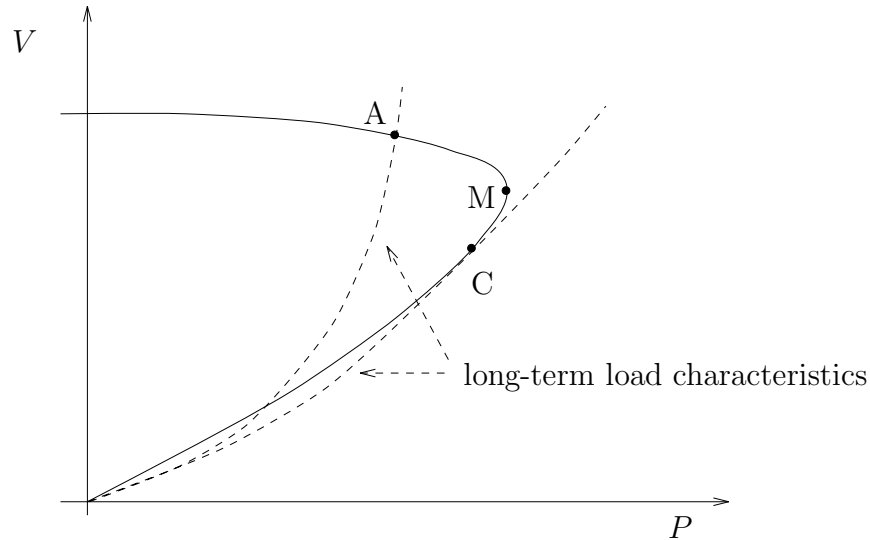


Figure 2.10-3. Example 2.

- (1) All equilibria above C (e.g. S) are stable.
- (2) All equilibria in between C and X (e.g. U) are unstable.
- (3) All equilibria below X (e.g. S') are again stable.

Again, C is a saddle-node bifurcation, separating stable and unstable operating points.

Apparently strange, the third result is explained by the particular nature of long-term equilibrium X. Indeed, at this point, the *transient* load characteristics is tangent to the network PV curve. Hence if we slightly increase the slow state variable  $r$  the transient load characteristics no longer crosses the network PV curve. The system loses its fast dynamics equilibrium or, equivalently, the transient dynamics becomes unstable through a saddle-node bifurcation of the fast dynamics (for this purpose  $r$  is considered to be a slowly moving parameter and an increase in  $r$  causes the saddle-node bifurcation).

Up to now, we have assumed fast and stable transient dynamics while focusing on the stability of the long-term dynamics. This assumption stops being valid at point X. At that point, the modeling with the transient dynamics neglected has a *singularity*. That is, algebraic equations representing the fast dynamics equilibrium manifold are singular and we have a singularity induced bifurcation. To avoid the singularity induced bifurcation (as far as this is deemed useful!) we should resort to a more detailed modeling including transient dynamics. This more detailed model would then exhibit a saddle-node bifurcation at point X.

## 2.10.2 Large Disturbance Examples

### 2.10.2.1 Example 4

We come back to the system of Example 1, imposing now a large disturbance, such as a sudden increase in reactance between the generator and load. This causes the network PV curve to shrink, as shown in Figure 2.10-5. In this figure, the disturbance has been assumed so severe that the vertical line representing the long-term load characteristics does not intersect the new network PV curve. Thus it will be impossible to restore load power to its predisturbance level; this is equivalent to saying that the ULTC cannot restore voltage  $V_2$  to its set point value  $V_2^0$ . In other words, the system has lost its equilibrium, a typical long-term voltage instability mechanism.

The way the system undergoes instability is shown by the dotted lines in Figure 2.10-5. In its (hopeless) attempt to restore the secondary voltage, the ULTC increases  $r$ . The transient load characteristics, given by equation (2.5) are the dotted lines in Figure 2.10-5. The system thus moves from B to D to E to F.

Note that the system crosses point C where the saddle-node bifurcation conditions held in Example 1. However, this point is not a bifurcation point, because it is not an equilibrium: as already mentioned, there is no equilibrium any longer. We suggest to simply call C the critical point. Once it is identified, the critical point yields interesting information on what should be done to save the system.

Without further limitation, the system would converge to zero voltage. In practice however either the tap changers will hit their limits or the fast instability shown in the next example will occur.

In systems having a limited range of ULTC action (e.g. a single level between transmission and distribution) or a relatively low critical voltage, ULTCs could hit their limits before reaching the critical point. In such a case, it is essential to take into account self-restoration effects which will continue to degrade system conditions.

On the other hand, in systems having two or more levels of ULTCs in cascade or having a relatively high critical voltage (being thus voltage stability limited) the critical point is usually crossed before ULTCs reach their limits. In this case, load self-restoration effects are often “hidden” behind ULTC effects.

Similarly, when ULTC blocking is considered as a preventative action its interactions with load recovery and the actions of lower voltage ULTCs must be considered. ULTC blocking loses its effectiveness if and when the connected load restores its power demand. Indeed, the only effect of ULTC blocking lasting after the connected load readjusts to its previous value is a net increase in transmission losses.

### 2.10.2.2 Example 5

We come back to the system and load behavior of Example 3, imposing a large disturbance as in the previous case. The system and load characteristics are shown in Figure 2.10-6. Again, the main instability mechanism is the loss of equilibrium. In its attempt to restore the secondary voltage, the tap changer makes the system move from B to D to C to X. At point X however, the transient load characteristics is tangent to the network PV curve and for any subsequent increase in tap changer

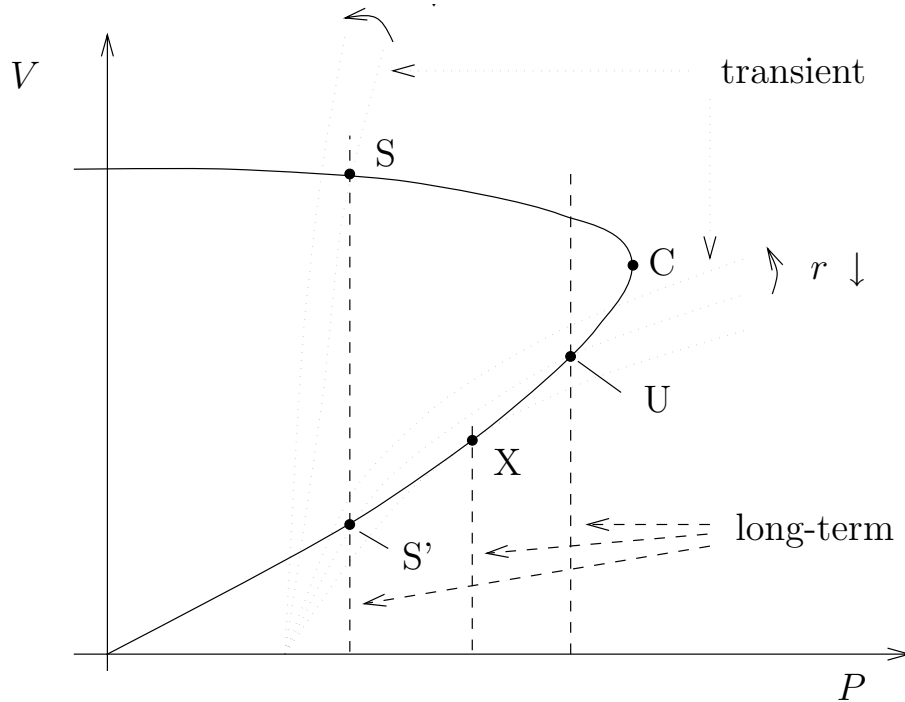


Figure 2.10-4. Example 3.

ratio, both characteristics will no longer intersect. As already quoted, this means that the fast dynamics equilibrium is lost: while negligible up to point  $X$ , the transient dynamics becomes significant again.

In the time domain, voltage versus time curves reveal a rather slow degradation due to long-term dynamics instability, followed by a faster system degradation due to transient dynamics instability. With detailed modeling, the final disruption might correspond to machines losing synchronism or motor stalling.

### 2.10.3 Corrective Actions in Large Disturbance Examples

In order for corrective action to stabilize a voltage unstable situation, an equilibrium must be restored by either one of the following mechanisms:

- (i) Decrease load by decreasing ULTC voltage set-points, shedding load, etc.
- (ii) Increase the maximum deliverable power by switching on shunt capacitors, switching off shunt inductors, increasing generator voltages, etc.

In addition these actions must take place fast enough in order the system to be attracted by the new equilibrium.

These aspects are illustrated in the next two examples.

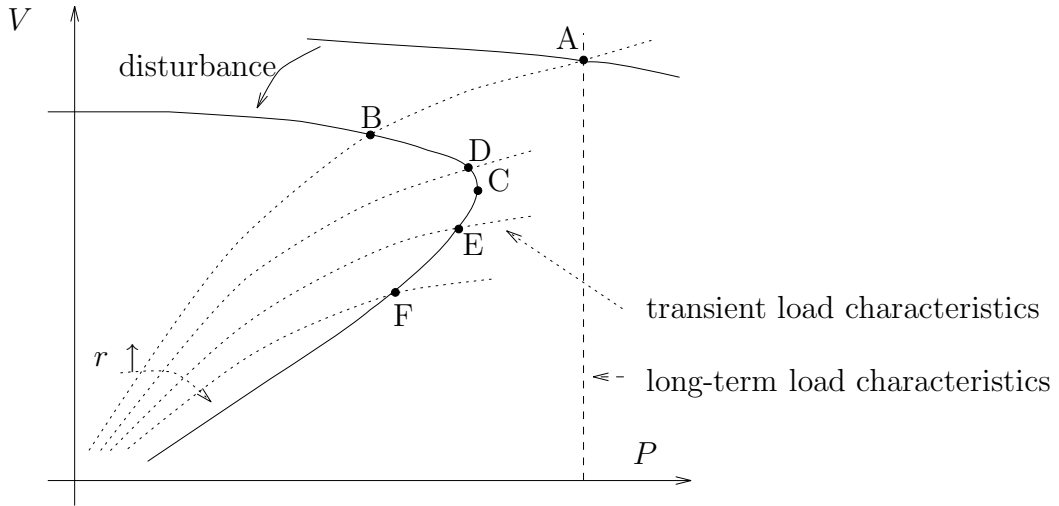


Figure 2.10-5. Example 4.

### 2.10.3.1 Example 6

Figure 2.10-7 illustrates a load shedding action. To create a new long-term equilibrium, it is required to decrease the load below the value corresponding to the critical point C. The vertical line of the new long-term load characteristics is shifted to the left, yielding the stable (resp. unstable) equilibrium S (resp. U).

Let  $t_1$  be the time load is shed and let  $P(t_1)$  be the operating point right after this action (see Figure 2.10-7). One easily verifies that the tap changer (or load self-restoration) will make the system move towards S. This is true as long  $P(t_1)$  is above the *unstable* equilibrium point U. Conversely, if the action is taken at time  $t_2 > t_1$ , the corresponding operating point  $P(t_2)$  (see Fig. 9) will not be attracted towards S and voltages will continue to drop. Otherwise stated, the domain of attraction of S is the portion O-S-C-U of the PV curve.

### 2.10.3.2 Example 7

Figure 2.10-8 illustrates the switching of a shunt compensation on the transmission system. The latter yields a new, “post control” network PV characteristics. Again, if the action is taken at time  $t_1$ , the operating point  $P(t_1)$  moves towards the stable equilibrium S, while if it is taken at time  $t_2$ , it does not.

The above examples inspire the following final remarks.

There is a minimal amount of corrective action to be taken. Not shown by our simplistic examples, there is also a most adequate location in the system for these actions. Analytical methods have been developed to identify these locations. The closer to this location, the smaller the required action.



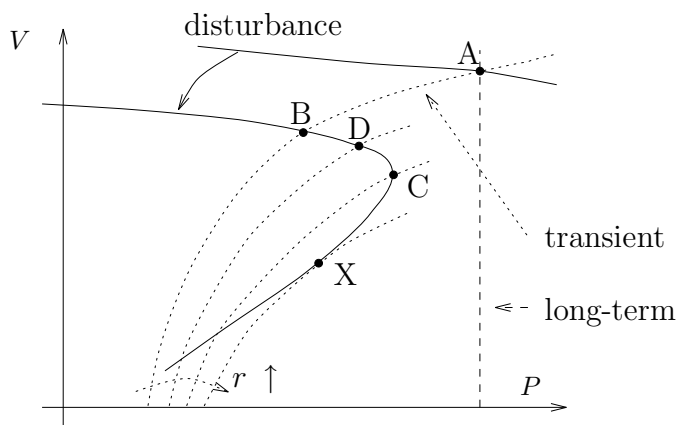


Figure 2.10-6. Example 5.

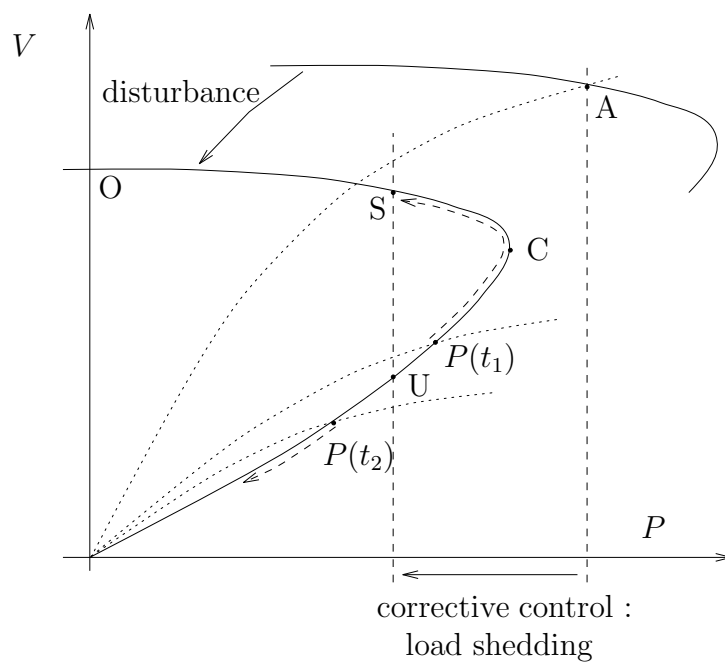


Figure 2.10-7. Example 6.

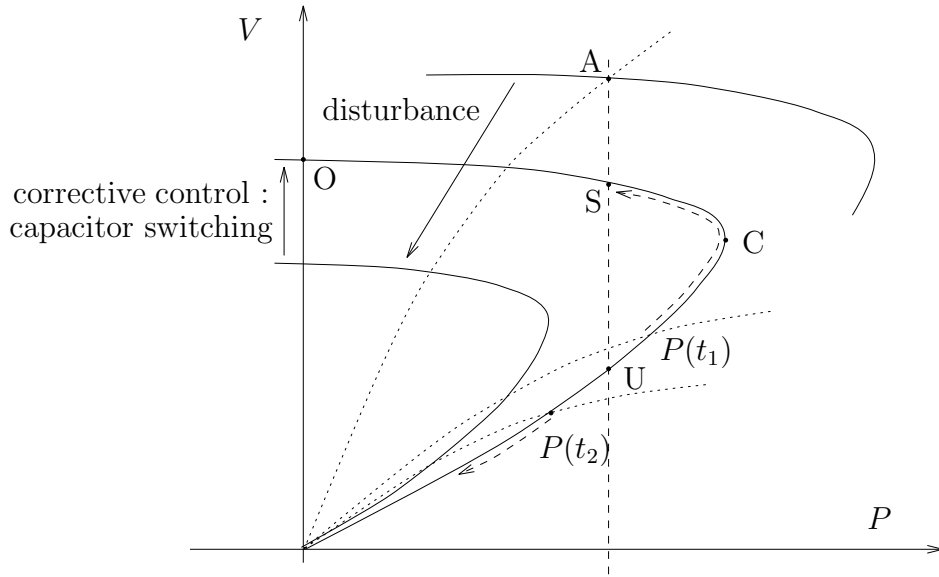


Figure 2.10-8. Example 7.

Corrective actions are usually triggered by protective devices monitoring low transmission voltages, low generator reactive power reserves, etc. For a given corrective action, the triggering threshold must be a compromise between false alarm and inefficient action. There are two risks associated with the latter. The first one is to have the action delayed so much that it cannot save the situation (as in Examples 6 and 7). The second is to reach a point of uncontrollable severe disruption (as in Example 5). Actions to slow down the system degradation (e.g. tap changer blocking) can mitigate the second risk.

## 2.11 A NUMERICAL EXAMPLE

The simple two bus system of Figure 2.11-1, proposed in [8] and used in one way or another throughout this chapter to illustrate the basic concepts discussed here, is studied in detail in this section, giving all equations and parameters so that the reader can reproduce the results presented and discussed here. Saddle-node and limit-induced bifurcations are analyzed in this example based on steady state and time domain simulations. A Transient Energy Function (TEF) is used to show the possible applications of these functions in voltage stability analysis, and to illustrate the effect of bifurcations in the stability of the sample system.

The example is basically set up to demonstrate the possible use of a TEF to determine the size and “connecting” time of shunt compensation and load shedding to recover a system after a simulated contingency. The contingency drives the system to collapse due to a saddle-node bifurcation or a limit-induced bifurcation, when the

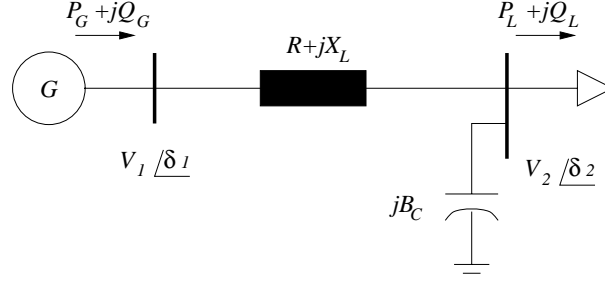


Figure 2.11-1. Sample system.

effect of generator Q-limits is considered in the problem.

The p.u. dynamic equations that represent this system, using a basic dynamic generator model and a frequency and voltage dependent dynamic model for the load, are given by

$$\begin{aligned}\dot{\omega} &= \frac{1}{M}[P_m - P_G(\delta, V_1, V_2) - D_G\omega] \\ \dot{\delta} &= \omega - \frac{1}{D_L}[P_L(\delta, V_1, V_2) - P_d] \\ \dot{V}_2 &= \frac{1}{\tau}[Q_L(\delta, V_1, V_2) - Q_d]\end{aligned}\tag{2.6}$$

where

$$\begin{aligned}\delta &= \delta_1 - \delta_2 \\ P_G(\delta, V_1, V_2) &= V_1^2 G - V_1 V_2 (G \cos \delta - B \sin \delta) \\ P_L(\delta, V_1, V_2) &= -V_2^2 G + V_1 V_2 (G \cos \delta + B \sin \delta) \\ Q_G(\delta, V_1, V_2) &= V_1^2 B - V_1 V_2 (G \sin \delta + B \cos \delta) \\ Q_L(\delta, V_1, V_2) &= -V_2^2 (B - B_C) - V_1 V_2 (G \sin \delta - B \cos \delta) \\ G &= \frac{R}{R^2 + X_L^2} \\ B &= \frac{X_L}{R^2 + X_L^2}\end{aligned}$$

$Q_G$  is used to represent generator reactive limits. If  $Q_{G_{\min}} \leq Q_G \leq Q_{G_{\max}}$ , the generator voltage  $V_1$  is assumed to be controlled to represent somewhat the control actions of a voltage regulator or AVR; thus, neglecting droop and the control system dynamics, the voltage regulator is modeled here by keeping the generator terminal voltage at the fixed value  $V_1 = V_{1o} = 1$ . To approximate the voltage control system limits, the voltage  $V_1$  is let free to change when  $Q_G$  reaches a maximum or minimum limit, which simulates loss of voltage control. Recovery from limits is allowed assuming no-windup limits, i.e., if  $V_1$  returns back to the controlled value  $V_{1o}$ , the voltage is immediately fixed and  $Q_G$  is then allowed to change. The generator inertia and damping constants are represented by  $M$  and  $D_G$ , and  $D_L$  and  $\tau$  stand for the dynamic load frequency and voltage time constants, respectively. The steady state

load demand is modeled through the parameter  $P_d$ , under the assumption that that reactive power load demand is directly proportional to the active power demand, i.e.,  $Q_d = kP_d$  (constant power factor load); this parameter is used here to carry out the voltage collapse studies. The shunt capacitance  $B_C$  is used to illustrate the effect of compensation on the system stability.

To simplify the stability analysis of this problem, the resistance is neglected ( $R = 0$ ), i.e.,  $P_m = P_d$ . The initial loading condition, as defined by the value of  $P_d$ , is chosen depending on whether generator limits are considered or not, as discussed below. The p.u. time constants are assumed to be  $M = D_L = \tau = 1$ ,  $D_G = 0.1$ ; the load power factor is assumed to be 0.97 lagging, i.e.,  $k = 0.25$ ; and the generator reactive power limits are defined as  $Q_{G_{\min}} = -0.5$  and  $Q_{G_{\max}} = 0.5$ . A transmission system contingency (e.g., outage of a line) is modeled by changing the value of  $X_L$  from an initial 0.5 to 0.6. Finally,  $B_C$  is given the values of 0, 0.5, or 1 to simulate different compensation levels.

For this system, a simple TEF can be used to study the effect of the different system parameters, i.e.,  $P_d$ ,  $X_L$  and  $B_C$ , on the stability of the system; this is the main reason why equations (2.6) were chosen to model the sample system and illustrate the voltage collapse problem. Thus, as discussed in [45, 46], the stability region for system (2.6) can be readily defined by

$$\begin{aligned} \vartheta(\omega, \delta, V) = & \frac{1}{2}M\omega^2 - B(V_1V_2 \cos \delta - V_{1o}V_{2o} \cos \delta_o) \\ & + \frac{1}{2}(B - B_C)(V_2^2 - V_{2o}^2) + \frac{1}{2}B(V_1^2 - V_{1o}^2) \\ & - P_d(\delta - \delta_o) + Q_d \ln \left( \frac{V_2}{V_{2o}} \right) - Q_G \ln \left( \frac{V_1}{V_{1o}} \right) \end{aligned} \quad (2.7)$$

where  $V_{1o}$ ,  $V_{2o}$  and  $\delta_o$  stand for the steady state values of the bus voltage magnitudes and angles, which depend on the values of the parameters  $P_d$ ,  $X_L$  and  $B_C$ . Observe that the generator reactive power  $Q_G$  term in this equation is not really “active” unless the generator hits a limit, in which case  $V_1 \neq V_{1o}$ .

### 2.11.1 Stability Analysis

For different values of  $X_L$  and  $B_C$ , the system presents a maximum loadability point  $P_{d_{\max}}$  corresponding to the “turning” points on the PV curves of Figures 2.11-2 and 2.11-3, for the system with and without generator limits, respectively. These maximum points are also known as the points of collapse, which in nonlinear systems theory can be shown to be either saddle-node bifurcation points for the system without generator limits (Figure 2.11-2), or limit-induced bifurcation points for the system with generator limits (Figure 2.11-3) [9, 24]. In these figures, the points “above” the bifurcation point (“high” voltage values) correspond to stable equilibrium points (s.e.p.), whereas the points “below” (“low” voltage values) are unstable equilibrium points (u.e.p.). Observe on these figures that, for both types of bifurcations, there are no equilibrium points, in parameter space, “beyond” the bifurcation point, which is the main reason for the voltage collapse in this example, as discussed throughout

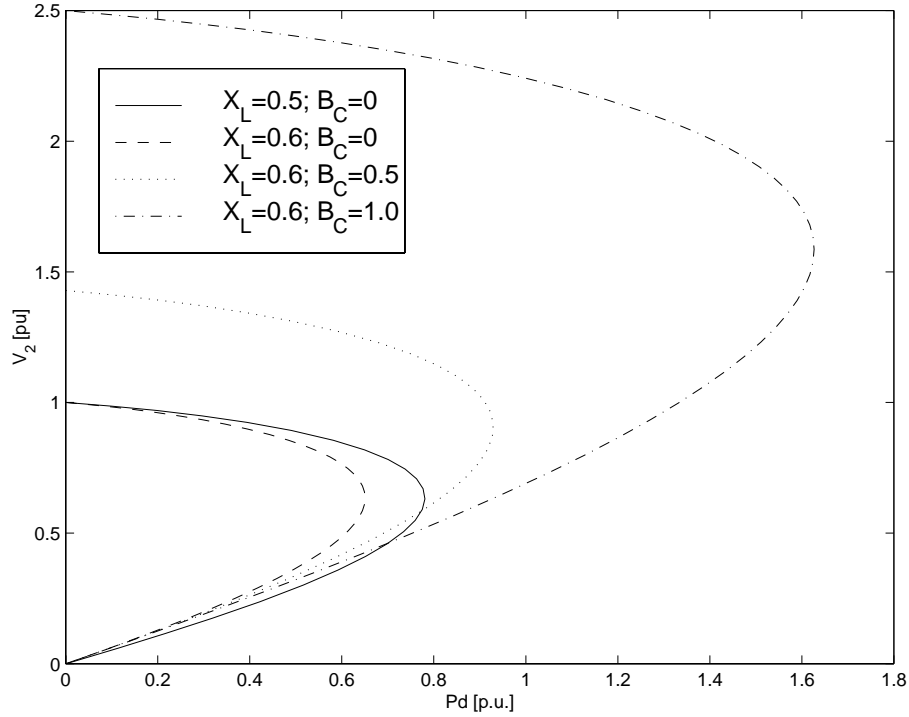


Figure 2.11-2. Bifurcation diagrams or PV curves for the test system without generator limits. The maximum value of  $P_d$  corresponds to a saddle-node bifurcation point.

this chapter and demonstrated by the time domain analysis of Section 2.11.2. (This sample system cannot have Hopf bifurcations due to  $R = 0$  [10, 12].)

Observe in Figures 2.11-2 and 2.11-3 that when the contingency is applied by increasing the value of  $X_L$ , the maximum loadability point is reduced. Generator limits have a negative effect on this point as well, as these limits reduced even further the maximum system loadability. On the other hand, as the compensation level increases by increasing the value of  $B_C$ , the maximum loadability point increases.

To illustrate how the stability of the system is affected by all these parameters, i.e.,  $P_d$ ,  $X_L$ ,  $B_C$  and generator limits, the corresponding TEF profiles are obtained by evaluating (2.7) at the corresponding u.e.ps. These energy profiles are depicted in Figures 2.11-4 and 2.11-5. Figure 2.11-4 shows the energy profile for the system without generator limits, whereas Figure 2.11-5 illustrates the negative effect that generator limits have on this region. Observe that the area decreases as the power demand  $P_d$  increases; it increases when  $B_C$  is applied; and decreases when  $X_L$  is increased (to simulate a contingency).

From these energy profiles, one can conclude that by applying shunt compensation or shedding load, i.e., increasing  $B_C$  or reducing  $P_d$ , respectively, the stability region of the system is increased, allowing the operator to recover the system after a fault. The question then is how fast this remedial measures should be taken to be able to recover the system; this problem is addressed in the next section.

It is interesting to see that as  $B_C$  is increased, the stability region increases and the bifurcations move away, i.e.,  $P_{d\max}$  also increases. However, there is a point where

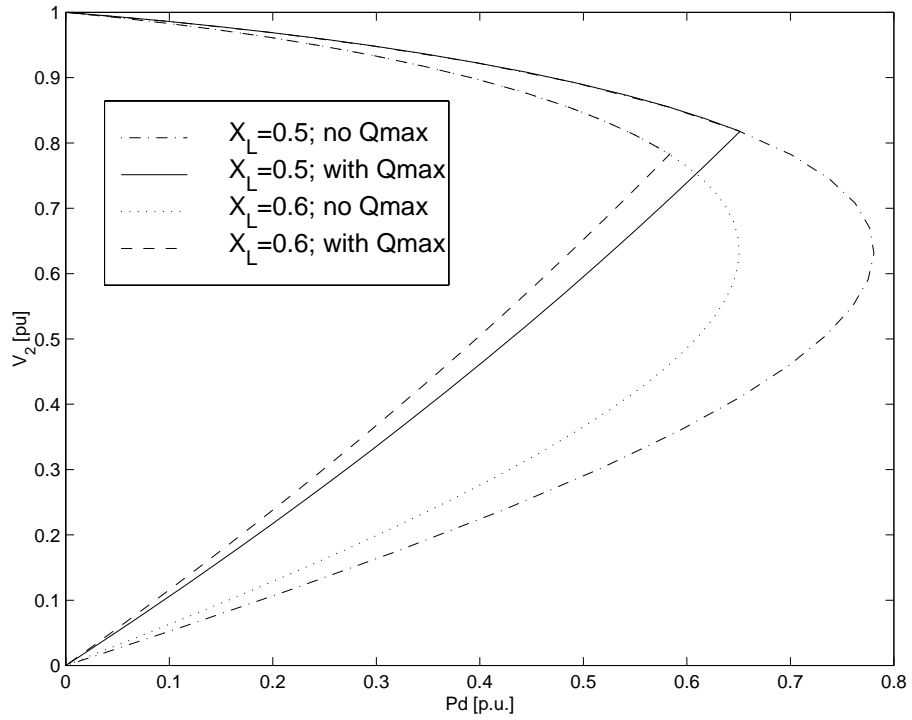


Figure 2.11-3. Effect of generator Q-limits in the bifurcation diagrams or PV curves for the test system. The maximum value of  $P_d$  corresponds to a limit-induced bifurcation point.

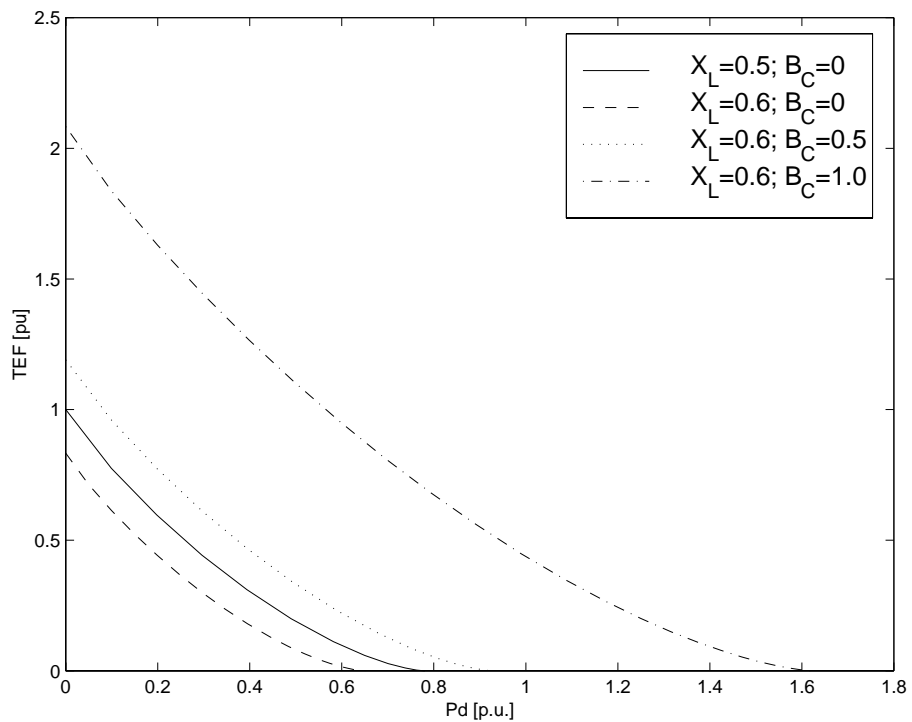


Figure 2.11-4. TEF profiles for the test system without generator Q-limits.

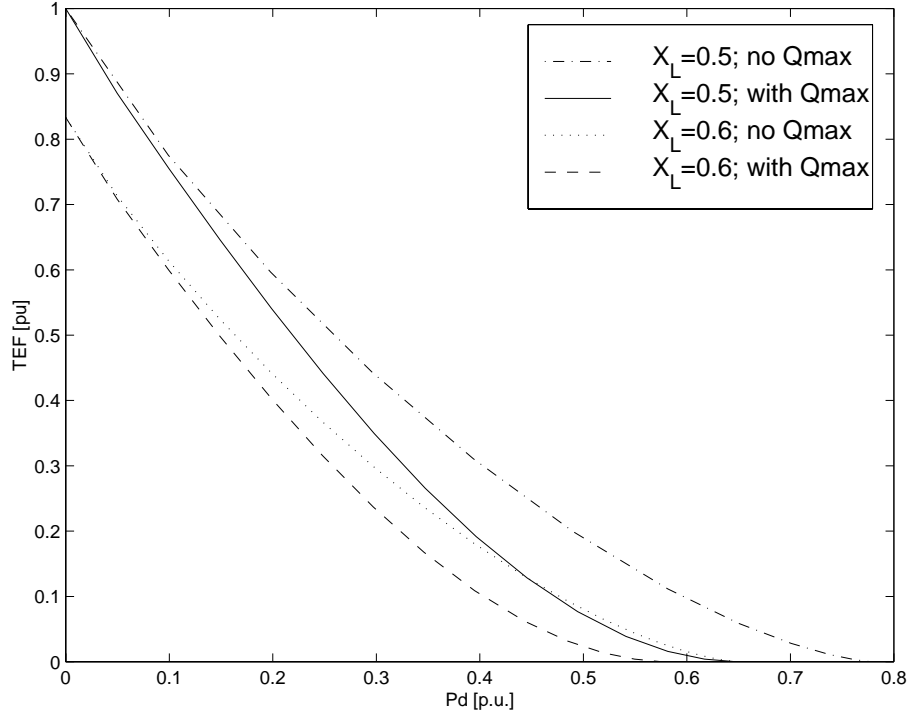


Figure 2.11-5. Effect of generator Q-limits on the TEF profiles for the test system.

this trend reverses, as explained in [8], which corresponds to a “maximum” bifurcation point; for this system, the maximum bifurcation points are obtained at  $B_C = 1/X_L$ .

### 2.11.2 Time Domain Analysis

1) *Neglecting Generator Limits:* A transmission system fault at a power demand level of  $P_d = 0.7$  is simulated by changing the value of  $X_L$  from 0.5 to 0.6, yielding a system collapse, as the system has no s.e.p. at the operating condition defined by  $P_d = 0.7$  and  $X_L = 0.6$  (see Figures 2.11-2 and 2.11-4). The “fault” is applied at 1 s, resulting in the collapse of voltage  $V_2$  and the corresponding monotonic increase of the system frequency  $\omega$  and angle  $\delta$  (the fault trajectories for these variables are similar to the ones depicted in Figure 2.11-6).

For this fault trajectory, the “potential” energy, which is obtained by subtracting the “kinetic” energy term  $1/2 M\omega^2$  from the total TEF defined in (2.7), is tracked for each post-contingency equilibrium point defined by the values of  $X_L$ ,  $B_C$  and  $P_d$ . The point where this energy reaches a maximum corresponds to the point where the system “leaves” the stability region; this point is known as the Potential Energy Boundary or PEB [46]. The point in time where this maximum occurs can be used as an estimate for the “critical clearing” time, i.e., the time at which the fault should be cleared or a control action such as shunt compensation or load shedding should take place. Thus, the critical times estimates obtained using the PEB technique are: 6.3 s to restore  $X_L$  to its original value of 0.5, i.e., “clear” the fault; 6.3 s and 7 s for applying shunt compensations of  $B_C = 0.5$  and  $B_C = 1$ , respectively; and 7.7 s for

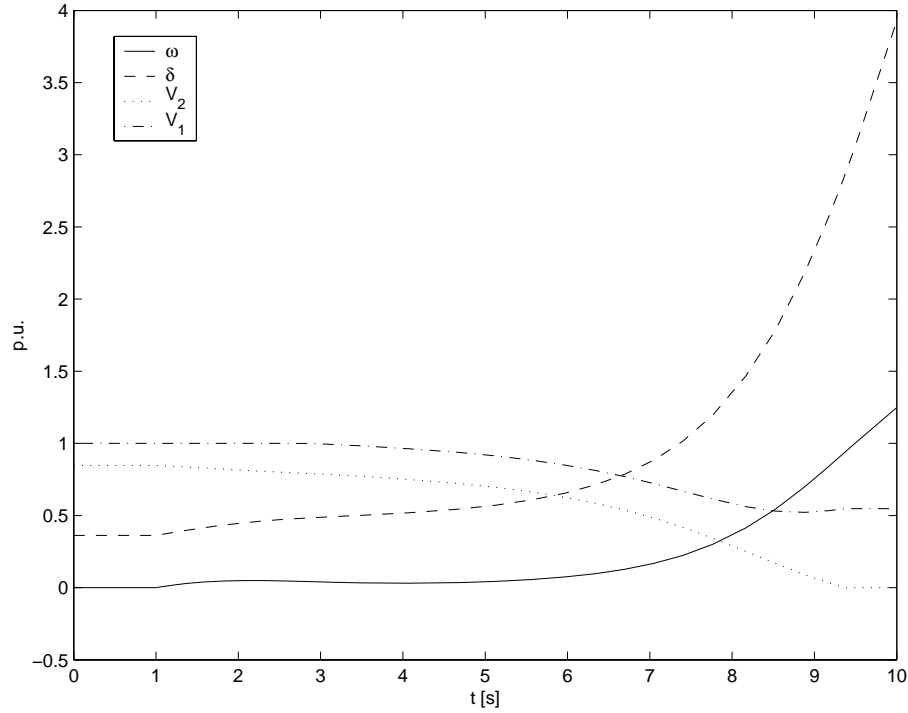


Figure 2.11-6. System trajectories for a fault simulated by increasing  $X_L$  from 0.5 to 0.6 at 1 s when Q-limits are considered. Generator voltage control is lost at about 3 s and the system collapses.

shedding load to  $P_d = 0.4$ .

These estimates are then used to determine the actual critical times through time simulation. Hence, for fault clearance, simulated by restoring  $X_L$  to its original value, the system recovers if the fault is cleared at or before 6 s, and does not recover if the fault is cleared at 6.1 s or longer. For a compensation level of  $B_C = 0.5$  applied at or before 6 s, the system recovers; for connection times of 6.1 s or longer, the system does not recover. For a compensation level of  $B_C = 1$ , the system recovers when applied at or before 6.8 s, and does not recover if applied at 6.9 s or longer. Finally, for load shedding, the system recovers when applied at or before 7.4 s, and does not recover when applied at 7.5 s or longer. A comparison of the computed and estimated “clearing” times for the different recovery options are summarized in Table 2.11-1; observe that these results basically validate the “energy” analysis.

2) *Considering Generator Limits:* In this case, a transmission system fault at a demand level of  $P_d = 0.6$  is again simulated by increasing the value of  $X_L$  from 0.5 to 0.6. The system also collapses due to lack of a faulted system s.e.p. at these operating conditions, as depicted in Figures 2.11-4 and 2.11-5. Observe that this system will not be able to operate at the previous demand level of  $P_d = 0.7$ .

The fault is applied at 1 s, obtaining the fault trajectory depicted in Figure 2.11-6, which is similar to the one obtained for the system without limits. Observe that generator control of voltage  $V_1$  is lost at about 3 s due to Q-limits, the voltage  $V_2$  collapses and frequency  $\omega$  and angle  $\delta$  monotonically increase. Furthermore, it can



Recovery Option	TEF Analysis	Time Analysis	
		Stable	Unstable
$X_d = 0.5$	6.3	6.0	6.1
$B_c = 0.5$	6.3	6.0	6.1
$B_c = 1.0$	7.0	6.8	6.9
$P_d = 0.4$	7.7	7.4	7.5

Table 2.11-1. Clearing times in seconds for different recovery options for the test system without Q-limits.

Recovery Option	TEF Analysis	Time Analysis	
		Stable	Unstable
$X_d = 0.5$	3.5	3.5	3.6
$B_c = 0.5$	6.3	6.0	6.1
$B_c = 1.0$	6.7	6.7	6.8
$P_d = 0.4$	6.7	6.3	6.4

Table 2.11-2. Clearing times in seconds for different recovery options for the test system when considering Q-limits.

be seen that the voltage first decreases slowly (1 to 6 s), to then rapidly collapse (6 to 9 s), as predicted by the theory; the rate of collapse is affected by the chosen value of the time constant  $\tau$  in the load model of equations (2.6).

Once more, the “potential” energy defined with respect to a given s.e.p., which depends on the values of  $X_L$ ,  $B_C$  and  $P_d$ , can be used to estimate the critical time for different recovery strategies, i.e., fault clearance ( $X_L$  recovery), application of shunt compensation (increase  $B_C$ ), and load shedding (reduce  $P_d$ ). Thus, the critical times are determined to be 3.5 s to clear the fault, 6.3 s for applying  $B_C = 0.5$  (see Figure 2.11-7), 6.7 s for applying  $B_C = 1$ , and 6.7 s for shedding load to  $P_d = 0.4$ .

Time domain analysis yields the following results: The system recovers if the fault is cleared by changing the value of  $X_L$  back to 0.5 at or before 3.5 s, and does not recover if it is changed at 3.6 or after. If shunt compensation  $B_C = 0.5$  is applied at or before 6 s, the system recovers (see Figure 2.11-8), and does not recover for application times of 6.1 s or longer. For a compensation level of  $B_C = 1$ , the system recovers if applied at or before 6.7 s; does not recover if applied at 6.8 s or longer. Finally, for load shedding of  $P_d = 0.4$ , the system recovers when applied at 6.3 s, and does not recover when applied at 6.4 s. A comparison of the computed and estimated “clearing” times for the different recovery options are summarized in Table 2.11-2; once again, these results validate the TEF analysis.

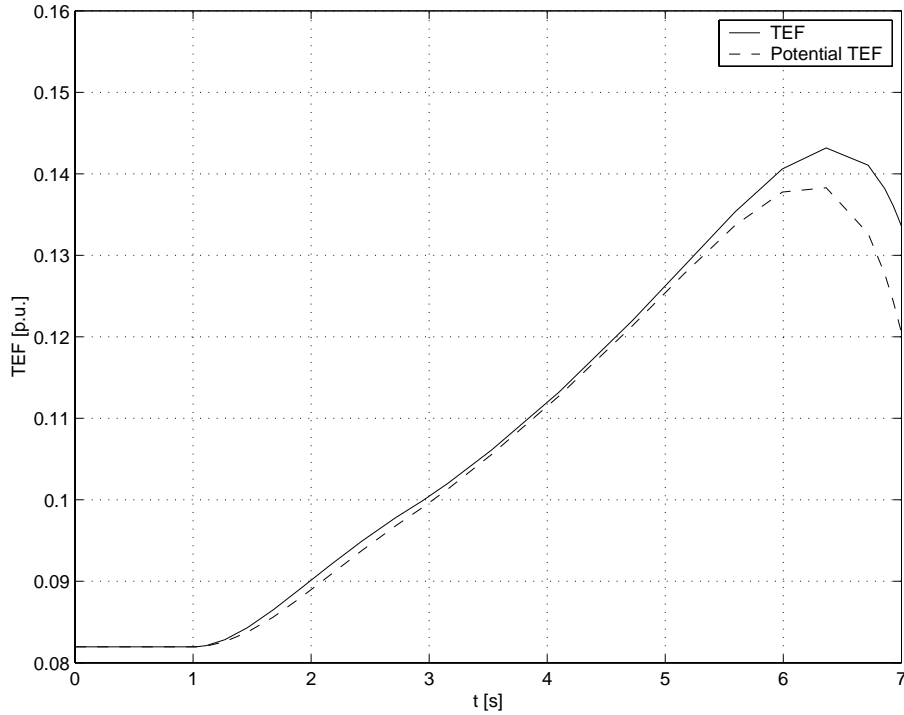


Figure 2.11-7. TEF trajectories for the faulted system when considering Q-limits and recovery by shunt compensation  $B_C = 0.5$ . The maximum point on the Potential TEF trajectory yields an estimate of the critical application time.

### 2.11.3 Conclusions

From the previous analyses, one can conclude that shunt compensation and load shedding have a positive effect on system recovery, as expected; however, the problem is to determine how much and how fast [56]. Observe that one could define “optimal” values of compensation and load shedding, i.e., the “minimum” compensation and/or load shedding that allows to recover the system within “reasonable” application times. The answer would depend on how much compensation and load to be shed is available, as well as the response times of the switching devices controlling these system elements. Furthermore, shunt and load location should also be considered, as it is well known that physical location of these elements has an effect on the stability of the system. Control limits, such as generator AVR limits, should also be factored into the analysis, as these have a significant negative effect on the stability regions, increasing the compensation and load shedding levels and reducing the associated application times required to recover the system.

Notice that the TEF is used in this simple example to illustrate the relative effect of compensation and load shedding on system stability, as well as to approximately determine optimal application times. Similar energy functions can be used in more realistic systems to carry out these types of studies; however, results are only approximate and should always be checked against time domain simulations. Various techniques based on TEF analyses have been proposed to determine “optimal” control

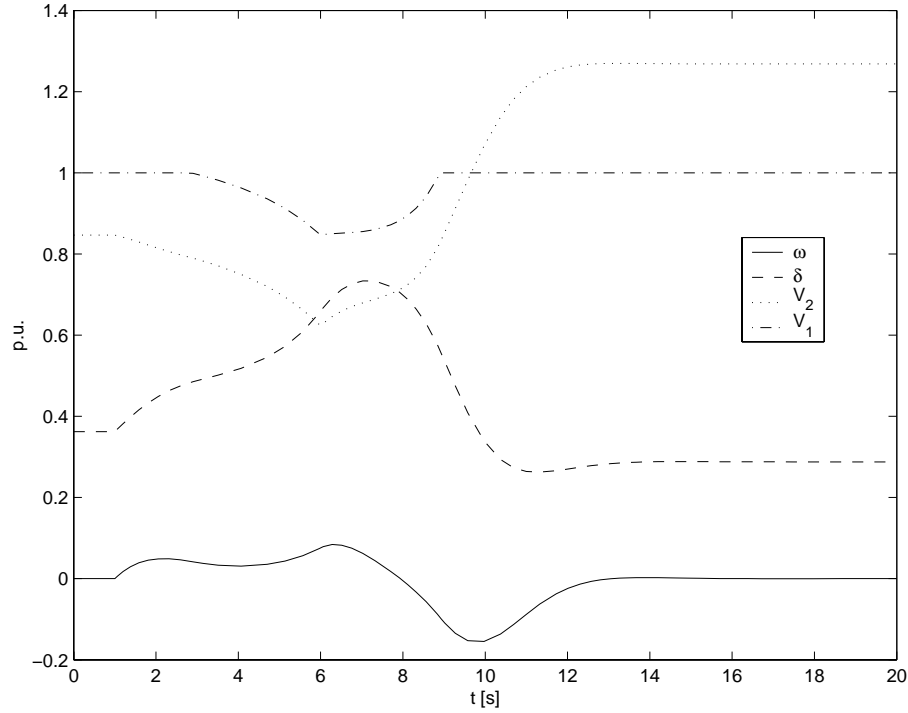


Figure 2.11-8. System trajectories for the faulted system when considering Q-limits for shunt compensation  $B_C = 0.5$  applied at 6 s. Generator voltage control is temporary lost but the system recovers.

strategies in realistic systems to avoid system collapse, as shown in [22].

## 2.12 GLOSSARY OF TERMS

This section explains some of the terms used in the chapter. Most of the explanations are informal. More formal definitions of some of the mathematical terms may be found in [32, 49].

**bifurcation:** A bifurcation is a qualitative change in the system, such as when an equilibrium disappears (saddle-node bifurcation) or the steady state changes from an equilibrium to an oscillation (Hopf bifurcation).

**bifurcation set:** The bifurcation set is those parameters (points in parameter space) at which a bifurcation occurs. The bifurcation set is often composed of hypersurfaces and their intersections.

**eigenvector, eigenvalue:** Eigenvectors and eigenvalues are associated with a matrix, which in our case is the Jacobian of power system differential equations evaluated at an equilibrium. This Jacobian describes the linear system which best approximates the differential equations close to the equilibrium. The eigenvalues and eigenvectors describe the modes of this linear system. Roughly speaking, a mode is a special transient behavior with a single time constant (in the case of a monotonically growing or decaying mode) or a single damping and frequency (in the case of an oscillatory

modes). Linear systems can be decomposed into modes and the usual behavior of the system is the result of many modes acting at once. (This explanation somewhat fudges the issue of nontrivial Jordan forms.) Each mode has an eigenvalue and right and left eigenvectors associated with it. For a monotonically growing or decaying mode, the associated eigenvalue is a real number which describes the modal damping (the eigenvalue is the negative of the reciprocal of the time constant). For an oscillatory mode, the associated eigenvalue is a complex number which describes the modal damping and frequency. (the real part of the eigenvalue describes the modal damping and the imaginary part describes the modal frequency). Each mode has a right eigenvector and a left eigenvector associated with it. The right eigenvector describes the relative participation of state variables in the mode. The left eigenvector describes the relative participation of each equation in the mode.

**equilibrium:** An equilibrium of a differential equation is a point in state space which does not move: if the state is initially at the equilibrium, it will stay there forever. (This description is idealized in the case of an unstable equilibrium because in practice a disturbance will displace the state from the equilibrium and then the unstable dynamics will cause a transient to occur moving the state away from the equilibrium.) A stable equilibrium of a power system model corresponds to an operating point of the power system.

**Jacobian:** The Jacobian of a set of  $n$  equations in  $n$  variables is an  $n \times n$  matrix of partial derivatives whose entries are the derivatives of each equation with respect to each variable. The Jacobian is often evaluated at an equilibrium and then used to study the small signal stability of the equilibrium. The Jacobian evaluated at an equilibrium of differential equations describes the linear system which best approximates the differential equations close to the equilibrium.

**periodic orbit:** A periodic orbit is a steady state oscillation. A periodic orbit is visualized in the state space as a closed loop which the state traverses once every period.

**quasistatic:** The quasistatic approximation regards the parameters as variable inputs to the system whose dynamics are neglected. Thus although the parameters can vary and pass through a value, the system dynamics are computed assuming that the parameter is fixed at that value. The quasistatic approximation holds when the parameter variation is slow enough compared to the dynamics of the rest of the system because then the parameters can be approximated as constant at the timescale of the dynamics of the rest of the system.

**stability:** There are many stability terms and concepts in voltage collapse studies. These terms and concepts arise in two ways: Firstly there are terms used to help classify or describe actual power system events and secondly there are quite different standard stability concepts which have precise meanings for particular power system models. There are also definitions which combine some aspects of both approaches [38]. One example from Section 2.1 is

An operating point of a power system is *small disturbance stable* if,

following any small disturbance, the power system state returns to be identical or close to the pre-disturbance operating point.

Since this chapter addresses detailed mechanisms of voltage collapse in power system models and attempts to explain how theorists think of voltage collapse, it is most useful here to discuss the stability terms which can be applied to power system models. These stability terms are fairly standard across most areas of mathematics, physics and engineering.

Stability is a property of a steady state such as an equilibrium or a periodic orbit. (In a nonlinear system such as a power system, it is important not to associate stability with the entire system because one equilibrium may be stable at the same time as other equilibria are unstable.) Suppose that the power system is modeled by a set of nonlinear differential equations. Then

An equilibrium of a power system model is *asymptotically stable* if, following any small disturbance, the power system state tends to the equilibrium.

This notion of small signal stability needs to be extended when the power system model is elaborated beyond differential equations. One elaboration is differential-algebraic equations. If the power system is modeled by differential-algebraic equations, the “stability” of the algebraic equations must be addressed. There is no problem if the small disturbance is assumed to satisfy the algebraic equations. If the small disturbance does not satisfy the algebraic equations, then to define and discuss stability some assumption must be made about whether and how the state changes to satisfy the algebraic equations (see Appendix 2.B). (Note that a useful definition of stability requires that the assumptions used in the stability definitions are consistent with the power system model being used and that the power system model is a reasonable approximation to the power system for the particular issue under study.)

Another elaboration is needed when the power system equations can change discretely as when generator reactive power limits change or when load tapchanging transformers are modeled with discrete taps. Then the state vector includes discrete quantities which, for example, describe which generators are limited and the tap positions. An equilibrium is a state in which both the continuous and discrete quantities do not change. Small signal stability of such an equilibrium would additionally require that any small disturbance not alter the discrete states.

Large disturbance stability of an equilibrium is best approached by considering the set of disturbances for which the resulting transient returns to the equilibrium. For example, if the disturbances are regarded as a change in state to a certain initial condition, then the set of initial conditions for which the resulting transient returns to the equilibrium is called the basin of attraction of the equilibrium. An equilibrium with a larger basin of attraction withstands a larger set of disturbances and is more stable in the large disturbance sense.

**state space:** The system state is a vector of quantities which vary during transients. The number and selection of states in the system state vector allow a complete description of the transient. If the system has three states, then the state vector has

three components and can be visualized as point in three dimensional space, and the state space is three dimensional. A similar concept applies when there are more than three states, say  $n$  states: the state vector is thought of a point in an  $n$  dimensional state space.

## 2.13 REFERENCES

- [1] S. Abe, Y. Fukunaga, A. Isono, B. Kondo, "Power System Voltage Stability," *IEEE Transactions on Power Apparatus and Systems*, Vol. PAS-101, No. 10, October 1982, pp. 3830–3839.
- [2] E. H. Abed, J. C. Alexander, H. Wang, A. M. A. Hamdan, H.-C. Lee, "Dynamic Bifurcations in a Power System Model Exhibiting Voltage Collapse," *International Journal of Bifurcation and Chaos*, Vol. 3, 1993, pp. 1169–1176.
- [3] E. H. Abed, P. P. Varaiya, "Nonlinear Oscillations in Power Systems," *International Journal of Electric Energy and Power Systems*, Vol. 6, No. 1, January 1984, pp. 37–43.
- [4] R. H. Abraham, C. D. Shaw, *Dynamics, the Geometry of Behavior*, vols. 1–4, Aerial Press, Santa Cruz, CA, 1988.
- [5] V. Ajjarapu, B. Lee, "Bifurcation Theory and its Application to Nonlinear Dynamical Phenomenon in an Electric Power System," *IEEE Transactions on Power Systems*, Vol. 7, February 1992, pp.424–431.
- [6] C. W. Brice et. al., "Physically Based Stochastic Models of Power System Loads," U.S. Dept. of Energy Report DOE/ET/29129, Sept. 1982.
- [7] C. A. Cañizares, "Conditions for Saddle-Node Bifurcations in AC/DC Power Systems," *Int. Journal Electrical Energy & Power Systems*, Vol. 17, No. 1, 1995, pp. 61–68.
- [8] C. A. Cañizares, "Calculating Optimal System Parameters to Maximize the Distance to Saddle-Node Bifurcations," *IEEE Transactions on Circuits and Systems-I*, Vol. 45, No. 3, March 1998, pp. 225–237.
- [9] C. A. Cañizares, F. L. Alvarado, "Point of Collapse and Continuation Methods for Large AC/DC Systems," *IEEE Transactions on Power Systems*, Vol. 8, No. 1, February 1993, pp. 1–8.
- [10] C. A. Cañizares, S. Hranilovic, "Transcritical and Hopf bifurcations in ac/dc systems," in [29], pp. 105–114.
- [11] H.-D. Chiang et al., "Chaos in Simple Power System," *IEEE Transactions on Power Systems*, Vol. 8, No. 4, November 1993, pp. 1407–1417.

- [12] H.-D. Chiang, F. F. Wu, "Stability of Nonlinear Systems Described by a Second-Order Vector Differential Equation," *IEEE Transactions on Circuits and Systems*, Vol. CAS-35, No. 6, June 1988, pp. 703–711.
- [13] M. L. Crow, J. Ayyagari, "The Effect of Excitation Limit on Voltage Stability," *IEEE Transactions on Circuits and Systems-I*, Vol. 42, No. 12, December 1995, pp.1022–1026.
- [14] T. Van Cutsem, "A Method to Compute Reactive Power Margins with Respect to Voltage Collapse," *IEEE Transactions on Power Systems*, Vol. 6, No. 1, February 1991, pp. 145–156.
- [15] T. Van Cutsem, Y. Jacquemart, J.-N. Marquet, P. Pruvot, "Extensions and Applications of a Mid-Term Voltage Stability Method," in [29], pp. 251–263.
- [16] T. Van Cutsem, "An Approach to Corrective Control of Voltage Instability Using Simulation And Sensitivity," *IEEE Transactions on Power Systems*, Vol. 10, No. 2, May 1995, pp. 616–622.
- [17] T. Van Cutsem, C. D. Vournas, "Voltage Stability Analysis in Transient and Mid-Term Time Scale," *IEEE Transactions on Power Systems*, Vol. 11, No. 1, February 1996, pp. 146–154.
- [18] T. Van Cutsem, C. D. Vournas, *Voltage Stability of Electric Power Systems*, ISBN 0-7923-8139-4, Kluwer Academic Publishers, Boston, 1998.
- [19] C. L. DeMarco, A. R. Bergen, "Application of Singular Perturbation Techniques to Power System Transient Stability Analysis," *International Symposium on Circuits and Systems*, Montreal, May 1984, pp. 597–601 (abridged version). Also Electronics Research Laboratory Memo. No. UCB/ERL M84/7, U.of CA, Berkeley (complete version).
- [20] C. L. DeMarco, A. R. Bergen, "A Security Measure for Random Load Disturbances in Nonlinear Power System Models," *IEEE Transactions on Circuits and Systems*, Vol. CAS-34, No. 12, December 1987, pp. 1546–1557.
- [21] C. L. DeMarco, "A New Method of Constructing Lyapunov Functions for Power Systems," *International Symposium on Circuits and Systems*, 1988, pp. 905–908.
- [22] E. De Tuglie, M. La Scala, P. Scarpellini, "Real-time Preventive Actions for the Enhancement of Voltage-Degraded Trajectories," *IEEE Tans. Power Systems*, Vol. 14, No. 2, May 1999, pp. 561–568.
- [23] I. Dobson, H.-D. Chiang, "Towards a Theory of Voltage Collapse in Electric Power Systems," *Systems and Control Letters*, Vol. 13, 1989, pp. 253–262.
- [24] I. Dobson, L. Lu, "Voltage Collapse Precipitated by the Immediate Change in Stability When Generator Reactive Power Limits are Encountered," *IEEE Transactions on Circuits and Systems-I*, Vol. 39, No. 9, September 1992, pp. 762–766.

- [25] I. Dobson, L. Lu, “New Methods for Computing a Closest Saddle Node Bifurcation and Worst Case Load Power Margin for Voltage Collapse,” *IEEE Transactions on Power Systems*, Vol. 8, No. 3, August 1993, pp. 905–913.
- [26] I. Dobson, “The Irrelevance of Load Dynamics for the Loading Margin to Voltage Collapse and its Sensitivities,” in [29], pp. 509–518.
- [27] Proceedings: Bulk Power System Voltage Phenomena Voltage Stability and Security, EPRI Report EL-6183, Potosi, Missouri, January 1989.
- [28] Proceedings: Bulk Power System Voltage Phenomena, Voltage Stability and Security, ECC/NSF workshop, ECC Inc., Deep Creek Lake, MD, August 1991,
- [29] Proceedings: Bulk Power System Voltage Phenomena III, Voltage Stability, Security and Control, ECC/NSF workshop, Davos, Switzerland, August 1994.
- [30] F. D. Galiana, E. Handschin, A. R. Fiechter, “Identification of Stochastic Electric Load Models from Physical Data,” *IEEE Transactions on Automatic Control*, Vol. AC-19, December 1974, pp. 887–893.
- [31] S. Greene, I. Dobson, F. L. Alvarado, “Sensitivity of the Loading Margin to Voltage Collapse with respect to Arbitrary Parameters,” *IEEE Transactions on Power Systems*, Vol. 12, No. 1, February 1997, pp. 262–272.
- [32] J. Guckenheimer, P. Holmes, *Nonlinear Oscillations, Dynamical Systems and Bifurcations of Vector Fields*, Springer-Verlag, NY, 1986.
- [33] P. Kokotović, H. K. Khalil, J. O’Reilly, *Singular Perturbation Methods in Control: Analysis and Design*, Academic Press, 1986.
- [34] P. Kundur, *Power System Stability and Control*, McGraw-Hill, New York, 1993.
- [35] W. Ji, V. Venkatasubramanian, “Dynamics of a Minimal Power System: Invariant Tori and Quasi-Periodic Motions,” *IEEE Transactions on Circuits and Systems-I*, Vol. 42, No. 12, December 1995, pp. 981–1000.
- [36] B. Lee, V. Ajjarapu, “Period-Doubling Route to Chaos in Electrical Power System,” *IEE Proceedings-C*, Vol. 140, No. 6, November 1993, pp. 490–496.
- [37] P.-A. Löf, G. Andersson, D. J. Hill, “Voltage Stability Indices for Stressed Power Systems,” *IEEE Transactions on Power Systems*, Vol. 8, No. 1, February 1993, pp. 326–335.
- [38] P.-A. Löf, D.J. Hill, S. Arnborg, G. Andersson, “On the Analysis of Long-Term Voltage Stability,” *Electric Power and Energy Systems*, Vol. 15, No. 4, 1993, pp. 229–237.



- [39] G. A. Manos, C. D. Vournas, "Bifurcation Analysis of a Generator-Motor System," *Proceedings of the fourth IEEE Mediterranean Symposium on New Directions in Control and Automation*, Maleme, Crete, Greece, June 1996, pp. 250–255.
- [40] "Voltage Stability of Power Systems: Concepts, Analytical Tools and Industry Experience," IEEE Special Publication, 90TH0358-2-PWR, 1990.
- [41] "Suggested Techniques for Voltage Stability Analysis," IEEE Special Publication, 93TH0620-5PWR, 1993.
- [42] NERC Interconnection Dynamics Task Force, *Survey of Voltage Collapse Phenomenon*, August 1991.
- [43] O'Malley, *Introduction to Singular Perturbation*, Academic Press, 1974.
- [44] T. J. Overbye, I. Dobson, C. L. DeMarco, "Q-V Curve Interpretations of Energy Measures for Voltage Security," *IEEE Transactions on Power Systems*, Vol. 9, No. 1, February 1994, pp. 331–340.
- [45] T. J. Overbye, C. L. DeMarco, "Voltage Security Enhancement Using Energy Based Sensitivities," *IEEE Transactions on Power Systems*, Vol. 6, No. 3, August 1991, pp. 1196–1202.
- [46] M. A. Pai, *Energy Function Analysis for Power System Stability*, Kluwer Academic, 1989.
- [47] P. W. Sauer, M. A. Pai, "A comparison of Discrete vs. Continuous Models Of Tap-Changing-Under-Load Transformers," in [29], pp. 643–650.
- [48] R. Seydel, *From Equilibrium to Chaos: Practical Bifurcation and Stability Analysis*, Second edition, Springer-Verlag, New York, 1994.
- [49] S. Strogatz, *Nonlinear Dynamics and Chaos: With Applications in Physics, Biology, Chemistry, and engineering*, Addison-Wesley, Reading, MA, 1994.
- [50] C.-W. Tan, M. Verghese, P. Varaiya, F.F. Wu, "Bifurcation, Chaos, and Voltage Collapse in Power Systems," *Proceedings of the IEEE*, Special issue on nonlinear phenomena in power systems, Vol. 83, No. 11, November 1995, pp. 1484–1539.
- [51] C. W. Taylor, *Power System Voltage Stability*, McGraw-Hill, New York, 1994.
- [52] J. M T. Thompson, H. B. Stewart, *Nonlinear Dynamics and Chaos: Geometrical Methods for Engineers And Scientists*, John Wiley, New York, 1986.
- [53] A. Tiranuchit, R. J. Thomas, "A Posturing Strategy Against Voltage Instabilities in Electric Power Systems," *IEEE Transactions on Power Systems*, Vol. 3, No. 1, February 1988, pp. 87–93.

- [54] V. Venkatasubramanian, H. Schättler, J. Zaborsky, “Voltage Dynamics: Study of a Generator With Voltage Control, Transmission, and Matched MW Load,” *IEEE Transactions on Automatic Control*, Vol. 37, No. 11, November 1992, pp. 1717–1733.
- [55] V. Venkatasubramanian, X. Jiang, H. Schättler, J. Zaborsky, “Current Status of the Taxonomy Theory of Large Power System Dynamics–DAE Systems with Hard Limits,” in [29], pp.15–103.
- [56] L. S. Vargas, C. A. Cañizares, “Time Dependence of Controls to Avoid Voltage Collapse,” *IEEE Transactions on Power Systems*, Vol. 15, No. 4, November 2000, pp. 1367–1375.
- [57] V. Venkatasubramanian, H. Schättler, J. Zaborsky, “Dynamics of Large Constrained Nonlinear Systems–A Taxonomy Theory,” *Proceedings of the IEEE*, special issue on nonlinear phenomena in power systems, Vol. 83, No. 11, November 1995, pp. 1530–1561.
- [58] C. D. Vournas, M.A. Pai, P.W. Sauer, “The Effect of Automatic Voltage Regulation on the Bifurcation Evolution in Power Systems,” *IEEE Transactions on Power Systems*, Vol. 11, No. 4, November 1996, pp. 1683–1688.
- [59] C. D. Vournas, M. Karystianos, N. G. Maratos, “Bifurcation Point and Loadability Limit a Solution of Constrained Optimization Problem,” *Proc. IEEE/PES Summer Meeting 2000*, Seattle, July 2000, pp.1883–1888.
- [60] K. T. Vu, C. C. Liu, “Dynamic Mechanisms of Voltage Collapse,” *Systems and Control Letters*, Vol. 15, 1990, pp. 329–338.
- [61] K. T. Vu, C. C. Liu, “Shrinking Stability Regions and Voltage Collapse in Power Systems,” *IEEE Transactions on Circuits and Systems–I*, Vol. 39, No. 4, April 1992, pp. 271–289.
- [62] H. O. Wang, E. A. Abed, A. M. A. Hamdan, “Bifurcations, Chaos, and Crises in Voltage Collapse of a Model Power System,” *IEEE Transactions on Circuits and Systems–I*, Vol. 41, No. 4, April 1994, pp. 294–302.
- [63] W. Xu, Y. Mansour, “Voltage Stability Analysis using Generic Dynamic Load Models,” *IEEE Transactions on Power Systems*, Vol. 9, No. 1, February 1994, pp. 479–493.

## Appendix 2.A HOPF BIFURCATIONS AND OSCILLATIONS

### 2.A.1 Introduction

A Hopf bifurcation is the onset of oscillatory behavior in a nonlinear system [4, 48, 49, 52]. A power system initially operating at a stable equilibrium typically starts oscillating when parameters change slowly so that a Hopf bifurcation occurs. A periodic orbit is a steady state oscillation. There are two ways to visualize a periodic orbit. The first way is that each state is plotted with respect to time and each of these graphs is a periodic waveform with the same period as shown in Figure 2.A-1(b). The second way is to imagine the state vector traversing a closed loop in the state space as shown in Figure 2.A-1(a). The state vector traverses the closed loop once every period. At a Hopf bifurcation of a stable equilibrium, the equilibrium becomes unstable by interacting with a periodic orbit. There are two types of Hopf bifurcation, called supercritical and subcritical, and what happens at these bifurcations is best explained by the examples of the next section.

### 2.A.2 Typical Supercritical Hopf Bifurcation

Figure 2.A-2(a) shows the state space of a dynamical model with two states; the arrows show the direction and magnitude of the movement of the states. At the center of Figure 2.A-2(a) is an equilibrium (an arrow of zero length indicates a place where the state has zero speed and does not change.) The equilibrium at the center of Figure 2.A-2(a) is stable; a perturbation of the state to the upper right hand corner of the plot leads to a transient which decays to the equilibrium in an oscillatory fashion. Figures 2.A-2(a) shows the position of the two states in state space as the transient evolves. The same transient is shown in Figures 2.A-2(b) which plots the two states against time.

Figure 2.A-3 shows the state space after the Hopf bifurcation has occurred. The equilibrium is now unstable and there is a stable periodic orbit near the equilibrium. For a stable periodic orbit, small perturbations lead to a transient which returns to the periodic orbit. If the state is initially near the unstable equilibrium, it will have increasing oscillations of increasing magnitude until it tends to the periodic orbit as shown in Figure 2.A-3. If the state is initially outside the periodic orbit, it will have oscillations of decreasing magnitude until it tends to the periodic orbit as shown in Figure 2.A-4.

The Hopf bifurcation is the critical case between Figures 2.A-2 and 2.A-3 and 2.A-4. In this case, the equilibrium is marginally stable and may be thought of as a periodic orbit of amplitude zero. Transients decay very slowly to the equilibrium in an oscillatory fashion. Thus at supercritical Hopf bifurcation of a stable equilibrium, the equilibrium becomes unstable and a stable periodic orbit forms. Before the bifurcation the state is at the stable equilibrium and after the bifurcation the state is oscillating according to the stable periodic orbit. The periodic orbit forms when the Hopf bifurcation occurs and grows from zero amplitude as the parameter is further changed. That is, an oscillation appears and grows.

### 2.A.3 Typical Subcritical Hopf Bifurcation

Figures 2.A-5 and 2.A-6 shows the state space of a dynamical model with two states. Before the bifurcation, there is a stable equilibrium at the center of Figure 2.A-5(a). Note the transient decaying to the equilibrium in an oscillatory fashion. There is also an unstable periodic orbit near the equilibrium. For an unstable periodic orbit, most small perturbations lead to a transient diverging from the periodic orbit. Figures 2.A-5 and 2.A-6 show examples of these transients. After the bifurcation, the periodic orbit disappears and the equilibrium becomes unstable as shown in Figure 2.A-7. Any perturbation from the equilibrium results in a oscillatory transient. The Hopf bifurcation is the critical case between Figures 2.A-5 and 2.A-6 and 2.A-7 when the unstable periodic orbit shrinks to zero amplitude and makes the equilibrium unstable.

Thus at subcritical Hopf bifurcation of a stable equilibrium, interaction with an unstable periodic orbit causes the equilibrium to become unstable. Before the bifurcation the state is at the stable equilibrium and after the bifurcation the state undergoes an oscillatory transient. The overall effect of slowly changing the system parameter so as to pass through the Hopf bifurcation is that the equilibrium becomes unstable and an unstable oscillation grows in amplitude.

### 2.A.4 Hopf Bifurcation in Many Dimensions

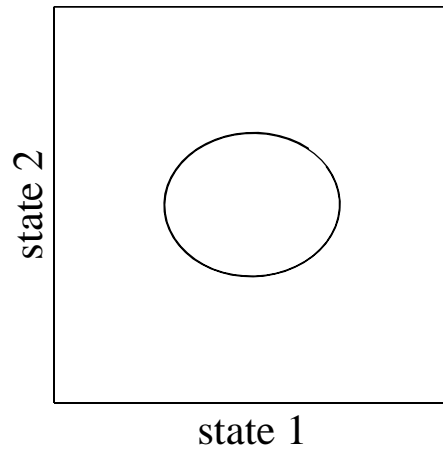
The Hopf bifurcation is explained above with two states and a single parameter. These small examples do in fact capture the essence of Hopf bifurcation in the large models of interest in power systems. Although in a large model all of the state variables would be involved in the Hopf bifurcation and oscillation to some extent, one could change coordinates in such a way that only the first two coordinates were involved in the Hopf bifurcation and all the remaining coordinates just decayed in a stable way. The first two coordinates would undergo the Hopf bifurcation in a way which is qualitatively identical to one of the small examples above. The extension to many parameters is analogous to the saddle node case: the set of parameters at which the Hopf bifurcation occurs is called the bifurcation set and it typically is composed of hypersurfaces in the parameter space.

### 2.A.5 Comparison of Hopf with Linear Theory

The Jacobian is obtained by linearizing the system about an equilibrium. The equilibrium involved in the Hopf bifurcation changes its stability as the bifurcation occurs and this is reflected in the Jacobian. In particular, a pair of complex eigenvalues cross the imaginary axis as the parameter is slowly varied. The Hopf bifurcation occurs when this pair of eigenvalues lies exactly on the imaginary axis.

Thus standard linear stability theory predicts the oscillatory instability of the equilibrium when a Hopf bifurcation occurs. The Hopf bifurcation results give additional information because it also takes account of the effect of nonlinearities. (These nonlinearities are present in power systems.) In particular, the presence and role of the periodic orbits and the two types of Hopf bifurcations cannot be understood from

(a) STATE SPACE



(b) TIME HISTORY

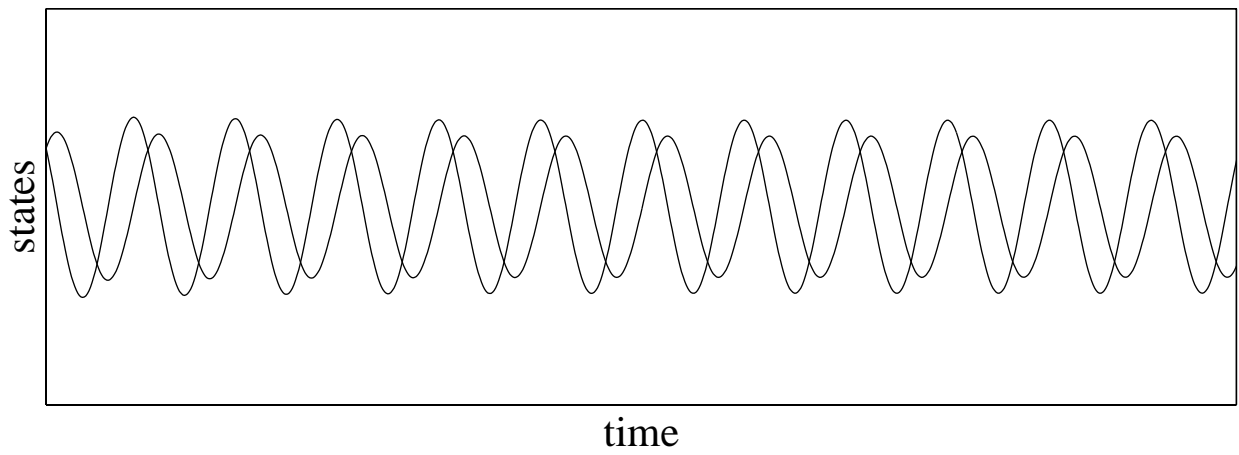


Figure 2.A-1. A periodic orbit.

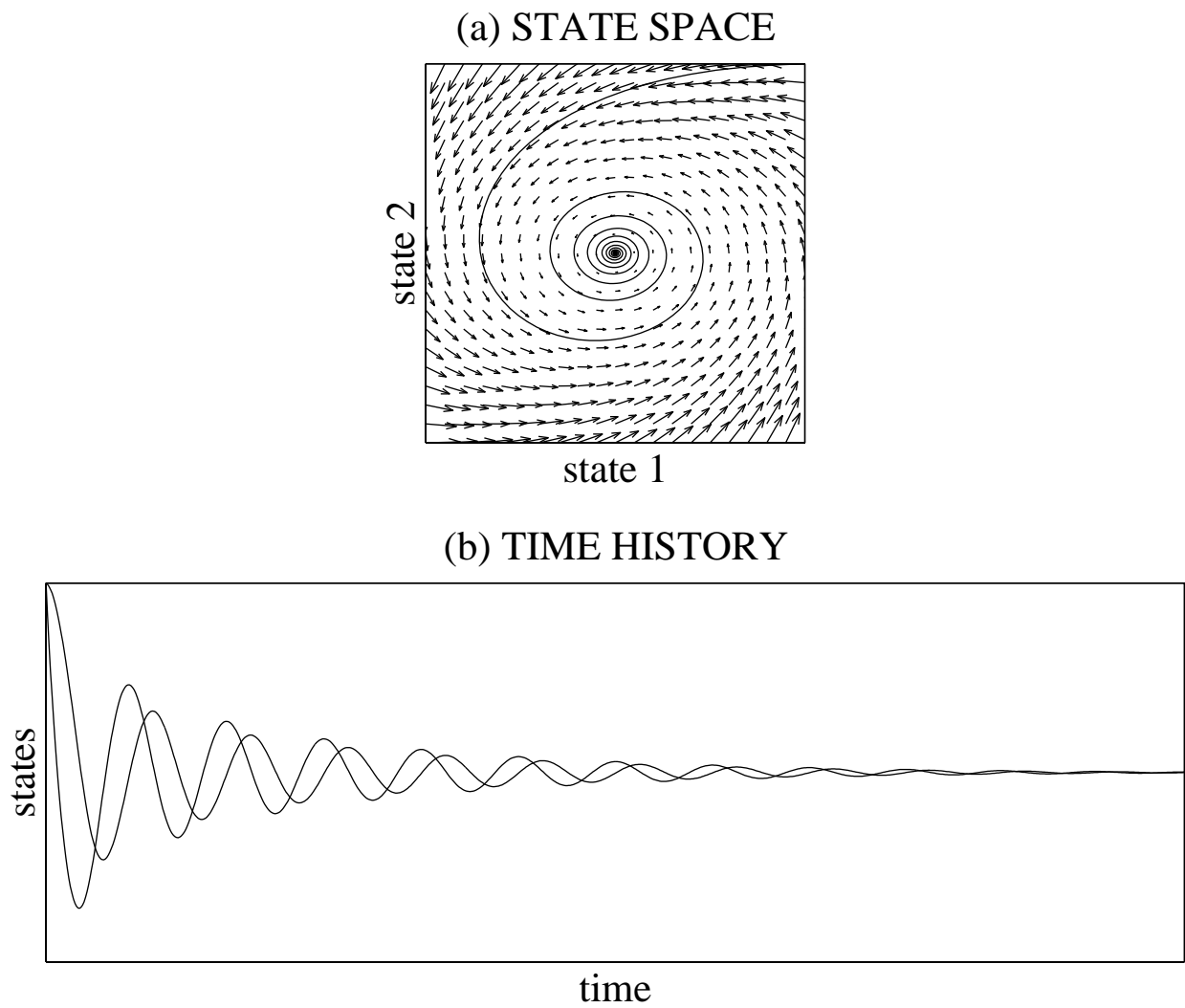


Figure 2.A-2. Before a supercritical Hopf bifurcation: stable equilibrium.

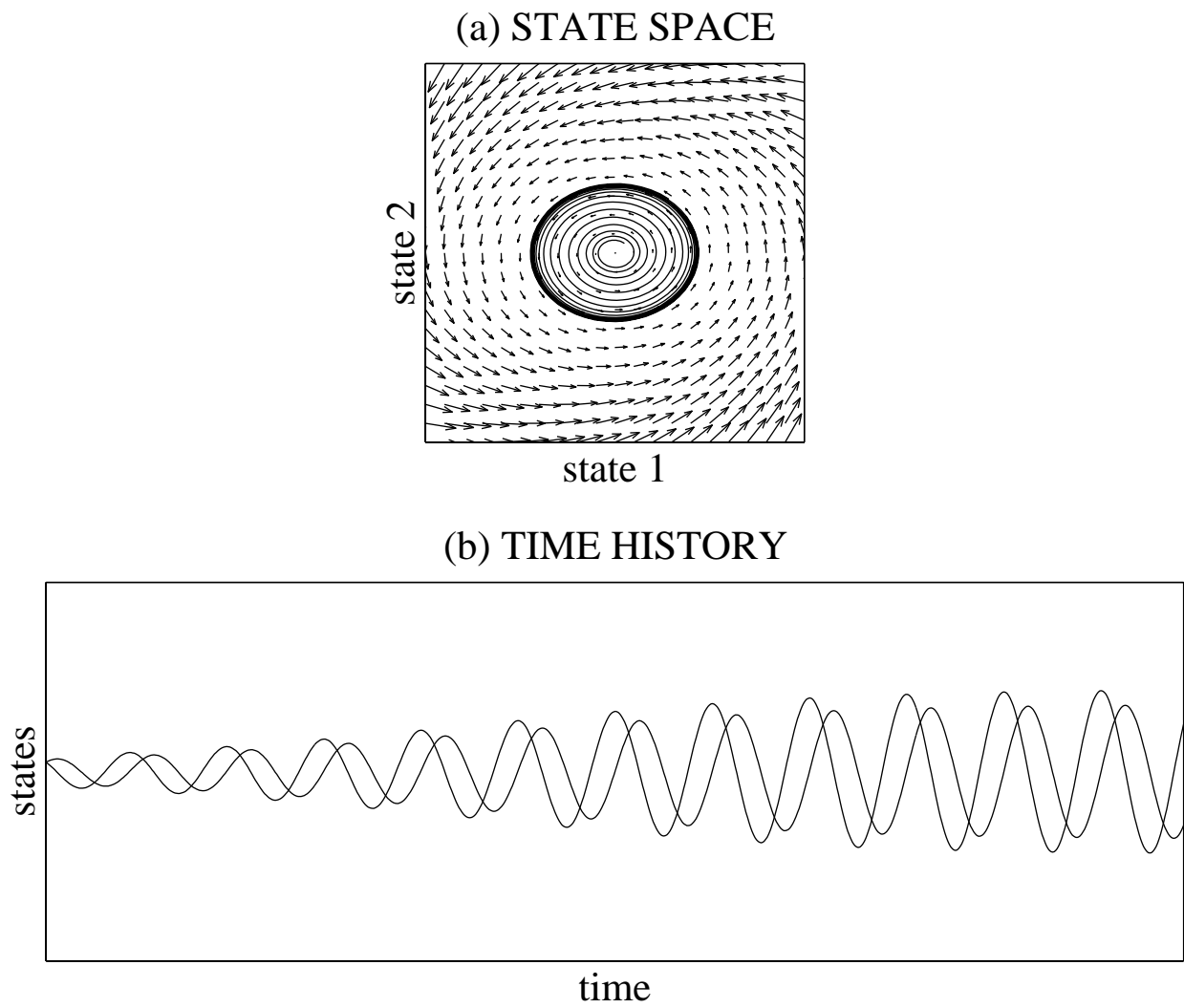
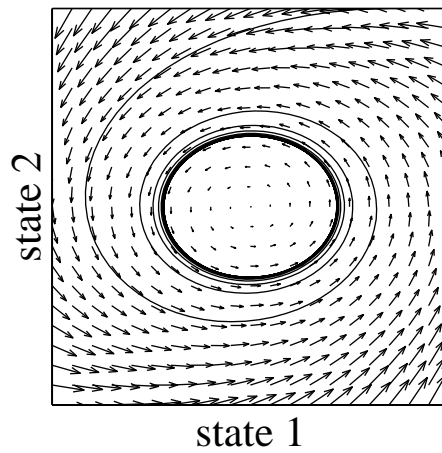


Figure 2.A-3. After a supercritical Hopf bifurcation: unstable equilibrium, stable periodic orbit.

(c) STATE SPACE



(d) TIME HISTORY

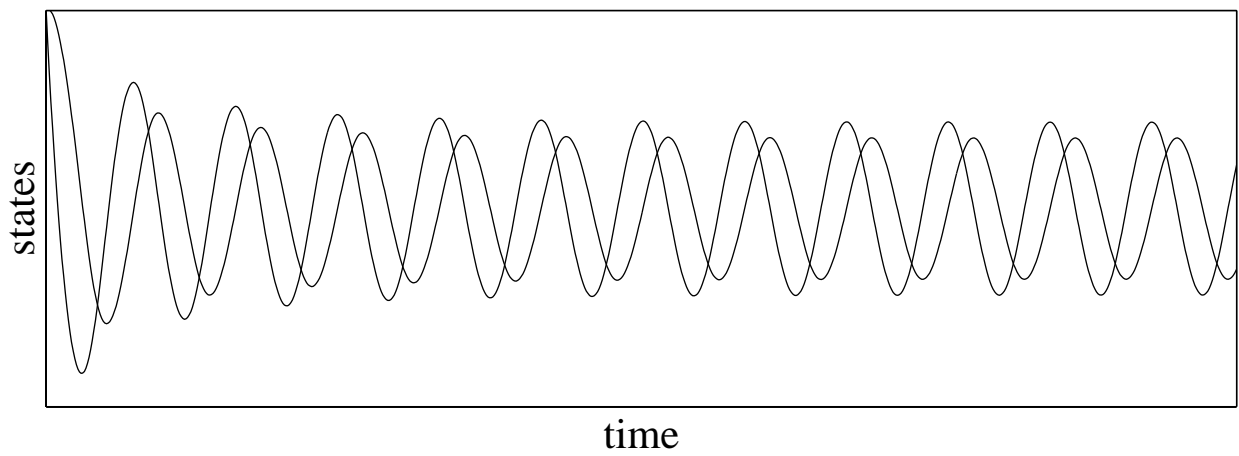


Figure 2.A-4. After a supercritical Hopf bifurcation: unstable equilibrium, stable periodic orbit.



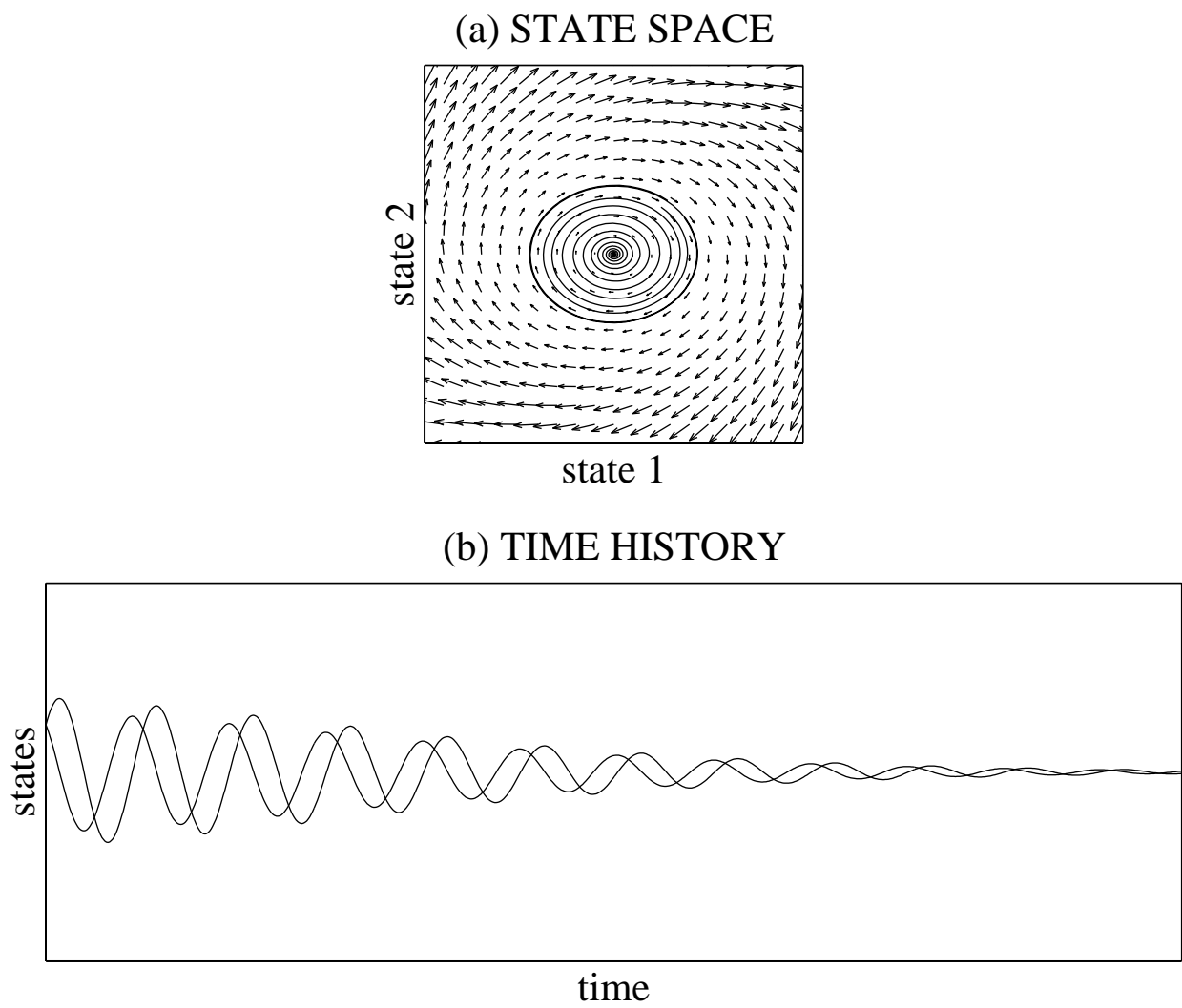
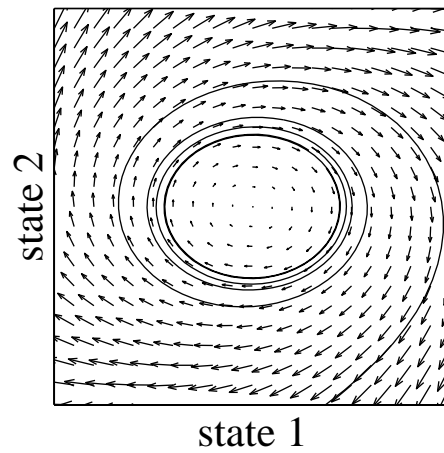


Figure 2.A-5. Before a subcritical Hopf bifurcation: stable equilibrium, unstable periodic orbit.

(c) STATE SPACE



(d) TIME HISTORY

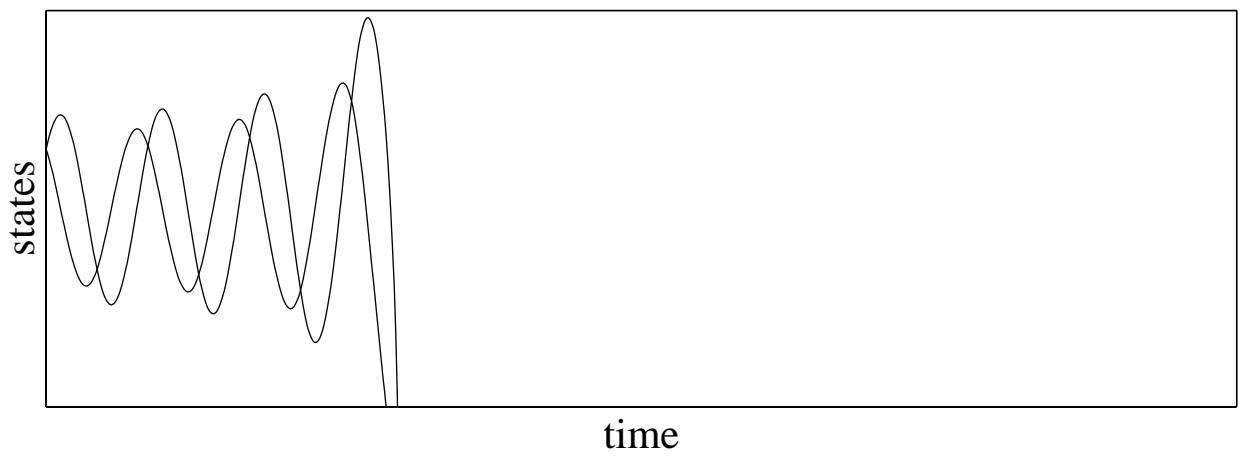


Figure 2.A-6. Before a subcritical Hopf bifurcation: stable equilibrium, unstable periodic orbit.

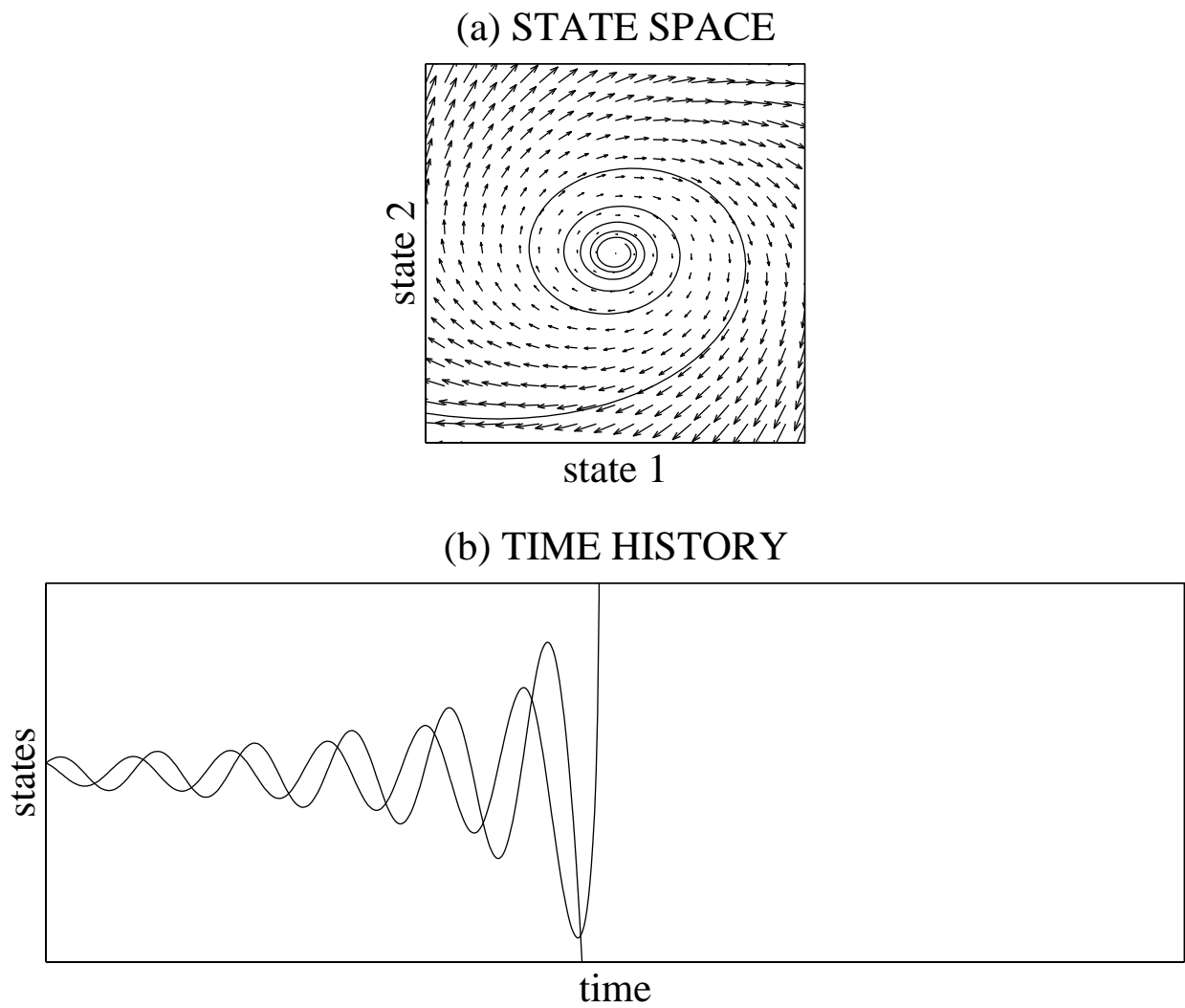


Figure 2.A-7. After a subcritical Hopf bifurcation: unstable equilibrium.

the linear theory. The two types of Hopf bifurcation of a stable equilibrium lead to quite different results: the supercritical bifurcation leads to a bounded oscillation whereas the subcritical bifurcation leads, at least initially, to a growing oscillatory instability. Thus the Hopf bifurcation gives a more complete picture than the linear theory of what happens in the power system when the instability is encountered.

### **2.A.6 Attributes of Hopf Bifurcation**

There are several useful indications of any Hopf bifurcation. All the following conditions occur at a Hopf bifurcation of a stable equilibrium and can be used to characterize or detect Hopf bifurcations:

- (1) A system which was previously in stable equilibrium begins a steady state oscillation in a periodic orbit or has a growing oscillatory transient as a parameter is slowly varied.
- (2) The system equilibrium persists as a parameter slowly varies, but it changes from stable to oscillatory unstable.
- (3) The system Jacobian has a pair of eigenvalues on the imaginary axis with nonzero frequency. That is, the system linearized about the equilibrium becomes unstable at a Hopf bifurcation by a pair of eigenvalues crossing the imaginary axis.

### **2.A.7 Modeling Requirements for Hopf Bifurcations**

Study of Hopf bifurcation requires the power system model to be differential equations with a slowly varying parameter. The parameter is often chosen to represent system loading. Alternatively, the power system model can be differential-algebraic if the algebraic equations are assumed to be enforced by underlying dynamics which are both fast and stable. Some studies may require the dynamics of loads to be represented.

### **2.A.8 Applications of Hopf Bifurcation to Power Systems**

The study of power system oscillations has a long history and the additional insights from Hopf bifurcation are appropriate in many contexts (e.g. [3, 5, 58]). Here we focus on briefly summarizing Hopf bifurcations observed in power system models designed for studying voltage collapse. Stressed power systems are more likely to undergo Hopf bifurcation and oscillate. There have been suggestions that unstable oscillations could be an additional phenomena associated with some voltage collapses but this possibility remains to be confirmed. This would imply that the power system was experiencing some combination of saddle node bifurcation and Hopf bifurcation at the same time. While this is perfectly possible in theory and can be observed in some small power system models [2, 35, 39], the evidence of problems with unstable oscillations from reported voltage collapse incidents is not conclusive. (Of course

any power system disturbance involves *stable* oscillations as swing dynamics act.) However unstable power system oscillations are of considerable importance even if they are not directly related to voltage collapse.

## Appendix 2.B SINGULARITY INDUCED BIFURCATIONS

### 2.B.1 Introduction

The generic local bifurcations saddle node bifurcations (related to zero eigenvalues) and Hopf bifurcations (related to purely imaginary eigenvalues) have been introduced in Section 2.4 and Appendix 2.A. In systems which are modeled by purely differential equations, saddle node and Hopf bifurcations are in fact the only two types of local bifurcations which are generically significant for understanding the small signal stability properties of the operating equilibrium.

On the other hand, realistic large scale power system models generally consist of two types of equations namely the differential equations (modeling the equipment behavior) which are constrained by a set of algebraic equations (modeling the transmission network behavior). In such differential-algebraic models, an additional type of local bifurcation (other than saddle node and Hopf) phenomenon emerges when the network algebraic equations have singularity problems at the operating point. The practical implications of these local bifurcations (associated with the singularity of network equations) demand a careful scrutiny owing to modeling limitations of the network equations in power system models. More details on these issues follow in this section.

### 2.B.2 Differential-algebraic Models

The midterm dynamics of the power system can be represented by the differential-algebraic model

$$\dot{x} = f(x, y) \quad (2.8)$$

$$0 = g(x, y) \quad (2.9)$$

The differential equations (2.8) represent the dynamics of the equipment (including generators and controls) and loads at the buses. The algebraic equations (2.9) represent the power transfer relationships between the buses as effected by the transmission network. The state variables  $x$  of (2.8) equations (such as generator angles, frequencies, and flux quantities, control state variables and dynamic load variables) are denoted the dynamic state variables. The  $y$  variables of the algebraic equations (2.9) are typically the power flow variables such as the bus voltages and angles.

Note that the dynamics within the transmission network (network transients) are much faster than the midterm dynamics of equipment and load (2.8). Therefore the network power flows are modeled to be instantaneous (2.9) in the differential-algebraic model (2.8)-(2.9) by assuming that the network variables  $y$  respond in a *quasi-stationary* or *quasi-steady state* fashion to changes in the dynamic state variables  $x$ .

The actual dynamics of the transmission network is quite complicated since each transmission line is a distributed parameter device and as such it is difficult to analyze the time domain behavior of network transients accurately. However, since the dynamics of interest in the model (2.8)-(2.9) is slower than 5 Hz or so (midterm

dynamics), we can employ the quasi-stationary or quasi-steady state assumption to simplify the network representation to lumped parameter circuits using the concept of quasi-stationary phasor representations. Instead of analyzing the actual dynamics of modulated sinusoidal time domain signals (which would require distributed parameter transmission line models), we only study the dynamics of the modulated envelope represented by phasor bus voltages and angles  $y$  by analyzing the dynamics in the quasi-stationary phasor domain. In the phasor domain, the familiar and useful concepts of real and active power also emerge which are powerful tools for understanding the flows of electric power through the transmission network.

However, it must be kept in mind that the concept of phasors as well as the lumped parameter representation of the transmission network which have been used in deriving the algebraic equations (2.9) are only valid under the quasi-stationary assumption. That is, the algebraic equation type phasor representation of network power flows (2.9) is only valid for quasi-stationary phenomena whenever the dynamics under investigation is slower than say 5 Hz or so. For studying faster dynamic properties, more detailed time domain models which carry out the analysis in terms of sinusoidal signals are necessary and these models are beyond the scope of quasi-stationary phasor domain models (2.8)-(2.9). In solving the phasor network equations (2.9), there arise certain conditions called the *singularity* where the quasi-stationary assumption of the phasor model (2.9) breaks down and more detailed models become necessary.

In numerical implementations and analysis of the model (2.8)-(2.9), the algebraic equations (2.9) can usually be solved for  $y$  as say  $y = h(x)$  given any value of  $x$  and this reduces the dynamic equations  $\dot{x} = f(x, y)$  into a set of unconstrained set of differential equations  $\dot{x} = f(x, h(x))$  purely in terms of  $x$ . (In computations, it is not necessary or desirable to actually perform this reduction to the differential equations, the necessary information can be deduced directly from the differential-algebraic equations.) If the algebraic constraints (2.9) are enforced by stable and sufficiently fast network dynamics, then these differential equations correctly describe the slow system dynamics of interest as long as the quasi-stationary phasor assumption is valid.

### 2.B.3 Modeling Issues Near a Singularity Induced Bifurcation

The electric power system is normally operating at a small signal stable equilibrium point. Equilibrium points of the differential-algebraic model (2.8)-(2.9) are defined by the solutions of the equations  $f(x, y) = 0$  and  $g(x, y) = 0$ . In power system small signal stability analysis, the first step is indeed the computation of the equilibrium condition for the variables  $x$  and  $y$ . Typically the equations  $f(x, y) = 0$  and  $g(x, y) = 0$  possess a large number of solutions. That is, the model (2.8)-(2.9) has a number of equilibrium points; however, typically one of these equilibrium points is small signal stable and this small signal stable equilibrium solution (when it exists) of  $f(x, y) = 0$  and  $g(x, y) = 0$  corresponds to the system operating point.

The small signal stability of an equilibrium point say  $(x_o, y_o)$  can be verified by

computing the eigenvalues of the associated Jacobian or the system matrix say  $A$  by linearizing the equations (2.8)-(2.9) at the equilibrium point  $(x_o, y_o)$  where

$$A = \left( \frac{\partial f}{\partial x} - \frac{\partial f}{\partial y} \frac{\partial g}{\partial y}^{-1} \frac{\partial g}{\partial x} \right) \bigg|_{(x_o, y_o)}$$

Note that the definition of the system matrix  $A$  requires the inversion of the matrix  $G_y = \frac{\partial g}{\partial y} \big|_{(x_o, y_o)}$  which represents the presence of network variables  $y$  in the power flow equations  $g(x, y) = 0$ . When this matrix  $G_y$  is singular at the operating point  $(x_o, y_o)$  clearly the inversion of  $G_y$  is not defined and hence the system matrix  $A$  is also not defined at the operating point. This condition of singularity of the matrix  $G_y$  at the operating point is defined as the *singularity induced bifurcation* [57].

Mathematically it can be proved that the system matrix  $A$  has eigenvalues at infinity (unbounded eigenvalues) at the singularity induced bifurcation when the matrix  $G_y$  is singular. This implies that the actual system will encounter some sort of instability problems resulting from fast interactions of network variables. However, it is not possible to predict the nature of the instability owing to modeling limitations on the network power flow equations.

The singularity of the matrix  $G_y$  at the operating point implies that the operating point lies in the vicinity of an algebraic singularity of the network equations  $g(x, y) = 0$  in the model (2.8)-(2.9). As stated earlier, the quasi-stationarity phasor assumption which is the underlying assumption in deriving the network equations  $g(x, y) = 0$  loses its validity in singularity domains. Therefore the differential-algebraic model (2.8)-(2.9) based on phasors is no longer valid near the singularity induced bifurcation. More detailed dynamic models are necessary for predicting the power system behavior near the singularity induced bifurcation.

## 2.B.4 Singularity Induced Bifurcation Definition

If the power system is operating at a stable equilibrium and parameters change slowly so that the algebraic equations become singular, a singularity induced bifurcation is said to have occurred. In other words, singularity induced bifurcation results when the matrix  $G_y$  becomes singular at the operating point under some parameter variation.

The following are mathematical attributes of a singularity induced bifurcation:

(1) The algebraic equations become singular in the sense that the Jacobian of the algebraic equations with respect to  $y$  becomes singular.

(2) An eigenvalue of the system Jacobian passes from the left half plane to the right half plane via infinity.

The infinite (unbounded) eigenvalue at this bifurcation implies that some of the slow dynamics  $x$  of the differential-algebraic model become very fast near the singularity induced bifurcation. The presence of the eigenvalue in the right half plane after the singularity induced bifurcation in the differential-algebraic model implies that the power system is small signal unstable after the bifurcation.

As explained in the previous subsection, the occurrence of singularity induced bifurcation in a differential-algebraic model raises some difficulties about the model



itself. In particular, the overall dynamics becoming fast near the bifurcation violates the quasi-stationary assumption of the network phasor equations. These difficulties suggest that the differential-algebraic equation model is incomplete for describing the system behavior near the singularity induced bifurcation.

Since singularity induced bifurcations do occur in some differential-algebraic power system models, these difficulties are under discussion. Indeed, encountering a singularity induced bifurcation is a typical occurrence in any differential-algebraic model when parameters are varied. The resolution of the difficulties may well lie in rederiving valid dynamic models in specific instances in which singularity induced bifurcations arise to more reliably determine the consequences of this phenomenon.

## **Appendix 2.C GLOBAL BIFURCATIONS AND COMPLEX PHENOMENA**

### **2.C.1 Introduction**

Parameter values at which the stability of equilibria change are bifurcations. Those parametric conditions where the system operating point a) loses its existence as an equilibrium (at saddle node bifurcations leading to voltage collapse) or b) loses its local stability (at Hopf bifurcations leading to oscillations) or c) possibly faces loss of stability at singularity of network equations (at singularity induced bifurcations in differential-algebraic models leading to per se indeterminable behavior) are the most important bifurcations in power system models. These bifurcations are called local bifurcations because they only concern the immediate vicinity of an equilibrium.

In addition to these local bifurcations which affect the local stability properties of equilibria, there exist different bifurcations called global bifurcations which change the global dynamic properties of power system models. Global in this sense refers to the behavior of the trajectories away from an equilibrium in the state space. Recently global bifurcations which are related to chaos and complicated phenomena have drawn a lot of interest in nonlinear system theory and also among power system researchers.

### **2.C.2 Four Types of Sustained Phenomena**

In nonlinear systems such as power system, there exist four different types of sustained phenomena. While normal system operation is always at stable equilibria, there exist three other types of sustained operating conditions where the system can get trapped into following large disturbances. The transitions between different types of operating conditions can occur at local or global bifurcations.

### **2.C.3 Steady State Conditions at Stable Equilibria**

All state variables remain at their steady state values at stable equilibria. These correspond to the normally acceptable operating condition for power system operation. Under parametric variations, stable equilibria lose their local stability at local bifurcations of previous subsections. Following these local bifurcations, the operation could possibly get attracted to one of the other three types of operation described below or can diverge away leading to system break up or voltage collapse.

### **2.C.4 Sustained Oscillations at Stable Periodic Orbits**

When a trajectory gets trapped into a stable periodic orbit, all the state variables exhibit periodic motions. The motion has a single principal frequency and harmonics of that principal frequency. The fluctuations of various state variables are different depending on the nature of the stable periodic orbit. While long-term operation at a stable periodic orbit could be harmful for power system equipment, temporary

operation at a stable periodic orbit is possible provided all the state variable fluctuations are within their respective acceptable limits. Indeed actual power systems have occasionally been operated at stable periodic orbits.

Typically the transition from operation at a stable equilibrium point to operation on a stable periodic orbit occurs at supercritical Hopf bifurcations (see Section 2.A.2). These stable periodic orbits can emerge from the interaction of device hard limits and transients.

Under parametric variations, equilibria lose stability at local bifurcations. Similarly, stable periodic orbits can lose their stability under parametric variations, and such parameter values associated with changes in stability phenomena of periodic orbits are called global bifurcations. Just like the disappearance of an operating equilibrium at saddle node bifurcation leads to voltage stability problems, the annihilation of the operating periodic orbit could also lead to voltage crisis.

While the stability of equilibrium points depends on the eigenvalues at the equilibrium, the stability of a periodic orbit is characterized by what are called Floquet multipliers for the periodic orbit. Floquet multipliers can be thought of as the eigenvalues of an associated discrete map (called the Poincaré map) which quantifies the local stability properties of a point on the periodic orbit. Like in discrete nonlinear systems, all Floquet multipliers of a periodic orbit must have moduli less than one for the periodic orbit to be a stable periodic orbit. When the Floquet multipliers of a periodic orbit cross the unit circle under parametric variations, global bifurcations result.

There are two types of local bifurcations associated with stability properties of equilibria, namely saddle node bifurcations related to zero eigenvalues and Hopf bifurcations associated with purely imaginary eigenvalues. Similarly, there exist three types of global bifurcations for the loss of stability of a periodic orbit. These are cyclic fold bifurcations, period doubling bifurcations and secondary Hopf bifurcations. Just as each type of local bifurcation has a different physical implication, each of these bifurcations leads to a different consequence as briefly summarized below.

1) Cyclic fold bifurcation: This bifurcation arises when under parameter variations, when the Floquet multiplier of the periodic orbit is at  $+1$ . This global bifurcation is very similar to the saddle node bifurcation of equilibria and hence it is called a saddle node bifurcation of periodic orbits. The characteristics of the cyclic fold bifurcation are as follows: a) before the bifurcation, the system is operating at a stable periodic orbit displaying sustained oscillations; b) at the bifurcation, the periodic orbit becomes poorly stable and trajectory starts to move away from sustained oscillatory conditions; c) after the bifurcation, the periodic orbit has disappeared and the trajectory diverges away. This divergence is slow then fast and the oscillation will continue as it diverges. Depending on the direction of divergence either a voltage crisis or a loss of synchronization could follow.

2) Period doubling bifurcation: This bifurcation occurs when under parametric variations, one Floquet multiplier of the periodic orbit is at  $-1$ . This bifurcation is quite special to periodic orbits and there is no counterpart in local bifurcations of equilibria. Period doubling bifurcations are characterized by the doubling of the period of the periodic orbit at the bifurcation as the name suggests. Geometrically,

the periodic orbit gets a twist onto itself so that the trajectory takes twice the time to wind on itself thus twice the time period as compared to the original periodic orbit. There are two subtypes in this case called supercritical and subcritical period doubling bifurcations depending on whether the period two periodic orbit after the period doubling bifurcation is stable (supercritical) or unstable (subcritical).

Subcritical period doubling bifurcations denote the end of operation at the previously existing periodic orbit since operation cannot continue on the this unstable periodic orbit after the bifurcation. The resulting transient would diverge away in an oscillatory fashion. This transient may either get trapped into some other operating condition such as into chaos or may not converge resulting in system break-up.

On the other hand, supercritical period doubling bifurcations denote the transition of operation from stable periodic orbit to another stable periodic orbit of twice the period as the original one. That is, the period of oscillations double at period doubling bifurcations. When an infinite sequence of these period doubling bifurcations occur over a short parametric interval, the period of the periodic orbit becomes very large (the periodic orbit has “infinite twists”) resulting in a very complicated “periodic orbit” called a strange attractor. This mechanism of an infinite sequence of period doubling bifurcations is called a period doubling cascade and we will discuss this in a little more detail in the subsection on chaos below.

3) Secondary Hopf bifurcation: This global bifurcation occurs when a pair of complex Floquet multipliers lie on the unit circle with moduli one. As the name suggests this bifurcation is very similar to the Hopf bifurcation of equilibrium points. There are again two subtypes called subcritical and supercritical secondary Hopf bifurcations.

At supercritical secondary Hopf bifurcations, the stable periodic orbit changes into a stable two dimensional periodic orbit called a stable invariant two torus. While a periodic orbit is periodic in one direction, an invariant two torus is periodic in two directions and there are two principal frequencies. More discussion of invariant tori follows in the next subsection. At a supercritical secondary Hopf bifurcation, the operation essentially changes from stable sustained oscillations of one frequency (at a stable periodic orbit) to sustained oscillations of two frequencies (at an invariant torus) called quasiperiodic motions.

At subcritical secondary Hopf bifurcations the stability of the periodic orbit is annihilated by an unstable torus so that the trajectory diverges away after the bifurcation. As in the case of subcritical period doubling bifurcation, the resulting oscillatory divergent trajectory could either diverge away or get trapped into another type of operation.

The discussion in this section can be summarized as follows. Suppose the system is temporarily operating at a stable periodic orbit following a severe disturbance. Under parameter variations, the periodic orbit could undergo one of the types of global bifurcations described above. The consequences of such a global bifurcation depends on the specific type of the global bifurcation: 1) after supercritical period doubling bifurcations, the period of the stable periodic orbit gets doubled; 2) after supercritical secondary Hopf bifurcations, the operation changes to a stable invariant two torus and quasiperiodic oscillations; 3) after any of a) cyclic fold bifurcation, b)

subcritical period doubling bifurcation, or c) subcritical secondary Hopf bifurcation, the periodic orbit either disappears (case a)) or loses its stability (cases b) and c)) so that the trajectory diverges away in an oscillatory fashion. The divergence could lead to either voltage problems or angle problems depending on global interactions of system nonlinearities.

### **2.C.5 Sustained Quasiperiodic Oscillations at Invariant Tori**

When the sustained oscillations display more than one frequency content the oscillations are said to be quasiperiodic oscillations. Quasiperiodic oscillations are familiar in power engineering when, for example, the basic 60 Hz power system oscillation has its amplitude varying periodically as occurs in interarea oscillations. These can be thought of as periodic orbits of periodic orbits (where the amplitude of the periodic orbit is oscillating with a second frequency) and so on. These exotic oscillations typically arise after supercritical secondary Hopf bifurcations of stable periodic orbits into stable invariant tori. The stable invariant tori could in turn lead to other global bifurcations under parametric variations so that the oscillations would become more complex. Of special interest in nonlinear theory is when the invariant tori “breaks up” in some sense so that chaotic motions could emerge.

### **2.C.6 Sustained Chaotic Oscillations at Strange Attractors**

Sustained oscillations which have a continuous frequency spectrum and which are aperiodic and irregular are said to be chaotic oscillations. These are certainly the most complicated of all operating conditions since operation at chaotic attractors leads to unpredictable system behavior. Recall that sustained oscillations result when the operation is trapped at a stable periodic orbit. Similarly, sustained chaotic phenomena result when the operation is trapped at a complex entity called a strange attractor. The main characteristics of chaotic behavior are as follows:

a) Even trajectories with very similar initial conditions could lead to entirely different time behavior. This sensitive dependence on initial conditions results from the fact that strange attractors are also unstable in some sense within themselves. However, the trajectories of a strange attractor are confined to some region of state space. The sensitive dependence on initial conditions can create problems in time domain simulations since some aspects of the computed trajectory will not match the behavior of trajectories with very slightly different initial conditions or, for that matter, the exact trajectory of the power system model.

b) As a whole, a strange attractor is locally stable in the sense that a trajectory near the attractor converges to the strange attractor. The trajectory once trapped onto the strange attractor remains within the strange attractor forever. However, there are also some unstable directions within the strange attractor so that even trajectories nearby diverge away exponentially fast from each other. This results in the unpredictable nature of chaotic motions.

c) The oscillations while being random remain bounded much like true noise. The boundedness of chaotic oscillations comes from the boundedness of the strange

attractor.

d) The dimension of a strange attractor is a fractal and is not an integer. Any attractor with an integer dimension is said to be a regular attractor. For a normal stable periodic orbit which displays sustained oscillations, the dimension is one; for an invariant two torus displaying quasiperiodic oscillations, the dimension is two; for a higher dimensional torus, the dimension is still an integer. However, a strange attractor is an irregular set in some sense so that the dimension is not an integer.

### 2.C.7 Mechanisms of Chaos in Nonlinear Systems

Typically chaotic motions result when the system operating at a stable periodic orbit undergoes a series of global bifurcations leading to the birth of a strange attractor under some parametric variations. There are four such mechanisms for the generation of chaos which have been commonly encountered and all these cases have been shown to be relevant in small power system models by several recent papers [11, 35, 36, 50, 62]. Three of these cases are summarized below and the reader is referred to [32, 49] for more details.

a) Period doubling cascade: when a sequence of supercritical period doubling bifurcations occur in a small parametric interval, a stable periodic orbit can change into a complicated cycle namely the strange attractor. A period doubling cascade is characterized by gradual doubling of the period of the oscillations at specific parameter values (at period doubling bifurcation points) so that eventually the period effectively becomes infinity and the behavior becomes chaotic.

b) Intermittency: When a stable periodic orbit changes into a chaotic set by an exchange of stability mechanism an intermittency type bifurcation occurs. Before the intermittency, the operation is on a stable periodic orbit displaying regular sustained oscillations. After the intermittency, the operation is chaotic displaying irregular aperiodic oscillations.

c) Break-up of invariant tori: When an invariant three torus breaks up, the operation could change from quasiperiodic oscillations at the invariant torus into chaos at a strange attractor.

Essentially chaos at strange attractors can exist in nonlinear systems such as the power system from the occurrence of global bifurcations described above. Once the power system gets trapped into chaos, irregular and noise like oscillations emerge. If these irregular oscillations have sufficient amplitude they would interfere with system operation and could cause equipment damage.

### 2.C.8 Transient Chaos

Strange attractors themselves can undergo global bifurcations just like global bifurcations of periodic orbits and these phenomena are more exotic owing to the complex nature of strange attractors. One special global bifurcation of strange attractor called the boundary crisis has been studied in [62] related to voltage collapse phenomenon.

When a strange attractor collides with a saddle point under parametric variations, a global bifurcation called an exterior boundary crisis results where the stability of

the strange attractor gets destroyed. The remnants of the strange attractor after the boundary crisis are together called a transient chaotic set. A transient chaotic set has all the properties of a strange attractor. That is, trajectory within a transient chaotic set is irregular and has sensitive dependence on initial conditions. However, a transient chaotic set, unlike a strange attractor, is unstable in some directions. Therefore any trajectory with initial conditions within the transient chaotic set would eventually diverge and leave the set. In [62], the diverging trajectory in a small power system model is identified as a voltage collapse.

Interestingly, owing to the chaotic nature of the dynamics within the transient chaotic set, when the trajectory will actually diverge from the transient chaotic set cannot be predicted. In other words, after the boundary crisis bifurcation of the strange attractor, we can predict that the trajectory would lead to divergence at some future time after first displaying a chaotic bounded time behavior. On the other hand, we cannot predict when the bounded chaotic oscillations would stop and when the divergence away from chaos will occur.

In general, the parametric conditions under which a power system could get trapped into any of the three operating conditions namely periodic, quasi-periodic and chaotic oscillations are not well understood at this point. More work is needed to be able to assess the significance of these more exotic behaviors for power systems. Now that we know what to look for, it would be helpful to gain experience on how often these phenomena occur both in real power system measurements and in more realistic power system models. The amplitude of these phenomena is also an issue: small amplitude chaos need not be a problem on the system; indeed, it is conceivable that this occurs without much fanfare already. On the other hand, any exotic phenomena of larger amplitude could pose a threat to system operation.